Nanoparticle and Gel Based Formulations for Enhanced Drug Delivery

by

Mohammed Aldawsari

A dissertation submitted to the Graduate Faculty of
Auburn University
in partial fulfillment of the
requirements for the Degree of
Doctor of Philosophy

Auburn, Alabama
Dec 16, 2017

Keywords: Nanoparticles, Hydrogel, Antiviral activity, Antioxidant, Epilepsy Treatment, siRNA Delivery

Approved by

Jayachandra Babu Ramapuram, Chair, Professor of Drug Discovery and Development
Robert D. Arnold, Co-Chair, Associate Professor of Drug Discovery and Development
William R. Ravis, Professor of Drug Discovery and Development
Daniel L. Parsons, Professor of Drug Discovery and Development
Allan E. David, Assistant Professor of Chemical Engineering

Abstract

Nanogel and hydrogel formulations have shown promising advantages for topical and trans-mucosal routes of administration. The nanoparticle drug within the gel matrix showed significant enhancement in the permeation of drugs in the topical and transdermal drug delivery. On the other hand, the clear hydrogel with the completely solubilized drug showed attractive results as a suitable vehicle for delivering drugs via buccal mucosa to the systemic circulation. In this dissertation, research data has been presented on a nanogel and hydrogel as drug delivery platforms. In addition, research has been presented on siRNA polyplex nanoparticles as a platform for incorporation of therapeutic siRNA molecules in the treatment of melanoma.

We developed and evaluated siRNA- polyethyleneimine (PEI) polyplex nanoparticles with varied molecular weights of PEI (low, moderate and high). The polyplex formation was optimized at different N/P ratios (gel retardation assay) and studied their cytotoxicity, and cellular uptake on B16BL6 melanoma cell line. Optimal polyplexes were achieved at 50:1. 10:1, 5:1 N/P ratios for PEI 1.8 KDa, PEI 10 KDa, and PEI 25 KDa, respectively. Based on these results, it was concluded that 1.8 KDa PEI-siRNA polyplex at 50:1 ratio is optimum for siRNA delivery due to its safety and efficacy in the cellular uptake of B16BL6 melanoma cell lines.

A nanogel formulation for enhancing the topical delivery of acyclovir was investigated. Since the topical efficacy of acyclovir is hampered by poor skin penetration, the goal was to enhance the percutaneous permeation of acyclovir via nanoparticles based gel formulation with or

without penetration enhancers. Acyclovir nanogel (F1) formulation showed an enhanced skin permeation by 2-folds higher flux compared to Zovirax® commercial product. Incorporating 10 % ethanol (F3) in the formulation showed a synergistic permeation enhancement with 24-folds higher flux compared to Zovirax®. Inclusion of propylene glycol (F5), or oleic acid (F4) showed negligible penetration enhancement. To understand if the permeation barrier exists in the stratum corneum or dermal layers, the permeation data were generated on the microneedle-treated skin; which showed a significant enhancement in the skin permeation as compared to passive diffusion, Again the highest enhancement was achieved for the F3 (10% ethanol). Acyclovir nanogel formulations with ethanol as a penetration enhancer demonstrated a pronounced effect on enhancing acyclovir skin permeability and skin content upon topical application.

A novel buccal midazolam gel formulation was developed and evaluated for efficacy in comparison to an intravenous solution in healthy dogs. The formulations T19 and T29 (HPMC K100M) with significantly higher release rates than T18 (Pluronic F127) were also effectively absorbed through buccal administration in dogs. At a dose of 0.3mg/kg, T19 and T29 produced a Cmax of 98.3±26.5 and 106.3±35.2 ng/ml respectively, which are approximately two-fold higher as compared to T18 (47.7±38.5 ng/ml). Furthermore, T29 at higher dose (0.6mg/kg) produced a Cmax of (187.0±104.3ng/ml). Results of this study show promise in the treatment of seizures in dogs by buccal midazolam gel.

Resveratrol has potent anti-oxidant properties and is believed to be beneficial in treating several diseases. Resveratrol as nanoparticles based gel formulation was developed and evaluated

for percutaneous permeation enhancement. The skin permeation studies showed 12-folds higher flux as compared to its conventional gel (suspended resveratrol microparticles). An enhancement of resveratrol skin levels was observed when nanogel formulation was compared to microparticles incorporated in a gel formulation.

Acknowledgments

I am very grateful for my dissertation committee members, Dr. Jay Ramapuram (Major Advisor), Dr. Robert Arnold (Co-advisor), Dr. William Ravis, Dr. Daniel Parsons and Dr. Allan David. They were very kind and supportive in many ways. I have learned a lot from them and their knowledge, I appreciate their extensive efforts to help students. I would like to express my gratitude to Dr. Jay Ramapuram for his support in related work, for his patience, motivation, and knowledge. His guidance helped me through my research work as well as the writing of this dissertation. Also, I would like to thank Dr. Kevin Huggins for serving as an outside reader of my dissertation. I would like to extend my thanks to Dr. Tim Moore for his support and efforts in enhancing the department outcomes in various aspects. My special thanks to Jennifer Johnson for her substantial help and guidance. I would like to express appreciation to my parents for their support and efforts to help me out through pursuing my doctoral degree. They have helped me to get over many challenges especially through tough times either financially or emotionally. Also, I would like to extend the appreciation to my wife for providing me with unfailing support and continuous encouragement. My brother Saad was one of a kind by his unconditional support for a long time. My sisters were very encouraging and helping to me all time. I would like to thank my friends and laboratory mates Ahmad Alsaqer, Hamad Alrbyawi and Haley Shelley for being kind, honest and helpful. Finally, I would like to thank Saudi government and Prince Sattam bin Abdulaziz University for their financial support through my scholarship assistance.

Table of Contents

List of Figures

List of Tables

List of Abbreviations

SC	Stratum Corneum
FA	Ferulic acid
UVA	Ultraviolet A
DS	Diclofenac sodium
HPMC	Hydroxypropyl methylcellulose
CMC-Na	Sodium carboxymethyl cellulose
siRNA	Short interference RNA
PC	Pachyonychia cogenita
AAV	Adeno-associated virus
RA	Rheumatoid arthritis
SLN	Solid lipid nanoparticles
RNAi	RNA interferences
ACD	Allergic contact dermatitis
CD86	Cluster of Differentiation 86
AA	Alopecia Areata
dsRNA	Double strands RNA

RISC	RNA induced silence complex
Ago-2	Argonuate-2
PEG	Polyethylene glycol
GFP	Green fluorescent protein
VEGF	Vascular endothelial growth factor
PLGA	Poly (Lactide-co-glycolic acid)
EGFP	Enhanced Green Fluorescent Protein
CD	Cyclodextrin
RRM2	Ribonucleotide reductase M2
PEI	Polyethyleneimine
DOPC	1,2- dioleoyl-sn-glycero-3-phosphocholine
Cap	Capsaicin
IMQ	imiquamod
hKC	Human keratinocytes
PLL	Poly-L-lysine
CPP	Cationic cell penetrating peptides

TAT	Trans-Activating Transcriptional activator
SPACE	Skin Permeating And Cell Entering
IL	Interleukins
GADPH	Glyceraldehyde 3-phosphate dehydrogenase
MN	Microneedle
TRBP	TAR RNA binding protein
DPBS	Dulbecco Phosphate Buffered Saline
EtBr	Ethidium Bromide
DMSO	Dimethyl sulfoxide
MTT	3- [4, 5-dimethylthiazol-2-yl]-2, 5-diphenyl tetrazolium bromide
N/P	Nitrogen to phosphate ratio
PBS	Phosphate buffered saline
PG	Propylene glycol
AUC	Area under the curve
Cmax	Peak concentration
Tmax	Time to observed peak concentration

t1/2	Plasma half-life
HPβCD	Hydroxypropyl-β-cyclodextrin
MRM	Multiple reaction monitoring

1. Hydrogel and Nanogel Applications on Topical and Trans-mucosal Drug Delivery

1.1 Introduction

It has been reported that 40% of approved drugs and nearly 90% of the developmental pipeline drugs consist of poorly soluble molecules (Loftsson et al., 2010). Conventional formulations of a poorly water-soluble drug are mostly accompanied with limited bioavailability. To overcome this issue, several formulation approaches were reported such as mixing aqueous formulation with organic solvent (e.g. ethanol) for solubility enhancement, complex formation (e.g. cyclodextrin and its derivatives), solid dispersion, pH and salt forms alteration (Sandip S Chavhan et al., 2011; Poonia et al., 2016; Tokumura et al., 2009). However, these approaches showed limited success in respect to overall bioavailability improvement. Enhancing the bioavailability of poorly water-soluble drugs can be achieved by following two methods: i) enhancing saturation solubility and dissolution rate (Sandip S Chavhan et al., 2011; Kobierski et al., 2009), ii) applying nanotechnology in the formulation design. Several nanoparticulated delivery systems were developed such as polymeric nanoparticles, liposomes, solid lipid nanoparticles, micelles, dendrimers, etc. (Papakostas et al., 2011). These techniques are generally more expensive and pose challenges in large-scale production. There is a need for simple and cost-effective methods for enhancing the solubility and bioavailability of poorly soluble drugs. The top down approaches such as micronizing or high pressure homogenization of drug particles showed a great success as evidenced by the commercialization of several drugs such as fenofebrate (tablets), sirolimus (tablets), aprepitant (capsules), griseofulvin (tablet), for enhancing the bioavailability of poorly soluble molecules. The micronization and nanocrystal approach by milling techniques dramatically increases the particle surface area which increases the dissolution rate of drugs

(Junyaprasert et al., 2015; Kobierski et al., 2009). Nanosuspension is a simple and effective strategy for a wide range of poorly soluble molecules such as danazol (Liversidge et al., 1995), naproxen (Vergote et al., 2002), and itraconazole (Mou et al., 2011). Nanosuspension is prepared by drug particles reduction into nanoparticle size range, this produces a colloidal dispersion which is further stabilized with a stabilizer to achieve the desired nanosuspension formulation. Nanosuspensions are further formulated as dosage forms for various routes of administration such as dermal, oral, pulmonary, ocular and parenteral (Sandip S Chavhan et al., 2011).

Nanocrystals in a suspension are in the high energy state, which tend to aggregate to keep the surface free energy at a minimum level. Hence these particles must be stabilized in a gel system to prevent aggregation. A gel is made up of organic macromolecules which are interlaced and inter-penetrated by a solvent system. They are primarily recognized based on continuous phase construction. Hydrogel comprises of aqueous phase as continuous phase while an organogel comprises apolar solvent as a continuous phase. Drug release rate of the hydrogel has superiority over organogel for a topical and transdermal application (Gupta et al., 2002; Sagiri et al., 2014; Singh et al., 2014). Hydrogel formulation has unique properties with respect to mechanical strength and swelling behavior, due to softness and hydrophilicity which makes it an attractive option as a drug carrier. Moreover, a gel formulation helps drug penetration across biological membrane by increasing the residence time on the applied surface which overall improves the drug bioavailability (Khairnar et al., 2010; Salamat-Miller et al., 2005; Salatin et al., 2016; Sivaram et al., 2015).

The nanoparticles or nanocrystals can be combined in a gel matrix system such as hydrogel or organogel for improved delivery of drugs by transdermal or trans-mucosal (buccal, nasal, rectal or

vaginal) routes (Salatin et al., 2016). Topical nanogels provide a suitable delivery system for drugs because they are less greasy and can be easily washed off from the skin as compared to ointments or creams. Generally, nanoparticles or microparticles are not recognized to be readily permeable through skin layers since skin serves as the main barrier for all exogenous agents such as viruses, allergens, dust or bacteria, all of them within a nano-size scale (Prow et al., 2011). Utilizing drug in the nanoparticles form for enhancing skin permeability is not based on the nano-size but based on other physicochemical properties of drugs such as improved solubility, dissolution, protecting cargo and enhanced contact for better absorption (S. S. Chavhan et al., 2011).

Nanogel is broadly a nanoparticulate system incorporated uniformly within a hydrogel or organogel matrix. The nanoparticles are located within the gel matrix itself or exterior nanoparticulate systems such as incorporating nanoemulsion, liposome or nanosuspension into a gel matrix (Priya Batheja et al., 2011; Shah et al., 2012).

Nanogel can provide a homogenous distribution of nanoparticles with an enhanced thermodynamic activity of drug within gel formulation, with an ability to form aqueous solution with higher colloidal stability, an ability to accommodate macromolecules such as peptide and proteins, capability to load a higher drug quantity with no chemical reaction and a sustained drug delivery for prolonged time (Prakash et al., 2012; Salatin et al., 2016; Sivaram et al., 2015).

Since our research focuses on nanogel and hydrogel for topical, transdermal and trans-mucosal applications for drug delivery, a brief description of the feasible administration routes is presented below.

1.2 Topical and Transdermal Routes of Administration:

Topical application is one of the most suited routes for gel dosage form administration. Topical and transdermal applications have several advantages such as the site of application is easily accessible, wide surface area for application, avoidance of the first pass effect as well as gastric degradation of drugs, maintaining therapeutic concentration during the application and controlling drug concentration within the therapeutic window for an extended time. In addition, a transdermal dosage form is a safe, non-invasive, patient friendly, and requires no hospital visit. Even though skin is an attractive and feasible site for topical and transdermal drug delivery, it is selectively permeable to small drug molecules (less than 500 Da) with balanced lipophilicity and hydrophilicity (Log P 1-3), lower melting point (less than 200 ^{0}C) (Bos et al., 2000; Brown et al., 2008; Phatak Atul et al., 2012; Sharma et al., 2013; Teo et al., 2005; Valenzuela et al., 2012). Skin is composed primarily of three distinctive layers; epidermis, dermis and hypodermis layers as shown in Figure 1. Epidermis layer is responsible for defense against external and harmful agents (Baroli, 2010; Kanikkannan et al., 2000; Valenzuela et al., 2012).

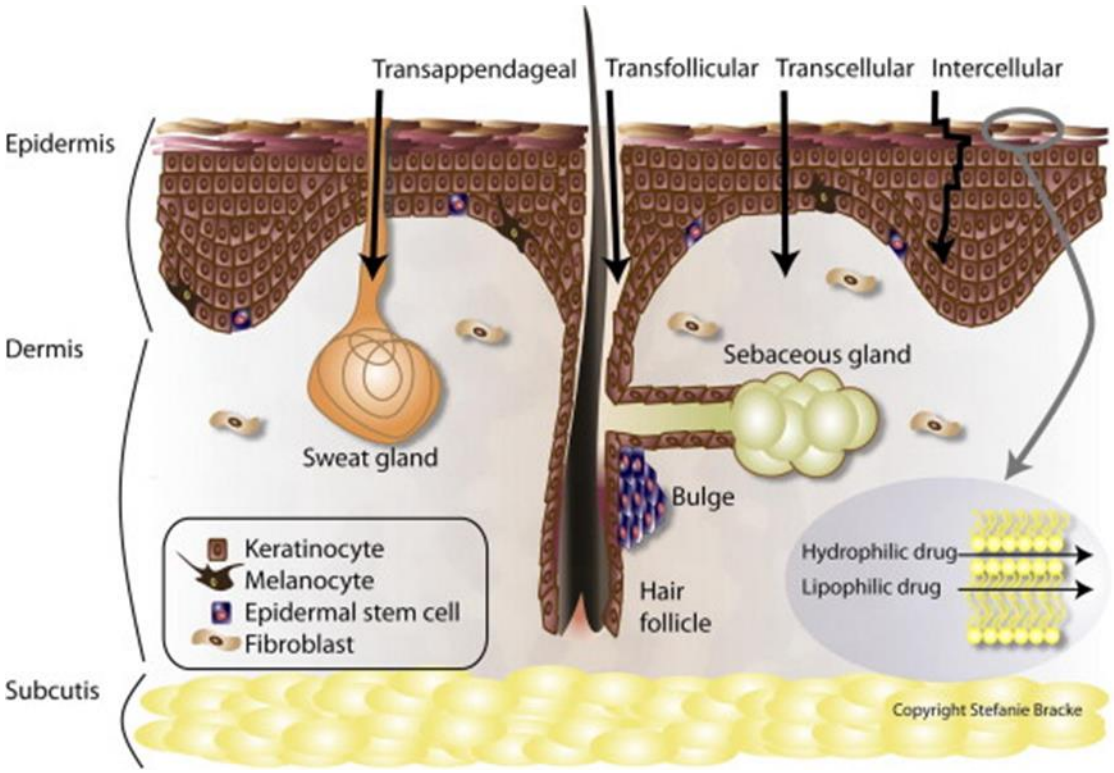

Figure 1.1 Skin structural representation, image describes main skin components and compositions; epidermis, dermis and subcutaneous layers. The figure is adapted from (Geusens et al., 2011).

The outermost layer of epidermis is a stratum cornum (SC), which represents the main barrier for skin permeation of drugs (Priya Batheja et al., 2011; Bouwstra et al., 2002). SC consists of stacked layers of corneocytes. They are interspersed in a lipid matrix which is uniquely organized in lamellar structure. This organization is referred as a brick and mortar structure as described in Figure 1.2 (Brown et al., 2008; Desai et al., 2010; Menon, 2002; Moser et al., 2001; Prow et al., 2011).

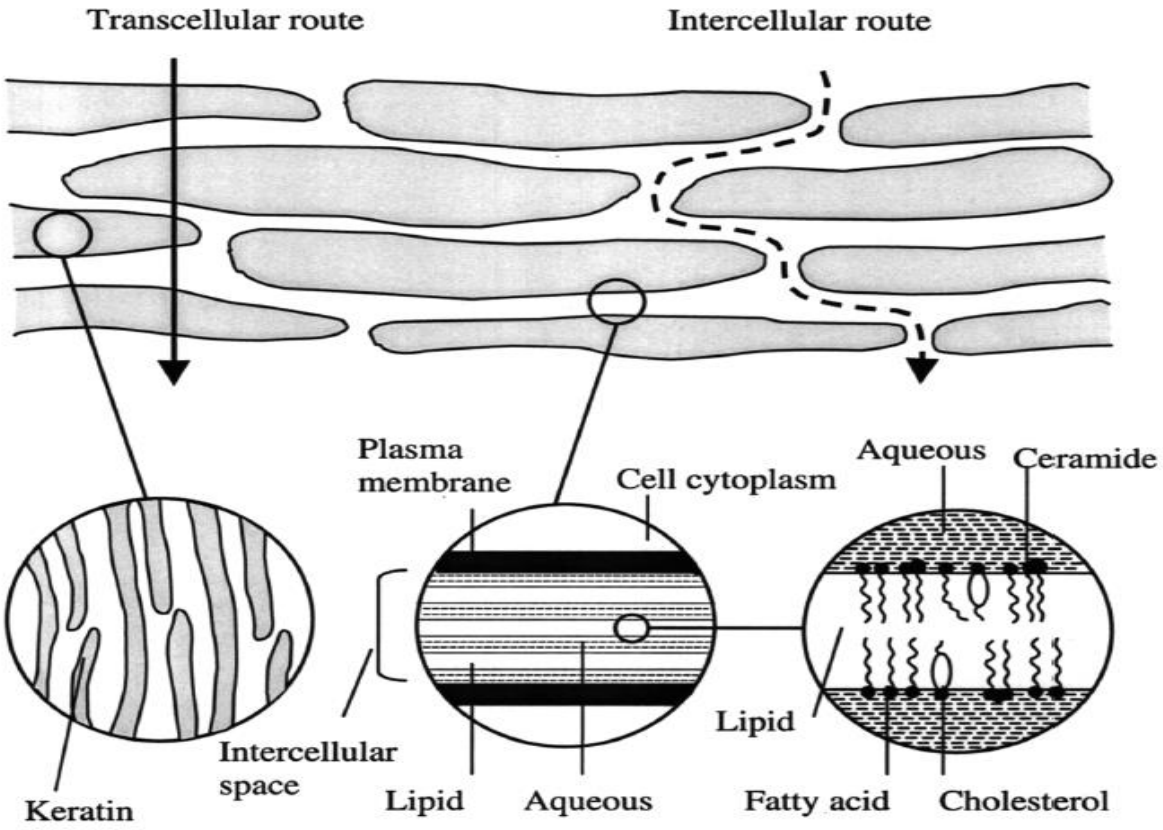

Figure 1.2 Illustrates the brick and mortar model structure of stratum corneum along with penetration pathways. The figure is adapted from (Moghimi et al.,1996)

Once the drug is able to cross the SC, it will be absorbed into dermis systemic circulation.

1.2.1 Penetration Pathways

Topically applied drugs can penetrate skin via three main routes; a- intercellular pathway which is across the lipid embedded in between keratinocytes. b- transcellular pathway which is mainly through keratinocytes. c- trans-appendageal pathway, which is through hair follicles, sweat ducts, sebaceous glands, this pathway is considered minor because the surface area occupied by the appendages is around 1% of the total area of the skin (Hadgraft, 2001; Moser et al., 2001; Prow

et al., 2011). However, intercellular penetration pathway is the most common route for drug penetration via passive diffusion (El-Nahas et al., 2011).

1.2.2 Permeation Enhancement Methods

Topical and transdermal drug delivery is limited to potent lipophilic drugs with the dose < 20 mg. For many drugs, drug permeability needs to be enhanced in order to deliver them in therapeutic quantities. Various permeation enhancement methods have been reported for successful transdermal drug delivery. These methods can be categorized broadly into chemical and physical enhancing methods (Moser et al., 2001). Chemical penetration enhancers are preferred over the physical methods for practical and patient compliance aspects. An ideal chemical penetration enhancer should be safe and non-toxic, non-irritant, and pharmacologically inert (Godin et al., 2003; Senel et al., 2001). Chemical penetration enhancers such as ethanol, surfactants, fatty acids, fatty acid esters, fatty alcohols, pyrrolidines, phospholipids, and terpenes are commonly utilized in transdermal formulations. Chemical penetration enhancers act via different mechanisms. a- disruption of the SC lipid organization. b- fluidization of lipid compositions of the SC. c- occlusive effect on skin based on hydration. d- enhance partitioning in between SC and drug or solvent, e- enhance the solubility of a given drug (Desai et al., 2010).

Merely adding a penetration enhancer to a formulation composition is not considered a right approach in order to achieve a desired permeation for a given drug. This is because the enhancer in a high incorporated percentage is commonly associated with irritation and toxicity (Li et al., 2013; Pegoraro et al., 2012).

Various active penetration enhancing methods such as microneedle arrays, ultrasound, iontophoresis, electroporation, laser radiation and jet injectors have been reported (Kumar et al.,

2007). Among these methods, iontophoresis and microneedle array patch are considered the most successful methods based on the number of commercial products available in the market such as Ionosys® patch, Intanza® patch etc.

Several research studies report the use of nanogel formulations for certain poorly soluble drugs with low skin permeability. A nanogel based formulation for enhancing ferulic acid (FA) permeability was developed. The gel was incorporated with a nanoemulsion made with isostearyl stearate (oil), labrasol (surfactant) and plurol isostearique (co-surfactant). The nanogel formulation revealed a sustained-releasing rate, a better permeability, and an enhanced protection against ultraviolet A (UVA) activity compared to conventional dosage form in a rat model. This study demonstrates the potential of nanogel for enhanced topical delivery for skin protection against UVA-induced damage (Harwansh et al., 2015).

In another study, Shen et al. formulated triterpenoids as a nanosuspension using a high-pressure homogenization technique and then suitably gelled with Carbopol. The drug permeation across rat skin by nanogel formulation was much higher than Carbopol gel. Moreover, nanogel formulation showed an increase in the cumulative amount of drug in epidermis five times in comparison to Carbopol gel. In addition, the nanogel formulation demonstrated a higher efficacy than Carbopol gel formulation in the treatment of frostbite which was corresponding to a higher cumulative amount of drug permeated in the epidermis for the nanogel formulation. This study demonstrated the superiority of nanogel based formulation over a conventional gel formulation for poorly soluble drugs on topical delivery (Shen et al., 2016).

Silver sulfadiazine as nanosuspension was optimized, which constituted of 5.5% each of Span 20 and Tween 80 as a dispersing agent and 0.5% Poloxamer 188 as a co-surfactant. This

nanosuspension was incorporated into a nanogel formulation with the addition of 1% AV-gel and 0.5% Carbopol 940. The releasing rate from nanogel formulation (77 ± 3%) was significantly higher compared to marketed formulation (43 ± 1.5%). Moreover, histopathological studies of nanogel formulations showed an enhancement on wound healing in rats upon 14 days of application compared to a marketed formulation (Barkat et al., 2017).

A Carbopol or HPMC gel formulation containing tyrosine-derived nanospheres was developed for effective skin application and enhanced permeation. Sparingly water-soluble diclofenac sodium (DS) and lipophilic Nile Red were used as model compounds. DS was used to determine the optimum polymer type, viscosity, and release properties of the gel while fluorescent Nile Red was used in in vitro and in vivo skin distribution studies. Dispersion of Nile Red-loaded nanospheres in 1% w/v HPMC gel produced a uniform and stable dispersion with suitable rheological properties for topical application, without any short-term cellular toxicity or tissue irritation. In vitro permeation studies using human cadaver skin revealed that the deposition of Nile Red via the nanosphere gel in the upper and lower dermis was 1.4 and 1.8-fold higher, respectively, than the amount of Nile Red deposited via an aqueous nanosphere formulation. In vivo, the HPMC gel containing Nile Red-loaded nanospheres significantly enhanced (1.4 fold) the permeation of Nile Red to the porcine stratum corneum/epidermis compared to the aqueous Nile Red-loaded nanospheres. An additional increase (1.4 fold) of Nile Red deposition in porcine stratum corneum/epidermis was achieved by incorporation of Azone (0.2M) into the nanosphere gel formulation (P. Batheja et al., 2011).

1.3 Trans-mucosal Route of Administration:

Oral cavity structure is composed of several regions including tongue, lips, soft palate, hard palate, cheek and other regions. The cheek mucosa represents the main target membrane for buccal administration of topically applied therapeutic agents (Harris et al., 1992). The mucosal membrane is generally classified into two types: Keratinized and non-keratinized. Keratinized is commonly presented on tough and hard places of the mouth. Keratinized tissues are employed for defense and protection against harmful effects. On the other hand, non-keratinized mucosa is commonly located in soft tissues such as cheek which is mainly covered with non-keratinized mucosa. Buccal mucosal simply consists of three distinctive layers; epithelium layer, basement membrane and connective tissues as described in Figure 1.3.

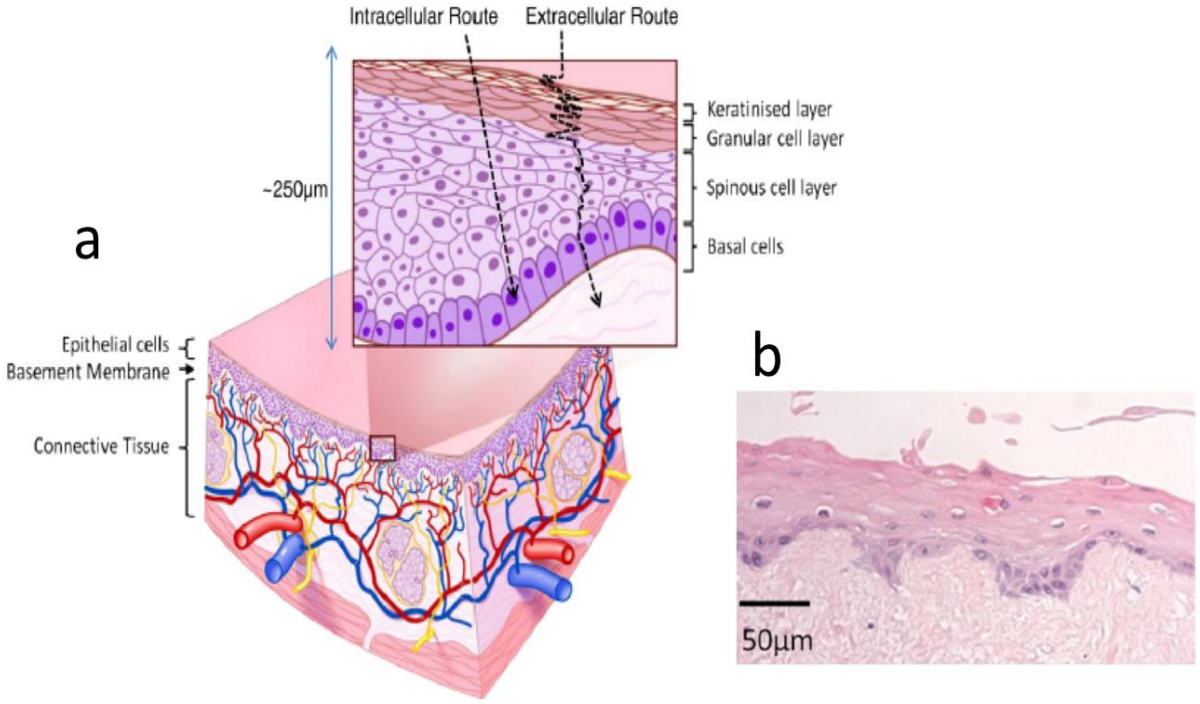

Figure 1.3 A- Schematic representation of oral mucosa demonstrates physiological structure as well as penetration pathways for therapeutic application. B- shows a microscopic cross section of human oral mucosal tissue that was stained with haematoxylin and eosin to emphasize the three distinct layers of oral mucosa; epithelial cells, basement membrane, and connective tissues. The figures are adapted with modification from article (Hearnden et al., 2012)/ Advanced Drug Delivery Reviews.

The thickness of the superficial layer in dogs, rabbits and human (epithelium layer) is in a range of 500 to 800 µm, all these species are similar in respect to the structural and functional aspect of the biological membrane. The turnover time for oral epithelial cells is around 5-7 days which reflects a brief time for regeneration and healing. Epithelium layer largely covers the surface of the buccal mucosa and acts as a barrier and support for subsequent layers (deeper tissues). Nonetheless, based on the soft nature of buccal mucosa, it represents a feasible and an accessible path for molecules to diffuse through and reach general circulation compared to other routes of administration (Caon et al., 2015; Laffleur, 2014; Nicolazzo et al., 2005; Sattar et al., 2014).

Trans-mucosal drug delivery, particularly via oral mucosa, serves as an attractive route for both local and systemic administration. For systemic delivery, sublingual and buccal mucosa are considered as the best suitable routes within an oral cavity. Although buccal mucosa is less permeable than sublingual mucosa, the former is more favorable as a suitable route of administration for systemic delivery. In the sublingual area, a steady and excess saliva washing affects the formulation retention for absorption. Moreover, the sublingual route is suitable for only limited number of drugs that are small molecules and high therapeutic potency. On the other hand, the buccal mucosa is preferred due to the wide feasibility as a route of administration for various drugs with less respective to potency and drug molecular size (Gilhotra et al., 2014; Jug et al., 2017; Sohi et al., 2010).

Buccal route of administration has several advantages such as avoidance of hepatic and intestinal metabolism, modulating applied therapeutic dose readily and easily in case of overdose administration, reduced enzymatic activity relatively which is favorable specifically for proteins and peptides based therapy, a relative low required dose owing to higher permeability compared to other oral routes of administration, high vasculature density which facilitates and enhances drug absorption readily to systemic circulation, avoidance of pain and discomfort of injection dosage form and applicability of buccal dosage form on patient who is unconscious (Boateng et al., 2015; Bos et al., 2000; Caon et al., 2015; Laffleur, 2014; Nielsen et al., 2000; Patel et al., 2011). However, this route has some limitations including: a limited accessible surface area for absorption, mucosal irritation with certain drugs, rapid clearance by saliva which intrudes residence time for absorption on buccal mucosa surface, low patient compliance due to unpleasant taste or mouth discoloration by certain drugs (Caon et al., 2015; Rehman et al., 2016; Satheesh Madhav et al., 2012; Sohi et al., 2010; Wu et al., 2015).

To achieve an effective drug delivery via oral mucosa route, the delivery system should satisfy certain conditions; applied drug formulation needs to be readily retained at absorption site for extended time, the drug should be completely released and available for adequate time to get a better absorption. Depending on the degree of mucosal permeability and drug diffusion properties, drug molecule will pass to systemic circulation and accomplish a desired pharmacological action. Certain factors may affect drug absorption in oral mucosa and alter the formulation efficacy such as enzymatic degradation, pH, mucosal integrity, cellular turnover and fluid volume, all these factors need to be taken into consideration in drug formulation development for enhanced drug delivery (Patel et al., 2011; Satheesh Madhav et al., 2012; Wu et al., 2015).

1.3.1 Absorption Pathways

Drug absorption through epithelial buccal mucosa occurs via passive diffusion, active transport (carrier-mediated transport) or other specific mechanisms. Passive diffusion mostly takes place in between lipid membranes which can be throughout transcellular, paracellular or both (Patel et al., 2011; Sattar et al., 2014; Thwala et al., 2017).

Hydrophilic and lipophilic drugs generally follow paracellular and transcellular diffusion pathway, respectively. Transcellular penetration route occurs mainly through transport from one adjacent cell to another till reach general blood circulation (Montero-Padilla et al., 2017; Rathbone et al., 1994; Shojaei, 1998; Thwala et al., 2017).

1.3.2 Penetration Enhancing Methods

For drugs with poor permeability (peptides and proteins), numerous absorption or penetration enhancers have been investigated (Li et al., 2013). Examples include: surfactants, fatty acids, bile salts, cyclodextrins and chitosan's derivatives are all considered as chemical penetration enhancers. In fact, penetration enhancers are not always considered safe and effective for buccal administration (Morales et al., 2014). Epithelial damage or irritation along with increased permeability for harmful microorganisms are some issues long term. A few penetration enhancers have proven their efficacy as well as their safety for enhancing the delivery of poorly permeable drug molecules through oral mucosae such as bile salts. For example, bile salt was utilized as penetration enhancer to increase the permeability of insulin (macromolecules therapy) across the oral mucosa. Buccal insulin is currently in clinical trials and can potentially reach to market in the near future (Hearnden et al., 2012).

A variety of dosage forms such as tablets, aqueous solutions, patches or films, gels, chewing gums, lozenges, and others have shown efficacy through oral trans-mucosal administration. Hydrogel formulation is simple and inexpensive to develop. In addition, hydrogel has a high capacity for drug loading, high releasing rate and enhanced drug penetration on mucosal membrane via increasing formulation retaining and contact time on the applied surface (Satheesh Madhav et al., 2012).

Buccal administration as a route for systemic absorption was potential for several drugs including acute seizure treatment. McIntyre et al. and his group initiated a clinical trial study to evaluate the safety and efficacy of buccal midazolam solution administration in comparison to rectal diazepam for managing and treating acute seizures in pediatric patients. They have observed a therapeutic success which was 56% (61 of 109) for buccal midazolam and 27% (30 of 110) for rectal diazepam (percentage difference 29%, 95% CI 16–41). The respiratory depression rate was not different in between the group of treatments. Buccal midazolam showed more efficacy compared to rectal diazepam for children presenting to hospital with acute seizures. Besides, buccal midazolam was not associated with an increased incidence of respiratory depression (McIntyre et al., 2005).

Karavana et al. evaluated a bioadhesive gel of benzidamine hydrochloride gels for oral ulcer curing. Gel formulations were developed with different hydroxypropyl methylcellulose (HPMC) grades (E5, E15, E50 and K100M) with varied ratios. In this study, increased drug concentration and gel viscosity leads to decreasing the release rate. The gel formulation with 2.5% HPMC K 100M was found to be the most appropriate formulation in providing suitable cohesion and bioadhesion (Karavana et al., 2009).

Chen et al. developed a buccal gel containing matrine for protection against enterovirus 71 which infects mouth, hand, and foot. The buccal gel formulation was prepared with Carbopol 971P, sodium carboxymethyl cellulose (CMC-Na) and HPMC K100M. All formulations were characterized for rheological and in vitro release behavior. The combinations of two polymers significantly improved mucoadhesion, especially Carbopol 974P blended with HPMC. Carbopol 974P to HPMC blend ratios of 1:1 and 2:1 provided better mucoadhesion. A ratio of 2.5:1 Carbopol 974P to HPMC showed the most sustained release behavior. Moreover, the gel containing 2.5% Carbopol 974P combined with 1% HPMC showed good mucoadhesion properties and sustained drug release (Chen et al., 2017).

Pignatello et al. prepared a hydrogel formulation of lidocaine hydrochloride with chitosan glutamate. Optimum hydrogel viscosity and rheological properties were achieved by incorporation of glycerin in the formulation. Local anesthetic activity of this gel was superior as compared to a commercial product, Xylocaine® gel at the same drug concentration (Pignatello et al., 2009).

In conclusion, hydrogel and nanogel formulations generally have shown promising advantages for topical /transdermal and trans-mucosal routes of administration. The nanoparticles suspension or nanoemulsion within the gel matrix showed significant enhancement of drugs by topical and transdermal drug delivery. Proposed permeation enhancement is speculated to be as a result of increasing the surface area based on decreasing particle size. The higher solubility which consequently increases the thermodynamic activity of the drug in the formulation, which provides enhanced permeability across skin. Furthermore, adding penetration enhancers may augment the penetration via altering the skin barrier. On the other hand, hydrogel alone showed attractive

results as a suitable vehicle for delivering several drugs via buccal mucosa in a rapid and controlled manner to the systemic circulation.

The general objective of this dissertation research was to develop and evaluate nanoparticle hydrogel with various drugs such as acyclovir, resveratrol, and midazolam to enhance the drug delivery of these agents and subsequently improve the overall bioavailability at intended sites of application. In addition, the therapeutic application of siRNA in a nano-platform for the treatment of melanoma cell lines has been explored.

This dissertation is written and organized into seven chapters. In chapter 1, a brief review of nanogel and hydrogel application in topical/transdermal and trans-mucosal routes of administrations has been presented. The chapter includes a description of the potential of hydrogel and nanogel for enhanced drug delivery. Also, it encompasses description of various barriers to permeation across skin and buccal mucosa, penetration pathways and enhancing methods.

Chapter 2 presents descriptive literature review about progress on gene delivery particularly siRNA delivery in nanoparticulate delivery systems for skin application. The chapter provides details on recent research on topical siRNA delivery utilizing various nanoparticles as non-viral carrier along with challenges, possible outcomes and enhancing techniques for topical applications.

Chapter 3 presents research on developing and investigating siRNA- polyethyleneimine (PEI) polyplex nanoparticles with varied molecular weights of PEI (low, moderate and high). The research data on polyplex formation optimization at different N/P ratios (gel retardation assay), cytotoxicity, and cellular uptake on B16BL6 melanoma cell line are presented. This chapter

emphasizes relationship between molecular weights of PEI and siRNA delivery in respect to efficacy and safety at a cellular level.

Chapter 4 presents research on utilizing nanogel formulation for enhancing the topical and transdermal delivery of acyclovir. Since the topical and transdermal efficacy of acyclovir is hampered by poor skin penetration, the goal of the study was to enhance the percutaneous permeation of acyclovir nanoparticles based gel formulation with and without penetration enhancers.

Chapter 5 presents research on developing and evaluating a novel buccal midazolam gel formulation for seizures managements in small animals. The efficacy of the buccal gel formulation in comparison to an intravenous solution was evaluated in a pharmacokinetics study in healthy dogs.

Chapter 6 presents research on developing resveratrol as nanoparticle based gel formulation. Resveratrol, a natural polyphenol found in grapes and berries, has strong anti-oxidant properties and is believed to be beneficial in treating many disease conditions including skin cancer. This compound is highly insoluble in many vehicles and poses a problem in topical product development. This emphasizes the necessity for developing a suitable formulation of resveratrol with enhanced transdermal drug delivery.

1.4 References:

Barkat, Harshita, Ahmad, Ali, Singh, Pottoo, Ahmad. (2017). Nanosuspension-Based Aloe vera Gel of Silver Sulfadiazine with Improved Wound Healing Activity. *AAPS PharmSciTech*. doi:10.1208/s12249-017-0817-y

Baroli. (2010). Penetration of nanoparticles and nanomaterials in the skin: fiction or reality? J. Pharm. Sci., *99*(1), 21-50.

Batheja, Sheihet, Kohn, Singer, & Michniak-Kohn. (2011). Topical drug delivery by a polymeric nanosphere gel: Formulation optimization and in vitro and in vivo skin distribution studies. *J Control Release, 149*(2), 159-167. doi:10.1016/j.jconrel.2010.10.005

Boateng, Okeke, & Khan. (2015). Polysaccharide Based Formulations for Mucosal Drug Delivery: A Review. *Curr Pharm Des, 21*(33), 4798-4821.

Bos, & Meinardi. (2000). The 500 Dalton rule for the skin penetration of chemical compounds and drugs. *Exp Dermatol, 9*(3), 165-169.

Bouwstra, & Honeywell-Nguyen. (2002). Skin structure and mode of action of vesicles. *Adv. Drug Deliv. Rev., 54*, S41-S55.

Brown, Traynor, Martin, & Akomeah. (2008). Transdermal drug delivery systems: skin perturbation devices. *Drug Delivery Systems*, 119-139.

Caon, Jin, Simoes, Norton, & Nicolazzo. (2015). Enhancing the buccal mucosal delivery of peptide and protein therapeutics. *Pharm Res, 32*(1), 1-21. doi:10.1007/s11095-014-1485-1

Chavhan, Petkar, & Sawant. (2011). Nanosuspensions in drug delivery: recent advances, patent scenarios, and commercialization aspects. *Crit Rev Ther Drug Carrier Syst, 28*(5).

Chen, Yan, Yu, & Wang. (2017). Formulation and In Vitro Release Kinetics of Mucoadhesive Blend Gels Containing Matrine for Buccal Administration. *AAPS PharmSciTech*. doi:10.1208/s12249-017-0853-7

Desai, Patlolla, & Singh. (2010). Interaction of nanoparticles and cell-penetrating peptides with skin for transdermal drug delivery. *Mol. Membr. Biol., 27*(7), 247-259.

El-Nahas, Fakhry, & El-Ghamry. (2011). Effect of various penetration enhancers concentrations on diclafenac sodium release from cellulose acetate phthalate polymeric film. *Asian J. Pharm., 5*(1), 33.

Geusens, Strobbe, Bracke, Dynoodt, Sanders, Van Gele, & Lambert. (2011). Lipid-mediated gene delivery to the skin. *Eur J Pharm Sci, 43*(4), 199-211. doi:10.1016/j.ejps.2011.04.003

Gilhotra, Ikram, Srivastava, & Gilhotra. (2014). A clinical perspective on mucoadhesive buccal drug delivery systems. *J Biomed Res, 28*(2), 81-97. doi:10.7555/JBR.27.20120136

Godin, & Touitou. (2003). Ethosomes: new prospects in transdermal delivery. *Crit Rev Ther Drug Carrier Syst, 20*(1), 63-102.

Gupta, Vermani, & Garg. (2002). Hydrogels: from controlled release to pH-responsive drug delivery. *Drug discovery today, 7*(10), 569-579.

Hadgraft. (2001). Modulation of the barrier function of the skin. *Skin Pharmacol Appl Skin Physiol, 14 Suppl 1,* 72-81. doi:56393

Harris, & Robinson. (1992). Drug delivery via the mucous membranes of the oral cavity. *J Pharm Sci, 81*(1), 1-10.

Harwansh, Mukherjee, Bahadur, & Biswas. (2015). Enhanced permeability of ferulic acid loaded nanoemulsion based gel through skin against UVA mediated oxidative stress. *Life Sci, 141*, 202-211. doi:10.1016/j.lfs.2015.10.001

Hearnden, Sankar, Hull, Juras, Greenberg, Kerr, Thornhill. (2012). New developments and opportunities in oral mucosal drug delivery for local and systemic disease. *Adv Drug Deliv Rev, 64*(1), 16-28. doi:10.1016/j.addr.2011.02.008

Jug, Hafner, Lovric, Kregar, Pepic, Vanic, Filipovic-Grcic. (2017). An overview of in vitro dissolution/release methods for novel mucosal drug delivery systems. *J Pharm Biomed Anal*. doi:10.1016/j.jpba.2017.06.072

Junyaprasert, & Morakul. (2015). Nanocrystals for enhancement of oral bioavailability of poorly water-soluble drugs. *Asian J. Pharm., 10*(1), 13-23.

Kanikkannan, Kandimalla, Lamba, & Singh. (2000). Structure-activity relationship of chemical penetration enhancers in transdermal drug delivery. *Curr Med Chem, 7*(6), 593-608.

Karavana, Guneri, & Ertan. (2009). Benzydamine hydrochloride buccal bioadhesive gels designed for oral ulcers: preparation, rheological, textural, mucoadhesive and release properties. *Pharm Dev Technol, 14*(6), 623-631. doi:10.3109/10837450902882351

Khairnar, & Sayyad. (2010). Development of buccal drug delivery system based on mucoadhesive polymers. *International Journal of Pharm Tech Research, 2*(1), 719-735.

Kobierski, Ofori-Kwakye, Muller, & Keck. (2009). Resveratrol nanosuspensions for dermal application--production, characterization, and physical stability. *Pharmazie, 64*(11), 741-747.

Kumar, & Philip. (2007). Modified transdermal technologies: Breaking the barriers of drug permeation via the skin. *Trop J Pharm Res., 6*(1), 633-644.

Laffleur. (2014). Mucoadhesive polymers for buccal drug delivery. *Drug Dev Ind Pharm, 40*(5), 591-598. doi:10.3109/03639045.2014.892959

Li, Yu, Faraji Dana, Li, Lee, & Kang. (2013). Novel engineered systems for oral, mucosal and transdermal drug delivery. *J Drug Target, 21*(7), 611-629. doi:10.3109/1061186X.2013.805335

Liversidge, & Cundy. (1995). Particle size reduction for improvement of oral bioavailability of hydrophobic drugs: I. Absolute oral bioavailability of nanocrystalline danazol in beagle dogs. *Int. J. Pharm., 125*(1), 91-97.

Loftsson, & Brewster. (2010). Pharmaceutical applications of cyclodextrins: basic science and product development. *J Pharm Pharmacol, 62*(11), 1607-1621. doi:10.1111/j.2042-7158.2010.01030.x

McIntyre, Robertson, Norris, Appleton, Whitehouse, Phillips, Choonara. (2005). Safety and efficacy of buccal midazolam versus rectal diazepam for emergency treatment of seizures in children: a randomised controlled trial. *Lancet, 366*(9481), 205-210. doi:10.1016/S0140-6736(05)66909-7

Menon. (2002). New insights into skin structure: scratching the surface. *Adv. Drug Deliv. Rev., 54*, S3-S17.

Moghimi, Williams, & Barry. (1996). A lamellar matrix model for stratum corneum intercellular lipids. II. Effect of geometry of the stratum corneum on permeation of model drugs 5-

fluorouracil and oestradiol. *Int. J. Pharm.*, 131(2),117-129. doi:10.1016/0378-5173(95)04307-1.

Montero-Padilla, Velaga, & Morales. (2017). Buccal Dosage Forms: General Considerations for Pediatric Patients. *AAPS PharmSciTech, 18*(2), 273-282. doi:10.1208/s12249-016-0567-2

Morales, & McConville. (2014). Novel strategies for the buccal delivery of macromolecules. *Drug Dev Ind Pharm, 40*(5), 579-590. doi:10.3109/03639045.2014.892960

Moser, Kriwet, Naik, Kalia, & Guy. (2001). Passive skin penetration enhancement and its quantification in vitro. *Eur. J. Pharm. Biopharm., 52*(2), 103-112.

Mou, Chen, Wan, Xu, & Yang. (2011). Potent dried drug nanosuspensions for oral bioavailability enhancement of poorly soluble drugs with pH-dependent solubility. *Int J Pharm, 413*(1-2), 237-244. doi:10.1016/j.ijpharm.2011.04.034

Nicolazzo, Reed, & Finnin. (2005). Buccal penetration enhancers--how do they really work? *J Control Release, 105*(1-2), 1-15. doi:10.1016/j.jconrel.2005.01.024

Nielsen, & Rassing. (2000). TR146 cells grown on filters as a model of human buccal epithelium: V. Enzyme activity of the TR146 cell culture model, human buccal epithelium and porcine buccal epithelium, and permeability of leu-enkephalin. *Int. J. Pharm., 200*(2), 261-270.

Papakostas, Rancan, Sterry, Blume-Peytavi, & Vogt. (2011). Nanoparticles in dermatology. *Arch Dermatol Res., 303*(8), 533.

Patel, Liu, & Brown. (2011). Advances in oral transmucosal drug delivery. *J Control Release, 153*(2), 106-116. doi:10.1016/j.jconrel.2011.01.027

Pegoraro, MacNeil, & Battaglia. (2012). Transdermal drug delivery: from micro to nano. *Nanoscale, 4*(6), 1881-1894. doi:10.1039/c2nr11606e

Phatak Atul, & Chaudhari Praveen. (2012). Development and evaluation of nanogel as a carrier for transdermal delivery of aceclofenac. *Asian J Pharm Tech, 2*(4), 125-132.

Pignatello, Basile, & Puglisi. (2009). Chitosan glutamate hydrogels with local anesthetic activity for buccal application. *Drug Deliv, 16*(3), 176-181. doi:10.1080/10717540902861267

Poonia, Kharb, Lather, & Pandita. (2016). Nanostructured lipid carriers: versatile oral delivery vehicle. *Future Sci OA, 2*(3), FSO135. doi:10.4155/fsoa-2016-0030

Prakash, & Thiagarajan. (2012). Transdermal drug delivery systems influencing factors, study methods and therapeutic applications. *Int. J. Pharm., 2*(2), 366-374.

Prow, Grice, Lin, Faye, Butler, Becker, Soyer. (2011). Nanoparticles and microparticles for skin drug delivery. *Adv. Drug Deliv. Rev., 63*(6), 470-491.

Rathbone, Drummond, & Tucker. (1994). The oral cavity as a site for systemic drug delivery. *Adv. Drug Deliv. Rev., 13*(1-2), 1-22.

Rehman, Hamid Akash, Akhtar, Tariq, Mahmood, & Ibrahim. (2016). Delivery of Therapeutic Proteins: Challenges and Strategies. *Curr Drug Targets, 17*(10), 1172-1188.

Sagiri, Behera, Rafanan, Bhattacharya, Pal, Banerjee, & Rousseau. (2014). Organogels as matrices for controlled drug delivery: a review on the current state. *Soft Materials, 12*(1), 47-72.

Salamat-Miller, Chittchang, & Johnston. (2005). The use of mucoadhesive polymers in buccal drug delivery. *Adv. Drug Deliv. Rev., 57*(11), 1666-1691.

Salatin, Barar, Barzegar-Jalali, Adibkia, Milani, & Jelvehgari. (2016). Hydrogel nanoparticles and nanocomposites for nasal drug/vaccine delivery. *Arch. Pharm. Res., 39*(9), 1181-1192.

Satheesh Madhav, Semwal, Semwal, & Semwal. (2012). Recent trends in oral transmucosal drug delivery systems: an emphasis on the soft palatal route. *Expert Opin Drug Deliv, 9*(6), 629-647. doi:10.1517/17425247.2012.679260

Sattar, Sayed, & Lane. (2014). Oral transmucosal drug delivery--current status and future prospects. *Int J Pharm, 471*(1-2), 498-506. doi:10.1016/j.ijpharm.2014.05.043

Senel, & Hincal. (2001). Drug permeation enhancement via buccal route: possibilities and limitations. *J Control Release, 72*(1-3), 133-144.

Shah, Desai, Patel, & Singh. (2012). Skin permeating nanogel for the cutaneous co-delivery of two anti-inflammatory drugs. *Biomaterials, 33*(5), 1607-1617.

Sharma, Saini, & Rana. (2013). Transdermal drug delivery system: a review. *Int. j. pharm. biomed. res., 4*(1), 286-292.

Shen, Xu, Shen, Min, Li, Han, & Yuan. (2016). Nanogel for dermal application of the triterpenoids isolated from Ganoderma lucidum (GLT) for frostbite treatment. *Drug Deliv, 23*(2), 610-618. doi:10.3109/10717544.2014.929756

Shojaei. (1998). Buccal mucosa as a route for systemic drug delivery: a review. *J Pharm Pharm Sci, 1*(1), 15-30.

Singh, Anis, Banerjee, Pramanik, Bhattacharya, & Pal. (2014). Preparation and characterization of novel carbopol based bigels for topical delivery of metronidazole for the treatment of bacterial vaginosis. *Mater Sci Eng C Mater Biol Appl, 44*, 151-158. doi:10.1016/j.msec.2014.08.026

Sivaram, Rajitha, Maya, Jayakumar, & Sabitha. (2015). Nanogels for delivery, imaging and therapy. *Wiley Interdiscip Rev Nanomed Nanobiotechnol, 7*(4), 509-533. doi:10.1002/wnan.1328

Sohi, Ahuja, Ahmad, & Khar. (2010). Critical evaluation of permeation enhancers for oral mucosal drug delivery. *Drug Dev Ind Pharm, 36*(3), 254-282. doi:10.1080/03639040903117348

Teo, Shearwood, Ng, Lu, & Moochhala. (2005). In vitro and in vivo characterization of MEMS microneedles. *Biomed. Microdevices., 7*(1), 47-52.

Thwala, Preat, & Csaba. (2017). Emerging delivery platforms for mucosal administration of biopharmaceuticals: a critical update on nasal, pulmonary and oral routes. *Expert Opin Drug Deliv, 14*(1), 23-36. doi:10.1080/17425247.2016.1206074

Tokumura, Muraoka, & Machida. (2009). Improvement of oral bioavailability of flurbiprofen from flurbiprofen/β-cyclodextrin inclusion complex by action of cinnarizine. *Eur. J. Pharm. Biopharm., 73*(1), 202-204.

Valenzuela, & Simon. (2012). Nanoparticle delivery for transdermal HRT. *Maturitas, 73*(1), 74-80.

Vergote, Vervaet, Van Driessche, Hoste, De Smedt, Demeester, Remon. (2002). In vivo evaluation of matrix pellets containing nanocrystalline ketoprofen. *Int J Pharm, 240*(1-2), 79-84.

Wu, Liu, Zhu, Shan, & Huang. (2015). Modification Strategies of Lipid-Based Nanocarriers for Mucosal Drug Delivery. *Curr Pharm Des, 21*(36), 5198-5211.

2. Progress in Topical siRNA Delivery Approaches for Skin Disorders

2.1. Abstract

The topical application of therapeutic agent has shown promising efficacy in the treatment of skin disorders. The siRNA based therapies have been used for treatment of various disorders including skin diseases. The topical delivery of siRNA has opened new perspectives for the treatment of skin disorders. The application of siRNA based therapy has limitations due to the rapid degradation siRNA and its poor cellular uptake. Also, the stratum corneum, the top layer of skin is the major barrier for siRNA delivery. clearly, there is unmet need for efficient topical formulations that will deliver the siRNA to the site of action and to overcome the limitations associated with siRNA stability. The topical delivery of siRNA has been achieved using viral or non-viral methods, and the combination of non-viral methods with active permeation enhancement methods such as iontophoresis, sonophoresis or microneedles. These delivery approaches have been tested in a preclinical setup and in few cases the results have shown promise for clinical trials. This review provides an update on the advances in the non-viral delivery approaches for siRNA for skin disorders and use of various delivery approaches for efficient delivery at the disease site.

2.2 Background of gene delivery and diseases related to gene disorders

Therapeutic gene delivery can provide effective treatments for certain types of diseases or genetic disorders at a cellular level (Gandhi et al., 2014; Pauley et al., 2013). The gene delivery is achieved by introducing the nucleic acid components into cells to correct some defects in the gene expression. The aberrant gene expression leading to production of proteins responsible for disease progression can be knocked-down using small interfering ribonucleic acid (siRNA) delivery (Dana et al., 2017; Sioud, 2015). This approach has been used to treat certain diseases like cancer, human immunodeficiency virus (HIV), organs failure, and diabetes (Chakraborty et al., 2017; W. Wang et al., 2013). siRNA therapy can be divided in to two methods: 1) Delivery of oligonucleotide or a specific plasmid to retrieve or initiate the protein expression. 2) Delivery of siRNA or antisense oligonucleotides that interfere with gene function and elicit silencing (Xu et al., 2012). Nucleotide blockade and antisense technology focuses on the study of function of specific proteins and intracellular expression. The sequence of a nucleotide chain that contains the information for protein synthesis is called the sense sequence. The nucleotide chain that is complementary to the sense sequence is referred to as the antisense sequence. The siRNA drugs bind to the nucleotide sense sequence of specific mRNA molecules preventing synthesis of unwanted proteins and destroying the sense molecules in the process (Grimm, 2009; Haigh et al., 2014).

In the last decade, a lot of research work has been reported on siRNA's role on silencing gene expression in several diseases (Grimm, 2009). The gene expression inhibition opened treatment options for certain type of diseases that are induced by aberrant gene expression. There are some clinical trials reported on siRNA based delivery to various organs such as kidney, eye, liver and

skin. This review is mainly focused on the non-viral based siRNA delivery approaches in the treatment of various skin disorders.

The skin represents the most accessible organ for topical siRNA delivery. Gene defects cause some skin diseases such as pachyonychia cogenita (PC), alopecia areata, melanoma, rheumatoid arthritis (RA), wounds, and psoriasis. These defects can be corrected by delivering an appropriate siRNA to the target region in the skin. Many pre-clinical studies have utilized the skin as the route for siRNA delivery (Chong et al., 2013; Desai et al., 2013; B. Geusens et al., 2010; Hsu et al., 2011; Thanik et al., 2007). Unfortunately, the skin has extreme barrier property for siRNA delivery due to its horny layer, stratum corneum (Aljuffali et al., 2016; Hegde et al., 2014). This barrier must be overcome to achieve successful delivery for siRNA. Thus, there is a need for penetration enhancing carrier systems to deliver siRNA to the skin. First, the carrier system should be able to encapsulate or form a complex with siRNA; second, the carrier system should possess the ability to cross the stratum corneum to reach the target cells in the skin. Third, the carrier system should release siRNA into cytosol which means the siRNA escapes into cytoplasm before getting degraded by lysosomes (Vicentini et al., 2013b).

2.3 Methods of Gene Delivery:

A) Viral Gene Delivery

The viral gene delivery constitutes approximately 68% of clinical trials conducted in gene delivery till 2010 (Kotterman et al., 2014). The viral vector is composed of two main components, genome, and capsids. Viral genome is utilized by inserting the therapeutic gene to substitute original gene (Xu et al., 2012). The Viral vector has the ability to invade the cells and exert the transfection into

the cells such as adenovirus and retrovirus. Lentiviral vectors were effective carriers of shRNA-encoding gene cassettes to human skin. Efficient lentiviral gene delivery to psoriatic skin and therapeutic applicability of anti-TNF-α shRNAs in human skin was demonstrated (Jakobsen et al., 2009). Despite its therapeutic efficiency, it presents immunogenicity and oncogenicity. There was an incident of death of a 36-year-old woman with RA. She received two injections of relatively high doses 10^{13} DRP/ml into the synovial joint using recombinant adeno-associated virus (AAV) as carrier for gene therapy to RA. After the injection immediately she died, this event demonstrated the serious issues regarding the safety for viral vectors in gene therapy (Evans et al., 2008). Therefore, there is unmet need for development of non-viral gene delivery systems that will achieve the effective gene delivery and will also overcome the limitations associated with viral gene (Dana et al., 2017; Vicentini et al., 2013a),(Geusens et al., 2011; Keasberry et al., 2017).

B) Non-viral Gene Delivery

Non-viral gene delivery gains attention due to its safety and effectiveness over the traditional viral delivery (Aied et al., 2013). Non-viral delivery methods can be categorized into two methods: Chemical methods and physical methods. We have further classified chemical methods based on the nature of the carriers system such as1- Lipid based system, and 2- Polymer-based system. The physical methods of delivery are classified as 1-Ultrasound, 2- Electroporation, 3- Iontophoresis, and 4- Microneedles.

Lipid-based system has a significant effect on the cell membrane due to its similarity to the components of the membrane. Even though this system has a desirable efficiency, it has some drawbacks such as poor stability and reproducibility of the method (Vicentini et al., 2013a). The lipid-based system for siRNA delivery includes: liposomes and solid lipid nanoparticles (SLNs).

Polymer based systems have gained attention for nucleic acids due to ease of preparation, biocompatibility, stability, high drug loading, and protection of nucleotides from degradation (Vicentini et al., 2013a), (Chakraborty et al., 2017; Zhang et al., 2013). Polymer based systems are categorized into natural polymer based systems and synthetic polymer based systems. The primary objective of this article is to emphasize siRNA concept, function, the topical barriers for siRNA delivery and the most efficient delivery approaches to the skin.

2.4 siRNA Based Therapy for Skin Disorders:

A) Skin as a Site for siRNA Delivery for Topical Skin Disorders

The skin is the most accessible and convenient organ for RNAi delivery. The advantages include easy application, termination, sampling of exposed skin area, and higher patient compliance. The skin has been used in many researches as a route or target for the treatment of genetic diseases such as melanoma, dermatitis, psoriasis, pachyonychia congenita, alopecia areata, wound healing, RA. However, the normal skin is a barrier for topical RNAi delivery as for many other drugs. Therefore, the delivery of therapeutic genes has to overcome this obstacle as the first step (Chong et al., 2013), (Vicentini et al., 2013b).

Psoriasis is one of the most common skin disorders affecting about 2% of the world population (Ko et al., 2009). It shows significant growth in keratinocytes that makes plaque in addition to the inflammatory component of the disease. There is a difference in protein expression in plaque psoriasis; the normal keratinocytes are more susceptible to apoptosis process than psoriatic patient (Lerman et al., 2011). The etiology of psoriasis is still not fully understood. However, there are certain factors that play a role in its progression mostly environmental factors like, infection, smoking, lack of humidity, and stress (Prieto-Perez et al., 2013). Mild to moderate psoriasis can

be usually treated topically by corticosteroids. These have several local and systemic side effects such as hypertension, fluid retention, weight gain, stinging, itching, irritation, dryness, atrophy, and hypopigmentation. It is highly desirable to find drug molecules with fewer side effects. Therefore targeting the primary cause of the disease genetically is better way in the treatment of psoriasis (Shepherd et al., 2013). Psoriasis can be genetically treatable by targeting a specific molecule that is responsible for the up-regulation of the pro-inflammatory cytokines. Tumor necrosis factor alpha represent an important target in the treatment of psoriasis. It was reported that the reduction of Tumor necrosis factor-alpha resulted in the improvement in psoriatic lesion in an animal model (Vicentini et al., 2013a).

Allergic contact dermatitis (ACD) has significant immunogenic component. The two common types of ACD, Atopic dermatitis and contact dermatitis, are commonly treated with topical corticosteroids and calcineurin inhibitors (Ko et al., 2009). However, these treatments mainly focus on the immune response, and it is for short-term treatment. In recent years, there is a high focus on the reasons behind the disease in genetic perspective (Wollenberg et al., 2013). It has been observed that an elevated expression of CD86 in the allergic skin in both animal and human models. The suppression of CD86 expression leads to a reduction of the inflammation and the response of immune system. The CD86 expression can be reduced in dendritic cells via use of CD86 targeting siRNA. This target can be considered as a therapeutic target for the treatment of atopic dermatitis and hypersensitivity (Vicentini et al., 2013a).

Pachyonychia Congenita (PC) is an uncommon genetic disease that occurs due to mutations in one of the keratin genes. It is characterized by dystrophic, thickened nails, and painful palmoplantar keratoderma (Smith et al., 2008). It affects only 5 to 10 thousand people in the world (Goldberg et

al., 2013). PC patients complain from severe pain and an irregular function of the affected area, especially with one that is related to palmoplantar keratoderma (Leachman et al., 2008). It is classified into two subsets depending on the variation of the mutant gene. PC-1 is resulted in change in K6a gene; on the other hand, PC-2 is caused by a change in K6b gene (Smith et al., 2008). These changes due to a substitute of one nucleotide in keratin gene that is responsible of formation of keratin fiber (Rugg, 2008). The conventional treatment for PC is different from one subject to another; therefore, it is difficult to come up with one medication that works for all PC patients. For example, in case of a nail disorder in PC, the disease is commonly treated by surgical or mechanical approaches. Whereas in follicular hyperkeratosis, it is usually treated with topical or oral retinoid, these different approaches of therapy demonstrate the diverse treatments for the PC disease. However, the outcomes from the these different treatments of PC are beneficial but has certain limitations (Goldberg et al., 2013). Therefore, targeting the mutation of the genes that are responsible for development of PC is the main goal in treating and preventing the disease, which can be achieved by utilizing siRNA to silence this mutation. The conventional treatment of retinoid has some drawbacks in respect to the therapeutic outcomes. Retionoids exhibit side effects such as down-regulation of the epidermis cells, which could lead to forming blisters instead of the overgrowth of keratin cells. Therefore, most patients of PC are not compliance with the medications. In other hand, targeting the mutant gene that leads to the protein expression of the disease is a valuable choice via utilizing the silence effect of siRNA (McLean et al., 2011).

Alopecia Areata (AA) is a disease that is caused by autoimmune action in respect to a gene initiated defect. It infects the hair follicles and leads to loss of hair. It represents a common skin disorder affecting one in 1000 people; the lesion can be extended to whole area of scalp and may extend to

the other hairy parts of the body (Nakamura et al., 2008). The number of the people who suffer from the disease is approximately between six and seven million in the United States. It happens due to a disorder, which involves the immune, genetic and nervous systems (Hordinsky, 2013). There are different kinds of conventional treatment for AA, topical minoxidil, immunosuppressants, anthralin, and steroids; all show some desirable outcomes (Shapiro, 2013). In the other hand, Investigation of the scalp area around hair follicles demonstrates a leakage of CD4, T lymphocytes and CD8 in patients with AA. Th1 represents a target for siRNA therapy to achieve a silence effect on aberrant gene expression in the AA (Vicentini et al., 2013a).

Melanoma can occur at the junction between the epidermis and dermis layers (Tran et al., 2008). It is characterized by a pigment deposition in the affected area. The genetic mechanism behind this disease is still not fully understood. A mutation of specific proteins is involved in the melanoma (Tran et al., 2008). The proteins, BRAF V600E and protein kinase B, are found to be changed in melanoma. Targeting of the mutant gene by siRNA to suppress the melanoma growth has been attempted (Vicentini et al., 2013a).

B) The Concept and Mechanism of siRNA

The introduction of long double strands RNA (dsRNA) into the body leading to a silencing effect (Fig. 2.1). This process depends on the cleavage of dsRNA into short nucleotides which represents siRNA parts (Geusens et al., 2009),(Fattal et al., 2008). siRNA consist of 21-23 nucleotides duplex, this short double strand RNA has an ability to silence a gene expression for a particular protein. siRNA is denoted as RNA interference due to its mechanism of action. Its silence action for a specific gene expression is powerful and reversible which makes it an excellent candidate as a new therapeutic agent for genetic disorders (Vicentini et al., 2013b).

siRNA initiates a degradation process for specific target messenger RNA (mRNA) through binding to RNA induced silence complex (RISC) (Geusens et al., 2011). In the cytoplasm, once dsRNA is inserted, it is taken up by an enzyme dicer (a component of RNase III group of certain ribonucleases). This process is is responsible for converting the long chain of dsRNA into a shorter chain with 21-25 nucleotides to get involved in the transcription process with complementary sequence to perform its expression. However, in case of siRNA insertion into cells, it binds instantly to RNAi complementary pathway without being involved for more steps like dsRNA cell insertion (Fig. 2.1)(Xin et al., 2017).

When siRNA gets in the cytoplasm, it binds to RISC to disassemble the duplex into two strands. a) the passenger strand, this strand is divided and evicted by a specific protein in the RISC which is called Argonuate-2 (Ago-2). b) the guide strand which is responsible for the recognition of the sequence of the complementary mRNA inducing the silence of mRNA (Guzman-Villanueva et al., 2012). RISC plays a significant role in effect of siRNA double strands silence by containing four parts which are helicase, exonuclease, endonuclease and homology searching domain. Helicase is responsible to cleave duplex siRNA into two strands as described above (Fattal et al., 2008). Once the silence process occurs, the split parts are degraded then RISC is available to be incorporated to target another silence process for mRNA (Guzman-Villanueva et al., 2012).

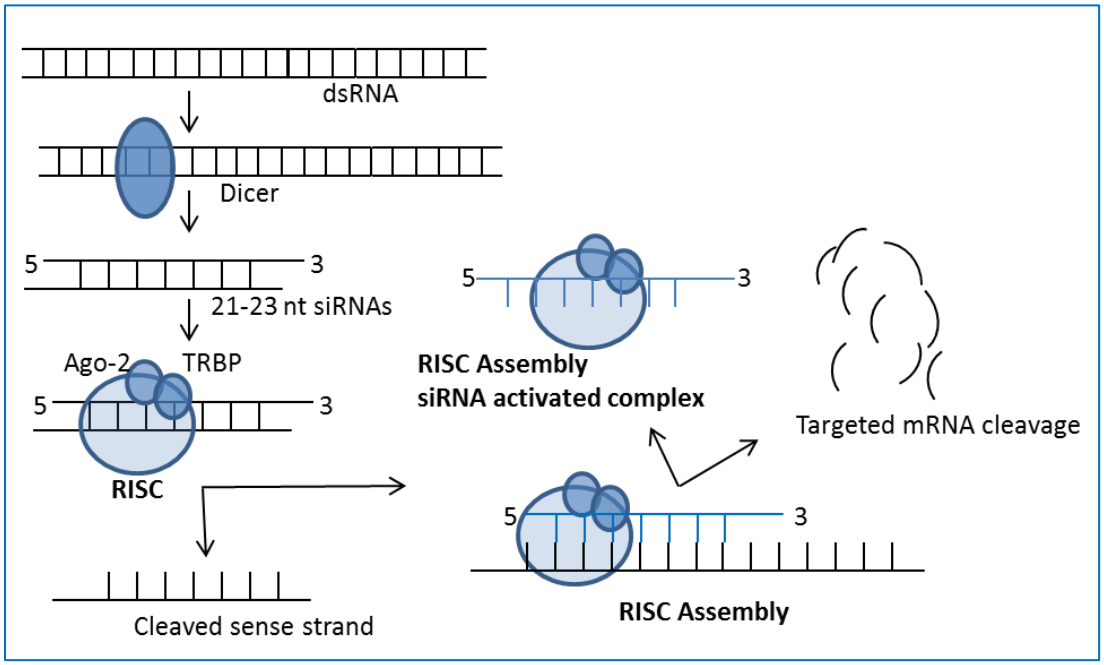

Figure 2.1 Mechanism of RNA interference. Different entry points for RNA-based (long dsRNA and synthetic siRNAs) siRNA drugs that enter and activate RNA-induced silencing complex (RISC) for gene silencing. Modified from Geusen et al. (Geusens et al., 2009).

Introduction of exogenous siRNA into cells is still vague. Even though, siRNA is permeated into the cells of invertebrate like Caenorhabditis Elegans. On the other hand, mammalian cells are not effectively permeable due to inability of naked siRNA to cross the cell membrane. The negative charge of siRNA and larger molecular weight make the siRNA impermeable across cells. The effectiveness of knock down of unmodified siRNA has been investigated in mammalian cell in vitro (cell culture), it showed no permeation of siRNA and action on the target genes (Fattal et al., 2008). However, the siRNA has to pass cell membrane and subsequently to the cytoplasm to exert its effect. The entry process into the cells occurs through certain pathways, which is diverse depending on the nature of the delivery system like, particle size, composition and the change of the cell membrane properties itself. Kaneda et al. reported the mechanism of introduction exogenous siRNA into cells; they explained the pathway of diffusion using a standard liposomal

transfection reagent which is undertaken by clathrin-mediated endocytosis in different cell lines (Kaneda et al., 2010). Once clathrin-coated vesicle has been formed and get inside the cells, the vesicle forms as endosome then later become as lysosome. Nevertheless, to deliver siRNA effectively it has to escape from the endosome before it gets mature and convert to lysosome by a lowering in PH which ends up degrading the cargo of siRNA. Kaneda et al. reported a new pathway to deliver siRNA into the cytoplasm that is independent from clathrin-mediated endocytosis. This pathway depends on lipid float mediated endocytosis, where the siRNA can be delivered to the cytoplasm with no demand for escape step from endosome (Kaneda et al., 2010).

C) siRNA Therapeutic Effects on Gene Expression

Targeting specific genes of proteins that initiate the causes of diseases is an excellent strategy. There are several diseases that can be treatable by silencing the gene expression of the causative disease. For example, the utilization of antisense oligonucleotide to suppress the genes that are responsible for hyperproliferation in keratinocytes in human cells through targeting Bcl-XL, siRNA has been applied in many cancer cells such as gastric adenocarcinoma (MGC-803), human hepatocellular carcinoma cells (HepG2) and human breast cancer cells (MCF-7). All of these cell lines have been targeted with Bcl-Xl siRNA and have shown an improvement in apoptotic action on the cells (Lerman et al., 2011).

In human keratinocytes, there is a receptor site called Insulin-like growth factor (IGF-1) that has important role in the regulation of cell viability with respect to transformation, differentiation, and apoptosis. The keratinocytes are very sensitive to its activation to play a role in the causes of certain skin disorders like psoriasis. The keratinocytes that are isolated from the psoriatic patient are more sensitive to IGF-1 activation than the keratinocytes in the normal people; it showed a

therapeutic effect on the reduction of the disease. siRNA was utilized in targeting IGF-1 receptor in addition to B-cell lymphoma extra-large (Bcl-xL) target which shows overexpression in case of psoriatic patient. It has shown efficiency in induction of apoptosis and an improvement on their sensitivity to UV radiation. On the other hand, it might be applicable in other skin disorders that cause hyperproliferation as therapeutic approach (Lerman et al., 2011). In case of PC disease, K16 gene is dominated for mutation in the disease, the receptor for this gene was targeted to inhibit the overexpression, and it showed a desirable outcome. In this study, a therapeutic siRNA was injected in the foot of the mouse and observed a significant improvement at the lesion site and the pain which reflects the effectiveness of siRNA in targeting K16 mutant in the PC disease (McLean et al., 2011).

In another study, the gene silencing efficacy of topically applied siRNA in a mouse model was reported. In this study, two genes mpka1 and lamin A/C were targeted to demonstrate an efficient delivery from a topical matrix-based siRNA, there was a high reduction in the expression of the these two genes in open wound in a mouse model (Thanik et al., 2007). In melanoma development, there is a common alteration in normal moles in the cells; it results from a mutation in B-Raf genes. Also, the melanoma cells in advanced level become metastatic and show aberrant genes (B-Raf ^{V600E}) leading to cellular proliferation and overgrowth of cancer cells. There is also an increased level of Akt3 as a result of a deficiency of PTEN phosphatase function. Increased Akt3 level induces abnormal regulation of the apoptotic process which acts as inhibitor for causing cancer cells. Therefore, reducing these levels of proteins that result from mutations in specific genes could be a valuable method to fight the progression of melanoma in either early stages or the metastasis of these cells to other parts of the body. Utilizing siRNA can be a useful tool to silence the

expression of these proteins via silencing the mutant genes, so V600E/B-Raf or Akt3 represent valuable targets in curing the progression of melanoma in skin (Tran et al., 2008).

2.5 siRNA Delivery Approaches in Skin:

A) Barriers for siRNA Delivery in Skin

siRNA delivery into skin has considerable barriers, which depend on the physicochemical properties of siRNA and skin structure (Blagbrough et al., 2012). The barriers can be classified into two main categories: extracellular barrier and intracellular barrier, the extracellular barrier starts from the application site on skin until reaches to the targeted cells (Fig.2.2).

The skin is composed of three distinct layers: epidermis, dermis and subcutaneous, each layer has different cells and structures consequently various functions. The upper part of the epidermis is stratum corneum (Geusens et al., 2011); the stratum corneum consists of lipids such as ceramides, cholesterol and free fatty acid. These lipids make a support structure for the cells and act as barrier either for microbial intrusion or drug permeation (Nasrollahi et al., 2012). Therefore, the stratum corneum is the primary barrier for siRNA delivery (Uchida et al., 2011). The epidermis cells are connected by Tight junctions (TJ); the TJ is responsible for transporting small hydrophilic molecules through paracellular pathway. Various proteins control this pathway: claudin, occludin, and zonula occludens proteins (Uchida et al., 2011).

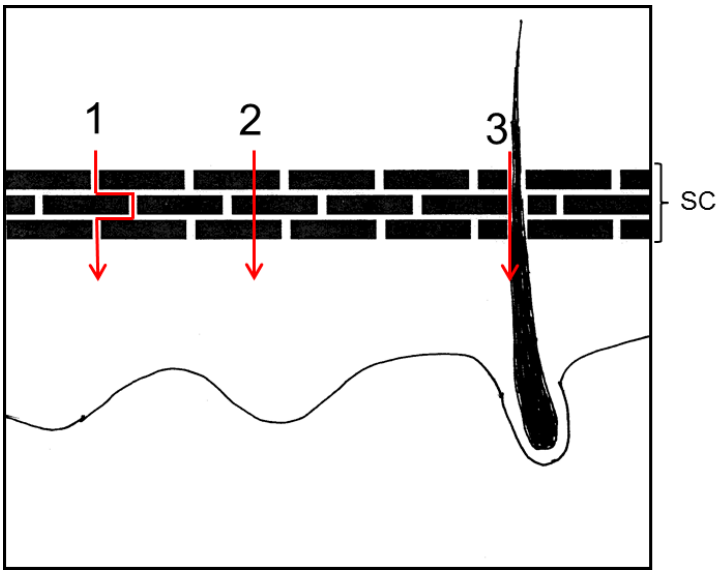

Figure 2.2 Routes of drug permeation across skin: (1) intercellular pathway, (2) transcellular pathway or (3) through the hair follicles. Modified from: Barry (Barry, 2001).

An entry of a foreign substance into skin layers is controlled by their size and a gradient, in addition, the physicochemical properties of a substance plays a role in the penetration of skin. In molecules prospective, small lipophilic (less than 500 D) and uncharged molecules are favorable for cutaneous penetration. However, siRNA is not applicable for these properties so; it encounters a difficulty in skin penetration to reach target cells and exert its action.

On the other hand, the intracellular barriers are extended from the cell membrane penetration until the siRNA exerts its effect on the cytoplasm as the following sequences: the entry of siRNA through cell membrane is considered as a barrier due the negative charge and the high molecular weight of siRNA. Even after a successful entry of siRNA by endocytosis, siRNA carrier has to protect siRNA from RNase degradation and to release siRNA from the endosome to the cytoplasm before the maturation of the endosome and the degradation by lysosome (Geusens et al., 2011),

(Ghonaim et al., 2010). Therefore, all these barrier have to be considered in order to design a delivery system for siRNA to overcome both extracellular and intracellular barriers in skin and get the desirable therapeutic effect (Blagbrough et al., 2012).

B) Topical siRNA Delivery Systems:

The topical delivery system on skin is non-invasive, easy to administer and reduced concentration of the drug to achieve the therapeutic value (Vicentini et al., 2013a). Topical delivery of small interference RNA represents an appealing site of application specifically to target a mutant gene locally and avoid the systemic exposure of siRNA to the whole body, which has consequences on the overall health and compliance regarding the off targeting and side effects (Thanik et al., 2007), (Vicentini et al., 2013b). The topical formulation should be able to protect the siRNA thereby achieving the delivery of siRNA to the desired site of action. The delivery systems such as liposome, polymeric nanoparticle, polymer–drug conjugate, dendrimer, oil nanoemulsion, mesoporous silica nanoparticle, and iron oxide nanoparticle have been studied (Fig. 2.3) (Keasberry et al., 2017). These systems are mainly used for delivery of small MW drugs, proteins, plasmids, and siRNA. The topical delivery of siRNA can be achieved with these delivery systems (Hu et al., 2012).

B.1. Lipid-based systems

The lipid-based system has been utilized to deliver siRNA via its incorporation in liposomes and solid lipid nanoparticles (S. Guo et al., 2014). The delivery of siRNA through these systems depends on certain factors like particle size, charge, lipid ratio and composition. In general, these

have some favorable features such as biocompatibility, low immune response, ease of application, safety, patient compliance and less cost (Geusens et al., 2011), (Guzman-Villanueva et al., 2012).

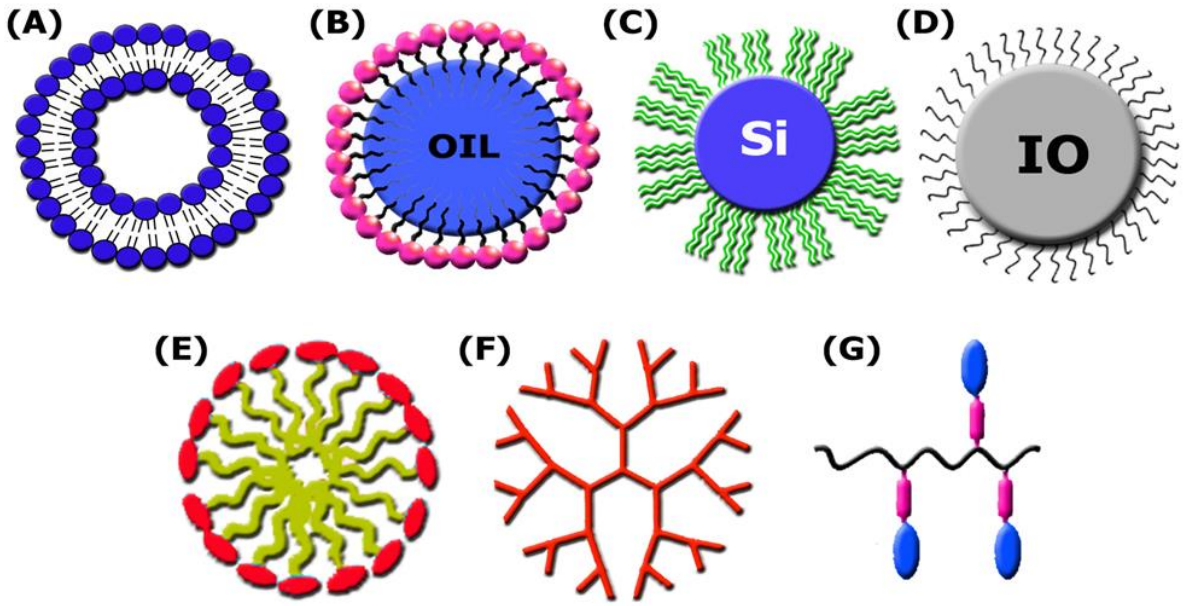

Figure 2.3 Schematic illustration of nanoscale carrier systems used for combinatorial drug delivery: (A) liposome, (B) oil nanoemulsion, (C) mesoporous silica nanoparticle, (D) iron oxide nanoparticle, (E) polymeric micelle, (F) dendrimer, and (G) polymer–drug conjugate. The combination of hydrophilic and/or hydrophobic therapeutic agents can be loaded in these nanoscale carrier systems.

Liposomes are composed of a phospholipid bilayer with hydrophilic head and lipophilic tail groups within the lipid structure, once expose to aqueous media, it forms an enclosed liposomal vesicles to protect the lipophilic material inside the carrier while exposing the hydrophilic head to aqueous medium (de Gier et al., 1968). Liposomal system has several advantages such as its capability to

entrap both hydrophilic and lipophilic materials, similarity to the composition of the cell membrane which improves its uptake into cells, biodegradability and safety (Geusens et al., 2011). In topical application on skin, liposome has been utilized due to its ability to act as reservoir in the stratum corneum (Fireman et al., 2011). Liposomes are widely used as in vitro transfection, but it is uncommon to be used in vivo even though it's safe and effective (Zhang et al., 2013). Cationic liposomes is very desirable for siRNA encapsulation due to the negative charge of siRNA, so there is an electrostatic interaction that has an ability to encapsulate and protect the siRNA from degradation in addition to its high transfection ability and low toxicity (Shegokar et al., 2011). siRNA liposomal delivery systems are mainly applied for systemic administration. However, the delivery of siRNA via traditional liposomes as carrier is limited for skin application. Due to the retardation of liposomes in the superficial layer of skin (stratum corneum), instead of penetration deeply into viable layers (B. Geusens et al., 2010). Nevertheless, there are some carrier systems utilizing liposomes in combination with lipid or physical methods, as it has been studied in cutaneous melanoma. A cationic liposome with a diameter of 50 nm showed an ability to incorporate, conserve and release siRNA into targeted cells on cutaneous melanoma (Tran et al., 2008). siRNA delivery was shown efficiency to silence the cells with a high level of Akt3 or ^{V600E}B-Raf after the application of ultrasound technique. Moreover, no sign of toxicity on targeted cells was observed when siRNA delivered to the melanoma cells by topical application (Tran et al., 2008).

Solid lipid nanoparticles (SLN) consist of four common components: the encapsulated therapeutic agent, emulsifier, solid lipid, and water. SLN's preparation depends on the incorporated therapeutic materials (S. Guo et al., 2013). SLNs are prepared using the liquid form of lipid in an

oil/water emulsion with the solid state of the lipid; the solid is composed of either two or more lipids. SLN consists of 0.1 to 30% w/w solid lipid in aqueous medium, the addition of surfactant is necessary to stabilize the formulation. The therapeutic agent is entrapped in the core of the SLNs, and the typical particle size of the system is ranged from 40 nm to 1 um (Fireman et al., 2011). SLNs have some significant advantages over the conventional lipid-based delivery system such as liposome in regard to the low toxicity and biodegradability (Shegokar et al., 2011). SLNs are considered as modification of cationic lipid formulation for siRNA delivery; it has been designed to overcome some problems that occur with cationic lipid-based system like, weak stability and toxicity in systemic delivery. SLNs have been surface modified to overcome the pharmacokinetic problems (Jeong et al., 2011; Xin et al., 2017). Modification of SLN-siRNA conjugated with PEG on the surface showed improved stability and reduced aggregation between the nanoparticles and consequently lead to increased delivery in systemic circulation and a reduction on the expression of GFP by 59% and VEGF by 54% (Jeong et al., 2011).

There are some examples utilizing SLN for the systemic delivery of siRNA. However, there are no reported studies about topical applications. For examples, in xenograft cancer model, siRNA incorporated lipid coated calcium nanoparticles were injected around the tumor and investigated for transfection efficiency (Shegokar et al., 2011). Also, the nanoparticles were surface modified with PEG and investigated for systemic delivery of siRNA.

B.2. Polymer based systems

In recent years, polymer-based delivery systems were investigated for gene therapy because of several advantages such as ease of preparation, biocompatibility and diverse properties (Gandhi et al., 2014). Also, they form complexes with siRNA depends on the electrostatic charge of the nucleic acid (negative charge) and a positive polymer charge, which improves the transfection efficiency (Kaczmarek et al., 2017; Vicentini et al., 2013a). However, the polymer based system has some disadvantages regarding toxicity due to its cationic charge and non-biodegradability. Therefore, the trend of utilizing polymer as a carrier for siRNA is increasing toward using biodegradable polymers like PLGA and chitosan polymers (Vicentini et al., 2013a). The polymer based systems are categorized into three classes: natural polymer, synthetic polymer, and inorganic polymer.

Chitosan is a natural polymer which has been extensively used for gene delivery (Ragelle et al., 2013). It possess several features like biodegradable, non-toxic, non-allergic and cationic charge that makes this polymer a favorable candidate in nucleic acid delivery (Acharya et al., 2017), here we focus on siRNA delivery with some examples utilizing chitosan as delivery system for different routes which is not specific for skin, however, it might be applicable for skin. The positive charge of chitosan due to the protonation of primary amines improves the encapsulation of siRNA into chitosan based on the negative charge of siRNA (Fig. 2.4). Also, the accessibility of chitosan for modification makes it an excellent candidate for developing a desirable carrier system for siRNA (Singha et al., 2011), such as PEGylated chitosan siRNA complex which improves the stability and extends the half-life of chitosan siRNA complex in blood stream for enhanced the systemic delivery of siRNA in the body (Nikitenko et al., 2013). There are several studies which utilized

chitosan in siRNA delivery. Chitosan aspartate, Chitosan glutamate, Chitosan Acetate and Chitosan hydrochloride were tested in vitro for siRNA delivery in EGFP expressing in HeLa cell. The weight ratio between siRNA and Chitosan complexes showed a positive effect on the transfection efficiency, but there was no significant impact of MW and the nature of the salts on the transfection efficiency. The highest transfection efficiency was observed in a weight ratio of 32 with a low molecular weight chitosan. In another report, hydroxy benzotriazole salt chitosan siRNA complex showed a gene silencing efficiency around 60% of EGFP in human carcinoma cell line as maximum transfection efficiency with a low molecular weight (20 KDa) at a weight ratio of 80. Another salt form of chitosan thiamine pyrophosphate showed a silence efficiency of 60-70% on EGFP gene due to the improved solubility and complexion with siRNA (Singha et al., 2011). Howard et al. (Howard et al., 2006) investigated the silence efficiency of anti-TNF-alpha siRNA chitosan complex in mice by injecting the complex in peritoneal area. It showed a reduction in the target anti-inflammatory gene expression. The reduction in the inflammation was approximately 44% (Nikitenko et al., 2013).

Cyclodextrin (CD) is cyclic (alpha-1, 4) linked oligosaccharide of beta-D-glucopyranose (Chaturvedi et al., 2011). CD has a cage-like structure, inside the cage is hydrophobic (due to oxygen bridges) and outside the cage is hydrophilic (due to hydroxyl groups). CD prevents the degradation of siRNA from nuclease in the body. One advantage of CD is that it has a low or no immune response when it delivers siRNA into the body. There are certain examples of CD applications in siRNA delivery. In one study, CD has been investigated for forming a complex with siRNA and a ligand for targeting (transferrin), this complex was designed to target oncogene in Ewing sarcoma cells, and it showed a reduction in the gene expression (Nikitenko et al., 2013).

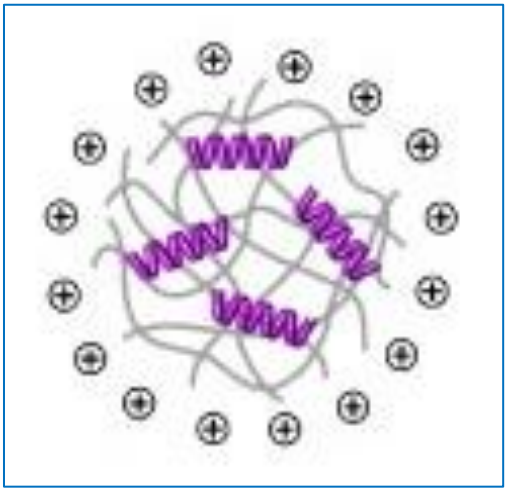

Figure 2.4 Chitosan-siRNA based nanoparticles. Modified from Mao et al. (Mao et al., 2010)

Another example of CD utilization in siRNA delivery is through targeting RRM2 gene in order to reduce the mRNA expression which represents a key faster for promoting a tumor growth by acting as an enzyme to catalyze the conversion of ribonucleotides into deoxyribonucleotides. In this study, it has been noticed that an inhibition on the conversion into deoxyribonucleotides leads to antitumor effects.The delivery system is named by anti-RRM2-siRNA nanoparticles, it showed a high reduction in RRM2 protein level as a result of reduction of mRNA level for RRM2 gene (Nikitenko et al., 2013). Despite all previous advantages of CD as delivery system for siRNA, there is an issue regarding the incapability of endosomal escape at intracellular site which possess some difficulties to develop an efficient siRNA delivery system. However, in one report, it was demonstrated that this issue can be overcome by modifying the CD with imidazole group, the imidazole group acts as a buffer in the endosomal vesicle and it showed improved siRNA delivery as compared with unmodified one (Singha et al., 2011). All previous studies and examples of this natural polymer as delivery system for siRNA is meant for systemic delivery. However, CDs are

not usually employed in the delivery of siRNA for skin.

Poly (Lactide-co-glycolic acid) [PLGA] is a safe polymer with biodegradable and biocompatible properties. PLGA is water insoluble, and it has been widely used for drug delivery in the form of micro and nanoparticles (Pandita et al., 2014). PLGA polymer in siRNA delivery is useful because it protects siRNA from degradation, and it has an ability to accommodate a high load of siRNA. Also, it can be modified through its surface to improve its biological properties (Zhang et al., 2013). PLGA has been utilized in vivo applications in gene delivery. At cellular level, the PLGA readily penetrates and facilitates the entry of siRNA into cells by endocytosis and release the payload quickly to the cytoplasm before lysosome degrades siRNA (Patil et al., 2009). In addition, PLGA polymer as microspheres offers protection for siRNA against enzymatic degradation, sustain release over time and increase the transfection efficiency by improving the cellular uptake. PLGA microspheres polymer were utilized to deliver siRNA into the articular tissue in a purpose to reduce the inflammation of joints by targeting TNF-a, which is the responsible for inflammation. It showed an effective inhibition of TNF-α in vitro in murine monocytic cell line (J774) (Presumey et al., 2012).

From previous characterizations, PLGA is considered as an appropriate carrier for siRNA, however, it has been observed in one report that the use of PLGA alone with siRNA has limitations on encapsulation efficiency, drug release and transfection efficiency. These issues may specific to the nature of siRNA in respect to anionic charge and the polarity (Uchida et al., 2011). PEI was incorporated with PLGA to improve the encapsulation efficiency and release of siRNA in the polymer as nanoparticles. In this study, PEI has imported a cationic charge to the PLGA polymer which improves retaining siRNA in the polymer and also helps to increase the release of the siRNA

into the cytoplasm via increasing the penetration of the water into the polymer matrix (Patil et al., 2009).

B.3. Nanoparticles conjugates

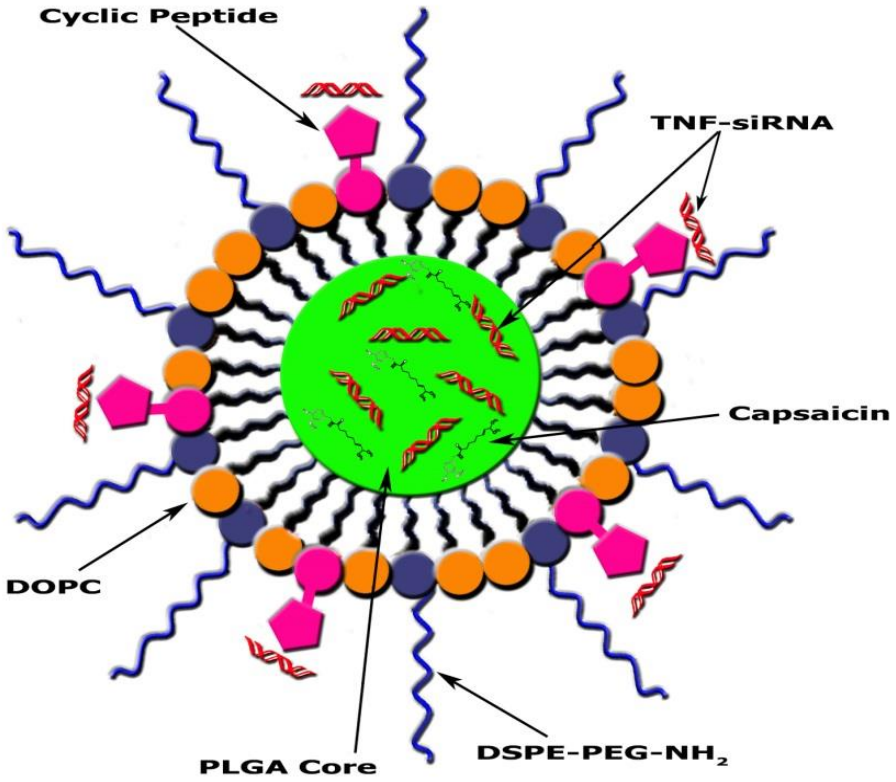

Figure 2.5 Formulation of CyLiPn. The CyLiPn comprises a hydrophobic PLGA core, a hydrophilic PEG shell and a lipid monolayer consisting of DOPC and a new cationic cyclic-head lipid at the interface of the hydrophobic core and hydrophilic shell. Modified from Desai et al. (Desai et al., 2013).

A nanocarrier that combines a biodegradable lipid-polymer system (noted as CyLiPn) was designed to contain a hybrid nanoparticle of hydrophobic PLGA in the core and a combination of

hydrophilic PEG in the shell with lipid layer consists of cyclic lipid and 1,2- dioleoyl-sn-glycero-3-phosphocholine (DOPC) .

This hybrid structure of 163 ± 9 nm was designed to incorporate a synergistic combination of Capsaicin (Cap) and siRNA to target and treat the inflammation (Fig. 2.5). Cap was retained in the core part, which represents the hydrophobic moiety; siRNA was incorporated in the shell to bind to the cationic lipid layer. The central idea for the combination between the Cap and siRNA was to attain the synergistic effect to reduce the inflammation.

Marepally et al. developed a novel fusogenic nucleic acid-based lipid particle (F-NALP) system containing two therapeutic nucleic acids, anti-STAT3 siRNA and anti-TNF-α siRNA (Marepally et al., 2014). A cationic amphiphilic lipid with oleyl chains was used to formulate the nanoparticles. F-NALPs co-loaded with anti-STAT3 siRNA and anti-TNF-α siRNA exhibited significant reduction in the expression of STAT3 and TNF-α mRNAs. The F-NALP formulation was superior anti-psoriatic activity in comparison with marketed Topgraf® formulation in an imiquimod induced psoriatic-like plaque model (Marepally et al., 2014).

Spherical nucleic acid nanoparticles conjugates (SNA-NC) system was developed to deliver nucleic acid for many different cell lines with 100% high efficiency (Rink et al., 2013; Rouge et al., 2014). The high efficiency was achieved due to the resistance toward nuclease degradation and the reduced immunogenicity. Also, it demonstrates no cellular toxicity at the optimum concentrations for transfection efficiency.

The spherical nucleic acid nanoparticle conjugates (SNA-NCs) with gold cores which was surrounded by a dense shell of highly oriented. The system covalently immobilized siRNA and

freely penetrate keratinocytes in vitro, mouse skin, and human epidermis within hours after application. These structures can be delivered in a moisturizer or phosphate-buffered saline, and do not require skin barrier disruption or transfection agents, such as liposomes, peptides, or viruses. This system was used for siRNA delivery to skin cells using spherical nucleic acid gold nanoparticles conjugates to target specific genes (EGFR in hKC) that are responsible for skin disorders (Fig. 2.6). EGFR in hKC cell line, SNA-NCs has been tested for 1- the silence efficiency of siRNA to the target gene. 2- The toxicity of this system on the cells. Moreover, this delivery system has been tested in human skin that simulates the in vivo condition. It showed reduction on EGFR expression by 75% when compared with control. Also, it showed no sign of toxicity under a light microscope examination of the treated skin (Zheng et al., 2012).

B.4. Miscellaneous siRNA delivery systems

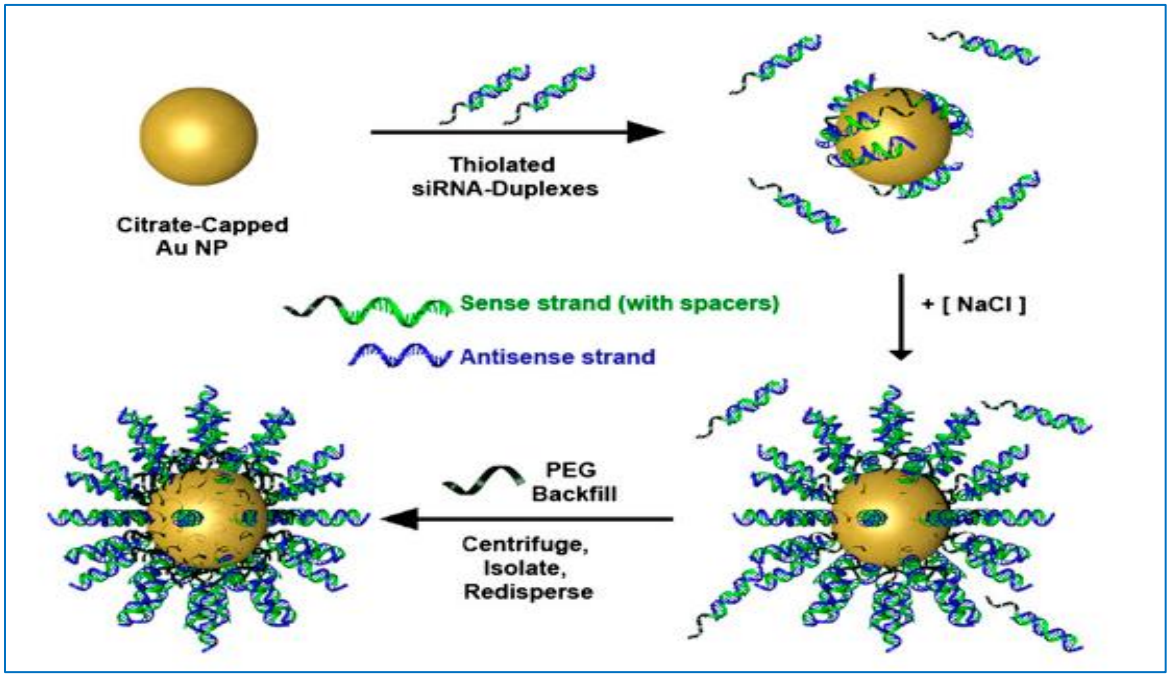

Figure 2.6 Synthesis scheme of siRNA-based SNA-NC. Hybridized siRNA duplexes were mixed with citrate stabilized gold colloid solution and conjugated via thiol gold chemistry. The salt was added to screen repulsive charges and formulate the densely functionalized nanoconjugates. The tested SNA-NCs has 13 nM core with densely arrayed approximately 30 siRNAs. Reproduced from Zheng et al. (Zheng et al., 2012).

Dendrimers are unique carriers for drug delivery based on several advantages such as the unique chemical structure and their capability to be modified as suitable drug carrier (Wu et al., 2013). Dendrimers consist of a core in the center of the whole structure which is connected into highly defined branched shapes. The terminal parts of the branched structures composed of reactive groups meant for conjunction of drug moieties (Biswas et al., 2013). In regard to siRNA delivery, diverse types of dendrimers were developed such as poly (amidoamine)dendrimers, poly(propylene imine) dendrimers, carbosilane dendrimers poly(L-lysine) dendrimers. All these dendrimers were utilized in siRNA delivery, as they give promising results. Poly (amidoamine) dendrimers (PAMAM), has a core of Ammonia or ethylenediamine: It interacts with siRNA by electrostatic interaction which attains desirable characters in improving the cellular uptake of siRNA. In addition, it promotes the release of siRNA from the endosome (Wu et al., 2013).

A cationic star-shaped polymer consisting of β-cyclodextrin (β-CD) core and poly(amidoamine) dendron arms (β-CD-[D3]7) was used as the gene carrier of MMP9-siRNA to reduce MMP9 expression for enhanced diabetic wound healing. The β-CD-(D3)7/MMP-9-siRNA complexes were taken up by fibroblast cells, resulting in the down-regulation of MMP-9 gene expression. Would healing experiments in diabetic rats revealed that the treatment by β-CD-(D3)7/MMP-9-siRNA complexes enhanced wound closure in diabetic rats on day-7 post-wounding (Li et al., 2014).

Poly-L-lysine (PLL) is one of the oldest polycation polymers that have been used in gene delivery (J. Guo et al., 2012). PLL showed effectiveness by itself, however; it was more efficient when it's incorporated into mesoporous silica nanoparticles to form a carrier for siRNA delivery. This provides protection against enzymatic degradation and in binding to gene targets. Hartono et al. developed and tested this carrier system for siRNA delivery to mini brain-related kinase and polo-like kinase in osteosarcoma cancer cells. This system has improved efficiency for siRNA delivery to target cancer cells. In addition, it showed a little toxicity up to 100 ug/ml and a high biocompatibility (Hartono et al., 2012).

PEI is commonly used polymer for incorporation of siRNA to be delivered to the targeted cells; it illustrates a high efficiency in transfection toward the gene target. PEI exists in two forms branched and linear; both have an impact on toxicity and effectiveness. The branched PEI has a high molecular weight and is more desirable for achieving high transfection efficiency (Riley et al., 2017; J. Wang et al., 2010), the high charge density which forms strong bonds with siRNA and keeps it safe from the degradation in the systemic circulation. However, it demonstrates more toxicity for exposed cells. This raises concerns for its use in the drug delivery application. On the other hand, linear PEI is less toxic toward the cell viability but it is less efficient in siRNA delivery to the targeted genes (Nikitenko et al., 2013). PEI was used as a carrier for targeting the siRNA to NMDA-R2B pain receptors to reduce the expression of protein that is responsible for inducing the pain. Moreover, it was utilized in targeting tumor receptors (cerbB2/neu (HER-2), it showed a high inhibition of tumor growth while the siRNA alone it did not show the same effect (J. Wang et al., 2010). Also, PEI was investigated in combination with siRNA-PEG conjugate, and it demonstrates 3.5-folders higher efficiency than the control one (no PEG). However, certain issues like non-

biodegradability and toxicity for body limit its uses as siRNA carrier (Jeong et al., 2011).

CPP is composed commonly of a short sequence of amino acids (no more than 30); also it has some desirable characters such as water solubility, cationic or amphiphilic in nature which is suitable to cross the cell membrane along with relatively large molecules (e.g. siRNA) at low concentration with efficient response and minimum toxicity. There are several CPPs in the market such as TAT (Trans-Activating Transcriptional activator), Penetratin, PEP-1, Trnasportan, and polyargini, these peptides were reported to be effective in delivering large therapeutic molecules in different cell lines. Several studies utilized CPP as delivery system in topical application of siRNA. TAT was used as CPP in siRNA delivery to skin in the form of nanoparticles. This study proposes that nanoparticles of >70 nm can penetrate via hair follicles (up to 200 nm in size), and those below 70 nm can pass through paracellular route of epidermis (Nasrollahi et al., 2012). In another study, a combination of TAT and AT1002 peptides were utilized to silence the effects of Rel-A in a mouse model with atopic dermatitis (Uchida et al., 2011). The nanoparticles penetrated via paracellular pathway in the epidermis layer by opening the tight junctions reversibly.

Hsu and Mitragotri reported a peptide enhancer called 'skin permeating and cell entering' (SPACE) peptide with a sequence AC-TGSTQHQ-CG that has unique properties in improve the penetration of siRNA into deep layers of skin (Hsu et al., 2011). The delivery of siRNA-SPACE conjugated peptide showed a high permeation through the stratum corneum and consequently demonstrated a high transfection efficiency of siRNA in targeting IL and GAPDH. Furthermore, the mechanism of SPACE peptide to improve the permeation via skin layers was found to be through macropinocytosis (Hsu et al., 2011).

Accell siRNAs (Dharmacon) based topical formulation that facilitates non-invasive epidermal delivery of unmodified and "self-delivery" siRNAs in a mouse model has been reported. Remarkably, a sustained > 40% luciferase gene inhibition was observed after two 1-hour topical treatments with Accell-siRNAs. Accell siRNAs have been rendered more cell permeable either by the addition of a small lipophile to the siRNA duplex or by modifying the highly charged siRNA backbone without compromising siRNA silencing activity (Hegde et al., 2014).

The nanosomes called surfactant-ethanol-cholesterolosomes (SECosomes) were prepared using DOTAP, cholesterol, sodium cholate, and ethanol. The SECosome-siRNA complex (SECoplex) was prepared from SECosomes. This novel formulation penetrates into the epidermis of freshly excised intact human skin and can enter into the keratinocytes. The stable SECosomes showed a significant skin penetration capacity after complexation with siRNA (Fig. 2.7). The SECoplexes had a mean diameter of 101 nm, surface charge of 56 mV, and 40 fold higher transfection efficiency than free siRNA. Furthermore, SECosomes showed ideal characteristics for siRNA encapsulation since the encapsulated siRNA was stable for at least 4 weeks. Also, they enabled highly efficient transfection of in vitro cultured cells. They were shown to transport siRNA delivery through intact human skin where changes in the keratinocyte cell state were demonstrated (Barbara Geusens et al., 2010). The DFB4 siRNA loaded SECosome inhibited the translation of the human β defensin-2 peptide. This resulted in the normalization of the psoriasis from epidermal phenotype in the human skin grafts (Haigh et al., 2014). Bracke et al. used a novel SECosome delivery system, to silence DFB4 gene, which encodes the antimicrobial peptide, human β defensin-2 (hBD2). This peptide induces intra-epidermal expression of psoriasis form in human skin grafts transplanted onto immune-deficient mice. Gene knockdown by SECosome-mediated

siRNA delivery prevented the translation of hBD2 and improved the psoriasis form features of treated skin grafts (Bracke et al., 2014; Keren et al., 2014)

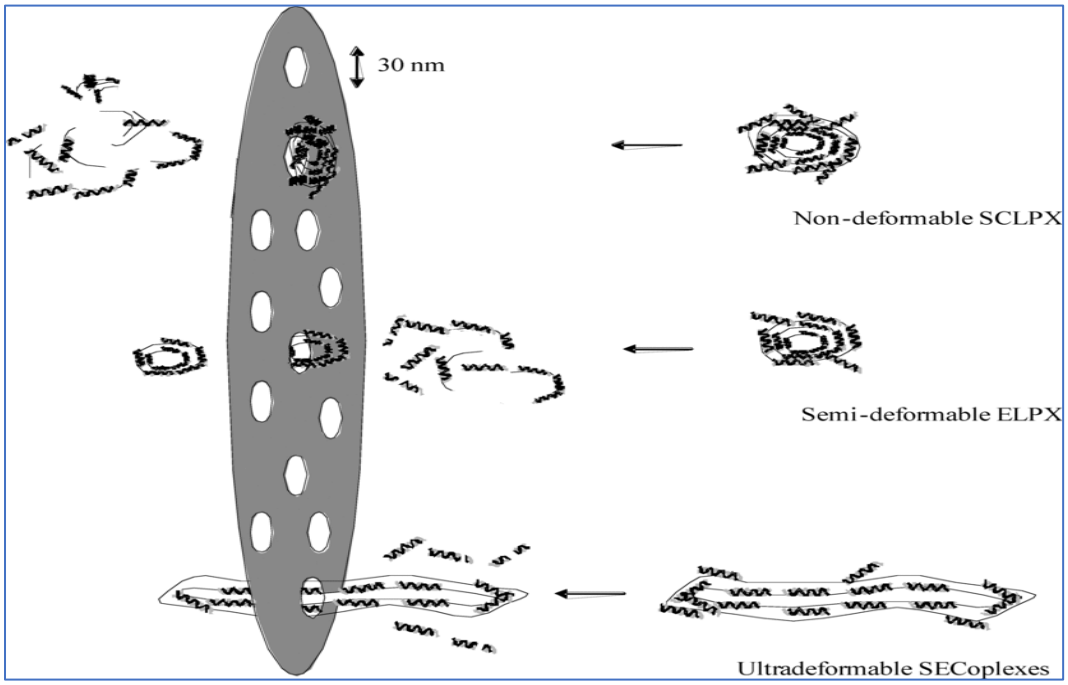

Figure 2.7 *Suggested mechanism of SECoplex membrane penetration during extrusion. External forced pressure in combination with small pore openings induces shear forces that break non-deformable SECosome-siRNA complex into fragments. Subsequently, siRNA molecules are released from the complexes and are broken down by RNases and/or physical forces. The ultra deformable character of the SECoplexes allows the complexes to adapt or "stretch" under an external force. This longitudinal stretching facilitates extrusion. As a result, the sandwiched siRNA molecules are now orientated perpendicular to the membrane's surface and are well protected by the SECosome. Reproduced from Geusens et al. (Barbara Geusens et al., 2010).*

Topical application of cream-emulsified CD86 siRNA ameliorated the clinical manifestations in murine contact hypersensitivity and atopic dermatitis -like disease. In this study, a co-stimulatory molecule, CD86, was induced on dendritic cells in situ after antigen uptake, and CD86-expressing dendritic cells migrate to the regional lymph nodes to present antigens to T cells (Azuma et al.,

2010).

Single-walled carbon nanotubes were formulated with non-covalent linkage with succinated polyethyleneimine to deliver the siRNA specific to Braf (Siu et al., 2014). The siRNA loaded carbon nanotubes were useful in Braf gene for in vitro against B16-F10 cell line. siRNA loaded carbon nanotubes exhibited significant cellular uptake of Cy3-labeled siRNA and Braf gene silencing in the tumor tissue in an C57BL/6 mice melanoma model. The treatment with C57BL/6 mice melanoma model attenuated the tumor growth for 25-days. These polymeric nanoparticle systems have provided a newer platform technology for topical siRNA delivery.

C) Physical Methods of Gene Delivery

The delivery of naked siRNA into skin to treat skin disorders is ineffective to penetrate skin layers and exerts its therapeutic effect on gene silencing expression (Vicentini et al., 2013a). There are several delivery methods to improve the delivery in skin layers as discussed previously. However, most of these methods have certain limitations either in the efficiency or the toxicity for the targeted cells. Therefore, there is a need to find a safe and effective delivery system for siRNA which overcomes the limitations associated with conventional delivery systems. There are several physical approaches that have been developed and employed alone or in combination to improve the delivery of siRNA across skin layers (Golzio et al., 2014; Haigh et al., 2014).

Iontophoresis utilizes current to improve the ionized drugs entry into cells (Pikal et al., 1990). This method has considerable advantages for drug delivery: reduces the systemic exposure, improves the skin permeation of the drug and facilitates the application (Vicentini et al., 2013a). Iontophoresis can be used to deliver a naked siRNA into deep skin layers non-invasively (a high

patient compliance). Iontophoresis was used for the delivery of a naked siRNA into skin layers with the help of a penetration enhancer (Ita, 2017; Kigasawa et al., 2010). Naked siRNA got accumulated in the epidermis (and not in the dermis) after iontophoretic delivery. In contrast, siRNA did not penetrate tape-stripped skin by passive diffusion. In a rat model of atopic dermatitis, skin was sensitized with ovalbumin to stimulate IL-10 mRNA expression as observed in skin lesions. Iontophoretic delivery of anti-IL-10 siRNA significantly reduced (73%) the level of IL-10 mRNA (Kigasawa et al., 2010). Electroporation is a technique that uses high voltage electric current (~50 V) pulses to create pores in a transient manner in the lipid components of the SC. This method facilitates the permeability of macromolecules (e.g. DNA) via skin administration (Singh et al., 2010),(Broderick et al., 2012).

Microneedle (MN) patch consists of tiny needles in micron-size, to make small pores on the SC without causing any pain in the application area (Alexander et al., 2012).This technique is simple and has several advantages such as the delivery of macromolecules, proteins across the skin by overcoming the barrier property of the stratum corneum (Coulman et al., 2006; Ita, 2017). Few studies utilized MN for siRNA delivery across skin (Haigh et al., 2014; Hickerson et al., 2013). Liposome encapsulated siRNA was delivered with help of micro projection arrays to enhance siRNA delivery across skin layers (Fig. 2.8). Transfection efficiency of siRNA on a reporter gene expression in vivo in mouse model was demonstrated (Coulman et al., 2006). In another study, Chong et al. investigated the efficiency of using coated microneedles to deliver siRNA into skin in vitro and in vivo on the efficiency of siRNA coating process and the functionality after its recovery from microneedle. This transfection efficiency was compared with a commercial transfection reagent, in HaCaT keratinocyte cell lines. The coated lamin A/C siRNA microneedles

were applied and evaluated the silence efficiency in a mouse model (Chong et al., 2013). Another type of MN, Motorized Microneedle Array Device (MMNA) which has the ability to adjust an appropriate amount of drug delivery was used. This method combines two techniques, the hypodermic action, and microneedle array. This device has been used commercially in cosmetic field. This system was utilized to deliver siRNA to epidermis layer for gene silencing. The siRNA was tagged to a fluorescent agent and detect the siRNA delivery across human and murine skin (Hickerson et al., 2013). A significant reduction ($78 \pm 5\%$) of CBL3 protein expression was observed in the skin epidermis in a group treated with CBL3 siRNA compared with nonspecific control.

Lara and coworkers showed that inhibition of CD44, a gene that is uniformly expressed throughout the epidermis, by a self-delivery siRNA (sd-siRNA) in cultured human epidermal skin equivalents as well as full-thickness human skin equivalents xenografted on immunocompromised mice. Treatment of human skin equivalents with CD44 sd-siRNA markedly decreased CD44 mRNA levels, which led to a reduction of the target protein as confirmed by immune-detection in epidermal equivalent sections with a CD44-specific antibody. Overall, these results demonstrate that sd-siRNA, delivered by microneedle arrays, can reduce expression of a targeted endogenous gene in a human skin xenograft model (Lara et al., 2012).

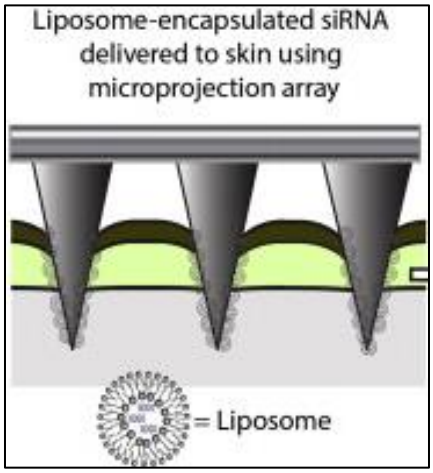

Figure 2.8 Gene silencing in the skin using liposome-encapsulated siRNA delivered by a micro projection array. Modified from Haigh et al. (Haigh et al., 2014).

Ultrasound uses high-frequency sound energy to open tight junctions on the epidermal layers to deliver macromolecules across skin (Azagury et al., 2014). A cationic liposomal carrier for siRNA to target ^{V600E}B-Raf or Akt3, (common promoters for melanoma) in combination with ultrasound energy was used. This formulation penetrated across skin to target melanoma cells (Tran et al., 2008). The ^{V600E}B-Raf siRNA and Akt3 siRNA loaded nano liposomal led to ~65% decrease in early or invasive cutaneous melanoma with minimal associated systemic toxicity.

2.6 Conclusion and Future Directions

There are number of challenges have to be addressed for the efficient topical delivery to skin diseases. The non-viral siRNA delivery approaches have shown promising effectiveness in delivering siRNA to the disease site. The delivery methods such as liposomes, lipid based polymer hybrid systems, spherical nucleic acid nanoparticles, and cationic cell-penetrating peptide based systems have been studied for topical delivery of siRNA. The selection of specific siRNA delivery systems will be based on skin penetration capability, protection of siRNA from degradation,

disease site and delivery of siRNA in the cytoplasm of cells. The skin penetration and cellular penetration are among the significant barriers for topical delivery of siRNA. The combination of non-viral delivery approaches with physical methods such as ultrasound, electroporation, iontophoresis, and microneedles will enable the efficient delivery of siRNA at diseases site. The preclinical studies with topical delivery of siRNA has shown promise for the treatment of skin disorder and a phase I clinical trial with TD101 siRNA which targets one of the PC keratin mutations, K6a for the treatment of Pachyonychia Congenita has been completed. It is anticipated that there will be more of progression and development in the field of siRNA based therapeutic in skin disorders in near future. With continuous development, the combination delivery system approaches for topical delivery of siRNA will ultimately lead toward better treatments for skin disorders.

2.7 Abbreviations:

siRNA: short interference RNA

PC: pachyonychia cogenita

AAV: adeno-associated virus

RA: rheumatoid arthritis

SLN: Solid lipid nanoparticles

RNAi: RNA interferences

ACD: Allergic contact dermatitis

CD86: Cluster of Differentiation 86

AA: Alopecia Areata

dsRNA: double strands RNA

RISC: RNA induced silence complex.

Ago-2: Argonuate-2

PEG: polyethylene glycol

GFP: green fluorescent protein

VEGF: Vascular endothelial growth factor

PLGA: Poly (Lactide-co-glycolic acid)

EGFP: Enhanced Green Fluorescent Protein

CD: Cyclodextrin

RRM2: Ribonucleotide reductase M2

PEI: Polyethyleneimine

DOPC: 1,2- dioleoyl-sn-glycero-3-phosphocholine

Cap: Capsaicin

IMQ: imiquamod

hKC: Human keratinocytes

PLL: Poly-L-lysine

CPP: Cationic cell penetrating peptides

TAT: Trans-Activating Transcriptional activator

SPACE: Skin Permeating And Cell Entering

IL: Interleukins

GAPDH: Glyceraldehyde 3-phosphate dehydrogenase

SC: stratum corneum

MN: Microneedle

TRBP: TAR RNA binding protein

2.8 References:

Acharya, Saha, Ray, Hazra, Mitra, & Chakraborty. (2017). siRNA-nanoparticle conjugate in gene silencing: A future cure to deadly diseases? *Mater Sci Eng C Mater Biol Appl, 76,* 1378-1400. doi:10.1016/j.msec.2017.03.009

Aied, Greiser, Pandit, & Wang. (2013). Polymer gene delivery: overcoming the obstacles. *Drug Discov Today, 18*(21-22), 1090-1098. doi:10.1016/j.drudis.2013.06.014

Alexander, Dwivedi, Ajazuddin, Giri, Saraf, Saraf, & Tripathi. (2012). Approaches for breaking the barriers of drug permeation through transdermal drug delivery. *J Control Release, 164*(1), 26-40. doi:10.1016/j.jconrel.2012.09.017

Aljuffali, Lin, & Fang. (2016). Noninvasive approach for enhancing small interfering RNA delivery percutaneously. *Expert Opin Drug Deliv, 13*(2), 265-280. doi:10.1517/17425247.2016.1121988

Azagury, Khoury, Enden, & Kost. (2014). Ultrasound mediated transdermal drug delivery. *Adv Drug Deliv Rev*. doi:10.1016/j.addr.2014.01.007

Azuma, Ritprajak, & Hashiguchi. (2010). Topical application of siRNA targeting cutaneous dendritic cells in allergic skin disease. *Methods Mol Biol, 623,* 373-381. doi:10.1007/978-1-60761-588-0_24

Barry. (2001). Novel mechanisms and devices to enable successful transdermal drug delivery. *Eur J Pharm Sci, 14*(2), 101-114.

Biswas, & Torchilin. (2013). Dendrimers for siRNA Delivery. *Pharmaceuticals (Basel), 6*(2), 161-183. doi:10.3390/ph6020161

Blagbrough, Metwally, & Ghonaim. (2012). Asymmetrical N(4),N(9)-Diacyl Spermines: SAR Studies of Nonviral Lipopolyamine Vectors for Efficient siRNA Delivery with Silencing of EGFP Reporter Gene. *Mol Pharm, 9*(7), 1853-1861. doi:10.1021/mp200428d

Bracke, Carretero, Guerrero-Aspizua, Desmet, Illera, Navarro, Del Rio. (2014). Targeted silencing of DEFB4 in a bioengineered skin-humanized mouse model for psoriasis: development of siRNA SECosome-based novel therapies. *Exp Dermatol, 23*(3), 199-201. doi:10.1111/exd.12321

Broderick, Chan, Lin, Shen, Kichaev, Khan, Sardesai. (2012). Optimized in vivo transfer of small interfering RNA targeting dermal tissue using in vivo surface electroporation. *Mol Ther Nucleic Acids, 1*, e11. doi:10.1038/mtna.2012.1

Chakraborty, Sharma, Sharma, Doss, & Lee. (2017). Therapeutic miRNA and siRNA: Moving from Bench to Clinic as Next Generation Medicine. *Mol Ther Nucleic Acids, 8*, 132-143. doi:10.1016/j.omtn.2017.06.005

Chaturvedi, Ganguly, Kulkarni, Kulkarni, Nadagouda, Rudzinski, & Aminabhavi. (2011). Cyclodextrin-based siRNA delivery nanocarriers: a state-of-the-art review. *Expert Opin Drug Deliv, 8*(11), 1455-1468. doi:10.1517/17425247.2011.610790

Chong, Gonzalez-Gonzalez, Lara, Speaker, Contag, Kaspar, Birchall. (2013). Gene silencing following siRNA delivery to skin via coated steel microneedles: In vitro and in vivo proof-of-concept. *J Control Release, 166*(3), 211-219. doi:10.1016/j.jconrel.2012.12.030

Coulman, Allender, & Birchall. (2006). Microneedles and other physical methods for overcoming the stratum corneum barrier for cutaneous gene therapy. *Crit Rev Ther Drug Carrier Syst, 23*(3), 205-258.

Dana, Chalbatani, Mahmoodzadeh, Karimloo, Rezaiean, Moradzadeh, Gharagouzlo. (2017). Molecular Mechanisms and Biological Functions of siRNA. *Int J Biomed Sci, 13*(2), 48-57.

de Gier, Mandersloot, & van Deenen. (1968). Lipid composition and permeability of liposomes. *Biochim Biophys Acta, 150*(4), 666-675.

Desai, Marepally, Patel, Voshavar, Chaudhuri, & Singh. (2013). Topical delivery of anti-TNFalpha siRNA and capsaicin via novel lipid-polymer hybrid nanoparticles efficiently inhibits skin inflammation in vivo. *J Control Release, 170*(1), 51-63. doi:10.1016/j.jconrel.2013.04.021

Evans, Ghivizzani, & Robbins. (2008). Arthritis gene therapy's first death. *Arthritis Res Ther, 10*(3), 110. doi:10.1186/ar2411

Fattal, & Bochot. (2008). State of the art and perspectives for the delivery of antisense oligonucleotides and siRNA by polymeric nanocarriers. *Int J Pharm, 364*(2), 237-248. doi:10.1016/j.ijpharm.2008.06.011

Fireman, Toledano, Neimann, Loboda, & Dayan. (2011). A look at emerging delivery systems for topical drug products. *Dermatol Ther, 24*(5), 477-488. doi:10.1111/j.1529-8019.2012.01464.x

Gandhi, Tekade, & Chougule. (2014). Nanocarrier mediated delivery of siRNA/miRNA in combination with chemotherapeutic agents for cancer therapy: current progress and advances. *J Control Release, 194*, 238-256. doi:10.1016/j.jconrel.2014.09.001

Geusens, Sanders, Prow, Van Gele, & Lambert. (2009). Cutaneous short-interfering RNA therapy. *Expert Opin Drug Deliv, 6*(12), 1333-1349. doi:10.1517/17425240903304032

Geusens, Strobbe, Bracke, Dynoodt, Sanders, Van Gele, & Lambert. (2011). Lipid-mediated gene delivery to the skin. *Eur J Pharm Sci, 43*(4), 199-211. doi:10.1016/j.ejps.2011.04.003

Geusens, Van Gele, Braat, De Smedt, Stuart, Prow, Lambert. (2010). Flexible Nanosomes (SECosomes) Enable Efficient siRNA Delivery in Cultured Primary Skin Cells and in the Viable Epidermis of Ex Vivo Human Skin. *Advanced Functional Materials, 20*(23), 4077-4090. doi:10.1002/adfm.201000484

Ghonaim, Li, & Blagbrough. (2010). N1,N12-Diacyl spermines: SAR studies on non-viral lipopolyamine vectors for plasmid DNA and siRNA formulation. *Pharm Res, 27*(1), 17-29. doi:10.1007/s11095-008-9764-3

Goldberg, Fruchter, Meilick, Schwartz, & Sprecher. (2013). Best treatment practices for pachyonychia congenita. *J Eur Acad Dermatol Venereol*. doi:10.1111/jdv.12098

Golzio, & Teissie. (2014). siRNA delivery via electropulsation: a review of the basic processes. *Methods Mol Biol, 1121*, 81-98. doi:10.1007/978-1-4614-9632-8_7

Grimm. (2009). Small silencing RNAs: state-of-the-art. *Adv Drug Deliv Rev, 61*(9), 672-703. doi:10.1016/j.addr.2009.05.002

Guo, Cheng, Gu, Ding, Qu, Yang, & O'Driscoll. (2012). Systemic delivery of therapeutic small interfering RNA using a pH-triggered amphiphilic poly-L-lysine nanocarrier to suppress prostate cancer growth in mice. *Eur J Pharm Sci, 45*(5), 521-532. doi:10.1016/j.ejps.2011.11.024

Guo, & Huang. (2014). Nanoparticles containing insoluble drug for cancer therapy. *Biotechnol Adv, 32*(4), 778-788. doi:10.1016/j.biotechadv.2013.10.002

Guzman-Villanueva, El-Sherbiny, Herrera-Ruiz, Vlassov, & Smyth. (2012). Formulation approaches to short interfering RNA and MicroRNA: challenges and implications. *J Pharm Sci, 101*(11), 4046-4066. doi:10.1002/jps.23300

Haigh, Depelsenaire, Meliga, Yukiko, McMillan, Frazer, & Kendall. (2014). CXCL1 gene silencing in skin using liposome-encapsulated siRNA delivered by microprojection array. *J Control Release, 194*, 148-156. doi:10.1016/j.jconrel.2014.08.021

Hartono, Gu, Kleitz, Liu, He, Middelberg, Qiao. (2012). Poly-L-lysine functionalized large pore cubic mesostructured silica nanoparticles as biocompatible carriers for gene delivery. *ACS Nano, 6*(3), 2104-2117. doi:10.1021/nn2039643

Hegde, Hickerson, Nainamalai, Campbell, Smith, McLean, & Leslie Pedrioli. (2014). In vivo gene silencing following non-invasive siRNA delivery into the skin using a novel topical formulation. *J Control Release, 196*, 355-362. doi:10.1016/j.jconrel.2014.10.022

Hickerson, Wey, Rimm, Speaker, Suh, Flores, Kaspar. (2013). Gene Silencing in Skin After Deposition of Self-Delivery siRNA With a Motorized Microneedle Array Device. *Mol Ther Nucleic Acids, 2*, e129. doi:10.1038/mtna.2013.56

Hordinsky. (2013). Overview of alopecia areata. *J Investig Dermatol Symp Proc, 16*(1), S13-15. doi:10.1038/jidsymp.2013.4

Howard, Rahbek, Liu, Damgaard, Glud, Andersen, Kjems. (2006). RNA interference in vitro and in vivo using a novel chitosan/siRNA nanoparticle system. *Mol Ther, 14*(4), 476-484. doi:10.1016/j.ymthe.2006.04.010

Hsu, & Mitragotri. (2011). Delivery of siRNA and other macromolecules into skin and cells using a peptide enhancer. *Proc Natl Acad Sci U S A, 108*(38), 15816-15821. doi:DOI 10.1073/pnas.1016152108

Hu, & Zhang. (2012). Nanoparticle-based combination therapy toward overcoming drug resistance in cancer. *Biochem Pharmacol, 83*(8), 1104-1111. doi:10.1016/j.bcp.2012.01.008

Ita. (2017). Dermal/transdermal delivery of small interfering RNA and antisense oligonucleotides-advances and hurdles. *Biomed Pharmacother, 87*, 311-320. doi:10.1016/j.biopha.2016.12.118

Jakobsen, Stenderup, Rosada, Moldt, Kamp, Dam, Mikkelsen. (2009). Amelioration of psoriasis by anti-TNF-alpha RNAi in the xenograft transplantation model. *Mol Ther, 17*(10), 1743-1753. doi:10.1038/mt.2009.141

Jeong, Park, & Kim. (2011). Self-assembled and nanostructured siRNA delivery systems. *Pharm Res, 28*(9), 2072-2085. doi:10.1007/s11095-011-0412-y

Kaczmarek, Kowalski, & Anderson. (2017). Advances in the delivery of RNA therapeutics: from concept to clinical reality. *Genome Med, 9*(1), 60. doi:10.1186/s13073-017-0450-0

Kaneda, Sasaki, Lanza, Milbrandt, & Wickline. (2010). Mechanisms of nucleotide trafficking during siRNA delivery to endothelial cells using perfluorocarbon nanoemulsions. *Biomaterials, 31*(11), 3079-3086. doi:10.1016/j.biomaterials.2010.01.006

Keasberry, Yapp, & Idris. (2017). Mesoporous Silica Nanoparticles as a Carrier Platform for Intracellular Delivery of Nucleic Acids. *Biochemistry (Mosc), 82*(6), 655-662. doi:10.1134/S0006297917060025

Keren, David, & Gilhar. (2014). Novel nanosome delivery system combined with siRNA targeting the antimicrobial gene DFB4: a new approach for psoriasis management? *Exp Dermatol, 23*(7), 464-465. doi:10.1111/exd.12397

Kigasawa, Kajimoto, Hama, Saito, Kanamura, & Kogure. (2010). Noninvasive delivery of siRNA into the epidermis by iontophoresis using an atopic dermatitis-like model rat. *Int J Pharm, 383*(1-2), 157-160. doi:DOI 10.1016/j.ijpharm.2009.08.036

Ko, Gottlieb, & Kerbleski. (2009). Induction and exacerbation of psoriasis with TNF-blockade therapy: a review and analysis of 127 cases. *J Dermatolog Treat, 20*(2), 100-108. doi:10.1080/09546630802441234

Kotterman, & Schaffer. (2014). Engineering adeno-associated viruses for clinical gene therapy. *Nat Rev Genet, 15*(7), 445-451. doi:10.1038/nrg3742

Lara, Gonzalez-Gonzalez, Speaker, Hickerson, Leake, Milstone, Kaspar. (2012). Inhibition of CD44 gene expression in human skin models, using self-delivery short interfering RNA administered by dissolvable microneedle arrays. *Hum Gene Ther, 23*(8), 816-823. doi:10.1089/hum.2011.211

Leachman, Hickerson, Hull, Smith, Milstone, Lane, Kaspar. (2008). Therapeutic siRNAs for dominant genetic skin disorders including pachyonychia congenita. *J Dermatol Sci, 51*(3), 151-157. doi:10.1016/j.jdermsci.2008.04.003

Lerman, Volman, Sidi, & Avni. (2011). Small-interfering RNA targeted at antiapoptotic mRNA increases keratinocyte sensitivity to apoptosis. *Br J Dermatol, 164*(5), 947-956. doi:10.1111/j.1365-2133.2010.10191.x

Li, Luo, Yang, Deng, Ren, Xie, Zhang. (2014). Cationic star-shaped polymer as an siRNA carrier for reducing MMP-9 expression in skin fibroblast cells and promoting wound healing in diabetic rats. *Int J Nanomedicine, 9*, 3377-3387. doi:10.2147/ijn.s66368

Mao, Sun, & Kissel. (2010). Chitosan-based formulations for delivery of DNA and siRNA. *Adv Drug Deliv Rev, 62*(1), 12-27. doi:10.1016/j.addr.2009.08.004

Marepally, Boakye, Patel, Godugu, Doddapaneni, Desai, & Singh. (2014). Topical administration of dual siRNAs using fusogenic lipid nanoparticles for treating psoriatic-like plaques. *Nanomedicine (Lond), 9*(14), 2157-2174. doi:10.2217/nnm.13.202

McLean, & Moore. (2011). Keratin disorders: from gene to therapy. *Hum Mol Genet, 20*(R2), R189-197. doi:10.1093/hmg/ddr379

Nakamura, Jo, Tabata, & Ishikawa. (2008). Controlled delivery of T-box21 small interfering RNA ameliorates autoimmune alopecia (Alopecia Areata) in a C3H/HeJ mouse model. *Am J Pathol, 172*(3), 650-658. doi:10.2353/ajpath.2008.061249

Nasrollahi, Taghibiglou, Azizi, & Farboud. (2012). Cell-penetrating peptides as a novel transdermal drug delivery system. *Chem Biol Drug Des, 80*(5), 639-646. doi:10.1111/cbdd.12008

Nikitenko, & Prassolov. (2013). Non-Viral Delivery and Therapeutic Application of Small Interfering RNAs. *Acta Naturae, 5*(3), 35-53.

Pandita, Kumar, & Lather. (2014). Hybrid poly(lactic-co-glycolic acid) nanoparticles: design and delivery prospectives. *Drug Discov Today*. doi:10.1016/j.drudis.2014.09.018

Patil, & Panyam. (2009). Polymeric nanoparticles for siRNA delivery and gene silencing. *Int J Pharm, 367*(1-2), 195-203. doi:10.1016/j.ijpharm.2008.09.039

Pauley, & Cha. (2013). RNAi Therapeutics in Autoimmune Disease. *Pharmaceuticals (Basel), 6*(3), 287-294. doi:10.3390/ph6030287

Pikal, & Shah. (1990). Transport mechanisms in iontophoresis. II. Electroosmotic flow and transference number measurements for hairless mouse skin. *Pharm Res, 7*(3), 213-221.

Presumey, Salzano, Courties, Shires, Ponchel, Jorgensen, De Rosa. (2012). PLGA microspheres encapsulating siRNA anti-TNFalpha: efficient RNAi-mediated treatment of arthritic joints. *Eur J Pharm Biopharm, 82*(3), 457-464. doi:10.1016/j.ejpb.2012.07.021

Prieto-Perez, Cabaleiro, Dauden, Ochoa, Roman, & Abad-Santos. (2013). Genetics of Psoriasis and Pharmacogenetics of Biological Drugs. *Autoimmune Dis, 2013*, 613086. doi:10.1155/2013/613086

Ragelle, Vandermeulen, & Preat. (2013). Chitosan-based siRNA delivery systems. *J Control Release, 172*(1), 207-218. doi:10.1016/j.jconrel.2013.08.005

Riley, & Vermerris. (2017). Recent Advances in Nanomaterials for Gene Delivery-A Review. *Nanomaterials (Basel), 7*(5). doi:10.3390/nano7050094

Rink, McMahon, Zhang, Chen, Mirkin, Thaxton, & Kaufman. (2013). Knockdown of intraislet IKKbeta by spherical nucleic acid conjugates prevents cytokine-induced injury and enhances graft survival. *Transplantation, 96*(10), 877-884. doi:10.1097/TP.0b013e3182a4190e

Rouge, Hao, Wu, Briley, & Mirkin. (2014). Spherical nucleic acids as a divergent platform for synthesizing RNA-nanoparticle conjugates through enzymatic ligation. *ACS Nano, 8*(9), 8837-8843. doi:10.1021/nn503601s

Rugg. (2008). Therapeutic interference: a step closer for pachyonychia congenita? *J Invest Dermatol, 128*(1), 7-8. doi:10.1038/sj.jid.5701065

Shapiro. (2013). Current treatment of alopecia areata. *J Investig Dermatol Symp Proc, 16*(1), S42-44. doi:10.1038/jidsymp.2013.14

Shegokar, Al Shaal, & Mishra. (2011). siRNA delivery: challenges and role of carrier systems. *Pharmazie, 66*(5), 313-318.

Shepherd, Taheri, & Feldman. (2013). Once-daily topical treatment for psoriasis: calcipotriene + betamethasone two-compound topical formulation. *Clin Cosmet Investig Dermatol, 7*, 19-22. doi:10.2147/CCID.S56673

Singh, Garland, Cassidy, Migalska, Demir, Abdelghany, Donnelly. (2010). Microporation techniques for enhanced delivery of therapeutic agents. *Recent Pat Drug Deliv Formul, 4*(1), 1-17.

Singha, Namgung, & Kim. (2011). Polymers in small-interfering RNA delivery. *Nucleic Acid Ther, 21*(3), 133-147. doi:10.1089/nat.2011.0293

Sioud. (2015). RNA interference: mechanisms, technical challenges, and therapeutic opportunities. *Methods Mol Biol, 1218*, 1-15. doi:10.1007/978-1-4939-1538-5_1

Siu, Chen, Zheng, Zhang, Johnston, Liu, Min. (2014). Non-covalently functionalized single-walled carbon nanotube for topical siRNA delivery into melanoma. *Biomaterials, 35*(10), 3435-3442. doi:10.1016/j.biomaterials.2013.12.079

Smith, Hickerson, Sayers, Reeves, Contag, Leake, McLean. (2008). Development of therapeutic siRNAs for pachyonychia congenita. *J Invest Dermatol, 128*(1), 50-58. doi:10.1038/sj.jid.5701040

Thanik, Greives, Lerman, Seiser, Dec, Chang, Saadeh. (2007). Topical matrix-based siRNA silences local gene expression in a murine wound model. *Gene Ther, 14*(17), 1305-1308. doi:10.1038/sj.gt.3302986

Tran, Gowda, Sharma, Park, Adair, Kester, Robertson. (2008). Targeting V600EB-Raf and Akt3 using nanoliposomal-small interfering RNA inhibits cutaneous melanocytic lesion development. *Cancer Res, 68*(18), 7638-7649. doi:10.1158/0008-5472.CAN-07-6614

Uchida, Kanazawa, Takashima, & Okada. (2011). Development of an efficient transdermal delivery system of small interfering RNA using functional peptides, Tat and AT-1002. *Chem Pharm Bull (Tokyo), 59*(2), 196-201.

Vicentini, Borgheti-Cardoso, Depieri, de Macedo Mano, Abelha, Petrilli, & Bentley. (2013a). Delivery systems and local administration routes for therapeutic siRNA. *Pharm Res, 30*(4), 915-931. doi:10.1007/s11095-013-0971-1

Vicentini, Depieri, Polizello, Del Ciampo, Spadaro, Fantini, & Vitoria Lopes Badra Bentley. (2013b). Liquid crystalline phase nanodispersions enable skin delivery of siRNA. *Eur J Pharm Biopharm, 83*(1), 16-24. doi:10.1016/j.ejpb.2012.08.011

Wang, Li, Ma, & Steinhoff. (2013). Non-viral gene delivery methods. *Curr Pharm Biotechnol, 14*(1), 46-60.

Wang, Lu, Wientjes, & Au. (2010). Delivery of siRNA therapeutics: barriers and carriers. *AAPS J, 12*(4), 492-503. doi:10.1208/s12248-010-9210-4

Wollenberg, & Feichtner. (2013). Atopic dermatitis and skin allergies - update and outlook. *Allergy, 68*(12), 1509-1519. doi:10.1111/all.12324

Wu, Huang, & He. (2013). Dendrimers as Carriers for siRNA Delivery and Gene Silencing: A Review. *Scientific World Journal*. doi:Artn 630654

Doi 10.1155/2013/630654

Xin, Huang, Guo, Huang, Zhang, & Jiang. (2017). Nano-based delivery of RNAi in cancer therapy. *Mol Cancer, 16*(1), 134. doi:10.1186/s12943-017-0683-y

Xu, Ganesh, & Amiji. (2012). Non-condensing polymeric nanoparticles for targeted gene and siRNA delivery. *Int J Pharm, 427*(1), 21-34. doi:10.1016/j.ijpharm.2011.05.036

Zhang, Wang, & Gemeinhart. (2013). Progress in microRNA delivery. *J Control Release, 172*(3), 962-974. doi:10.1016/j.jconrel.2013.09.015

Zheng, Giljohann, Chen, Massich, Wang, Iordanov, Paller. (2012). Topical delivery of siRNA-based spherical nucleic acid nanoparticle conjugates for gene regulation. *Proc Natl Acad Sci U S A, 109*(30), 11975-11980. doi:10.1073/pnas.1118425109

Pachyonychia Congenita Project. A Single-Center, Placebo-Controlled, Rising Dose to Tolerance and Safety Study of TD101, an siRNA Designed for Treatment of Pachyonychia Congenita. In: ClinicalTrials.gov [Internet]. Bethesda (MD): National Library of Medicine (US). 2000- [cited 2014 Mar 23]. Available from: http://clinicaltrials.gov/show/NCT00716014 NLM Identifier: NCT00716014.

3. Evaluation of siRNA-Polyethyleneimine (PEI) Polyplexes as a Suitable Delivery Platform for Melanoma Treatment

3.1 Abstract

Objective: Intracellular short interference RNA (siRNA) delivery confronts numerous challenges based on the properties of siRNA molecules, which are generally hydrophilic, negatively charged and labile for degradation. Hence there is need to protect the siRNA by means of a suitable delivery platform prior to delivery into the cells. Polyethyleneimine (PEI) was extensively investigated as a nano-carrier for gene therapy due to its ability to form a complex with many negatively charged molecules such as nucleic acids, ability to protect the molecules from degradation, and also its ability to enhance the cellular uptake. In this study, we focused on investigating the ability of PEI (varied molecular weights) to form polyplexes with an inert siRNA molecule (AccuTarget™ Negative Control siRNA) for intracellular delivery in melanoma (B16BL6) cell lines.

Methods: Three different molecular weights of PEI (1.8 KDa, 10 KDa and 25 KDa) were chosen for complexation with the siRNA (100 nM) at different polymer nitrogen (N) / siRNA phosphate (P) ratios (2:1, 5:1, 8:1, 10:1, 15:1, 20:1, 30:1, 50:1, 80:1, 100:1). These siRNA-PEI complexes were evaluated for complexation efficiency using agarose gel electrophoresis technique. The PEI at different concentrations in Dulbecco Phosphate Buffered Saline (10 nM-5000 nM) were evaluated for cytotoxicity in B16BL6 cell lines by MTT assay. Furthermore, selected PEI-siRNA polyplexes were evaluated for cytotoxicity by MTT assay, and cellular uptake by fluorescent microscopy.

Results: From gel electrophoresis, we found optimal polyplexes could be achieved at 50:1. 10:1, 5:1 N/P ratios for PEI 1.8 KDa, PEI 10 KDa and PEI 25 KDa, respectively. All three polymers

revealed a moderate to a high toxicity without complexation. However, all three polymers showed reduced or no toxicity at optimal polyplexes formation. The cellular uptake for polyplexes of PEI 1.8 KDa (50:1) and PEI 10 KDa (10:1) were compared with siRNA alone as control. siRNA alone had no cellular uptake as indicated by the absence of fluorescence in the cells while siRNA-PEI 1.8 KDa showed an intensity of the fluorescent siRNA. Likewise, siRNA-PEI 10 KDa showed a higher intensity of fluorescent siRNA inside the cells. This study demonstrated that the intracellular delivery siRNA-PEI polyplexes was achieved the N/P ratios 50:1 and 10:1 for PEI 1.8 KDa and PEI 10 KDa polymers, respectively.

Conclusion: This study establishes that 1.8 KDa PEI-siRNA polyplex at 50:1 ratio is the most optimum delivery platform for siRNA based on its safety and efficacy in the B16BL6 melanoma cell lines.

3.2 Introduction

Among various strategies, short interference RNA (siRNA) is emerging as one of the important treatments for cancer. RNA interference has gained a lot of attention in the treatment of various diseases due to high specificity, targetability, and fewer side effects (Xu et al., 2015). For cancer growth and development, cancerous cells go through successive steps or stages. Genetic mutation represents a key factor for certain cancers including melanoma. The mutation plays a vital role in the progressive phases of tumor development such as cell cycle and proliferation, cell death and survival, angiogenesis and chemotherapy resistance, invasion and metastasis. The genetic mutations in the cancer progression provide the basis for RNA interference therapy (Zhang et al., 2014).

In last decade, siRNA was discovered and utilized for the treatment of several diseases that are related to gene defects such as cancers, HIV, diabetes, brain injury, neurodegenerative illness and infections (Acharya et al., 2017; Zhang, Li et al., 2014). siRNA is basically composed of double strands in a manner similar to RNA sequence structure but relatively short. siRNA is typically in a range of 21-23 nucleic acids long. (Vicentini et al., 2013; Zhang, Li et al., 2014).

siRNA based treatment has been evolved as a strategy to treat and inhibit irregular functions of aberrant genes which eventually prevents protein expression associated with disease initiation and progression (Haigh et al., 2014). siRNA therapy has shown a high efficiency and selectivity on silencing the expression of aberrant genes (Geusens et al., 2011). The siRNA gene silencing effect can be achieved via the complementary base pairing of a single siRNA strand toward specific mRNA in order to prevent the transcription of targeted mRNA. Once siRNA successfully crosses cell membranes into the cytosol, it binds into RNA induced Silence Complex (RISC). This leads

the short double strand to unwind into a single strand and transforms to an active form (guide strand). This activation guides the complex for binding into targeted mRNA in order to degrade the specific mRNA and silence the expression of mutant genes (Chiu et al., 2004). Naked siRNA has numerous challenges for the delivery into cells and tissues. Since siRNA is generally hydrophilic, negatively charged and easily degradable, it demonstrates a poor permeability across the cell membrane and inefficient intracellular release. For successful siRNA based therapy, siRNA should be incorporated in the delivery system to overcome these challenges.

Based on siRNA delivery barriers, several delivery systems and strategies were exploited and employed to accommodate the following conditions and attain an effective delivery system: a- prevent siRNA from degradation and maintain its integrity for therapeutic activity. b- accumulate and permeate through blood vessels at targeted sites. c- enhance siRNA cellular uptake for cancer cells. d- promote endosomal escape upon cellular uptake to avoid lysosomal degradation in an enclosed vesicle (Bumcrot et al., 2006; Huang, 2011; Reischl et al., 2009; Zhang, Li et al., 2014). siRNA carriers are mostly classified into two main categories: viral and non-viral. Viral carriers are the most successful delivery approach in transfection efficiency perspective; however, they showed serious undesirable effects and limitations such as immune system stimulation, mutation susceptibility, safety issues and relatively high cost of production. On the other hand, non-viral carriers showed several promising platform candidates to deliver siRNA effectively into cytoplasm with enhanced efficacy and safety (Nam et al., 2016; Oh et al., 2009; Zhi et al., 2016).

Non-viral delivery systems can be categorized into three main classes: lipid-based carrier, inorganic nanoparticles and polymer-based carrier. In this study, we focused on polymer-based

delivery system, particularly PEI, due to its advantages such as enhanced stability, nuclease resistance, cellular uptake, and efficient siRNA carrier.

PEI is a cationic polymer with an ability to carry nucleic acids via electrostatic interaction. The electrostatic interaction is based on the negative charge of phosphate groups in the backbone of nucleic acid with an overall cationic charge of nitrogen in the polymer (PEI). PEI is a unique polymer due to the proton sponge effects upon cellular uptake. PEI has shown its efficacy to increase the transfection efficiency via improving endosomal escape upon endocytosis. This effect is achieved by primary nitrogen groups with strong positive charge. Experimentally, PEI demonstrates an optimum transfection efficiency with a range of molecular weights (10-30 KDa) (Chiper et al., 2017). Hence the objective of this research is to investigate the ability of PEI within a range of molecular weights and optimize the complexation ratio of PEI to enhance an inert siRNA (AccuTarget™ Negative Control siRNA) delivery in melanoma B16BL6 cell lines based on enhanced protection, efficiency, safety, and cellular uptake of the cargo.

3.3 Materials and Methods

3.3.1 Materials

AccuTarget™ Negative Control siRNA and AccuTarget™ Fluorescein-labeled Negative Control siRNA were obtained from Bioneer (Alameda, Ca). Polyethyleneimine branched 25 KDa was purchased from Sigma-Aldrich, Inc (Milwaukee, WI). Polyethyleneimine branched 1.8 and 10 KDa polymers were purchased from Polysciences, Inc (Warrington, PA). Dulbecco Phosphate Buffered Saline (DPBS) (1X) without Ca, and Mg was obtained from Lonza (Walkersville, MD). Agarose ^{TM} biotechnology grade was purchased from VWR life science (Solon, OH). Ethidium Bromide (10 mg/ml) and TAE buffer 50X were purchased from Bio-Rad laboratories (Hercules,

California). Fetal bovine serum, Dulbecco's Modified Eagle's Medium, and other reagents needed for cell culture were purchased from Mediatech (Manassas, VA). The mouse melanoma cell line (B16BL6) was obtained from the National Cancer Institute (Frederick, MD).

3.3.2 Complex Preparation

siRNA (AccuTarget™ Negative Control siRNA) was complexed with PEI of three different molecular weights (1.8 KDa, 10 KDa and 25 KDa, respectively). Based on nitrogen to phosphate ratios, PEI preparations were diluted in DPBS buffer appropriately to form a complex with siRNA at different N/P ratios (2:1, 5:1, 8:1, 10:1, 15:1, 20:1, 30:1, 50:1, 80:1, 100:1). The PEIs were complexed with siRNA to form siRNA-PEI complexes, the complexations were prepared via adding equal volumes of confirmed concentration of siRNA solution into DPBS solution of PEI directly and kept for 30 minutes at room temperature for further assessment (F. Wang et al., 2016).

3.3.3 Agarose Gel Electrophoresis

Agarose gel 1% (0.5 gm into 50 ml of TAE buffer) was prepared. (50mL) 1x TAE was added to the flask and swirled for homogenious mixing. The flask was heated for 1 minute using a microwave and left to cool for 4 minutes. (2.5ul) of ethidium bromide (10mg/mL) was added to the molten gel and swirled gently in both directions to blend the mixture thoroughly. The mixture was poured slowly into the mold. The molten gel was left for around 30-60 minutes to become solid. The samples were prepared in series and 20 ul of each sample was loaded using a pipette. In addition, enough quantity of the same buffer was prepared for running the gel electrophoresis with same EtBr concentration. The gel electrophoresis tank was filled with spiked running buffer (1X TAE) which contained EtBr (0.5 ug/ml). The immersed gel ran for 30 minutes at 80 V. Sample bands were visualized using UV trans-illuminator (Bio-Rad).

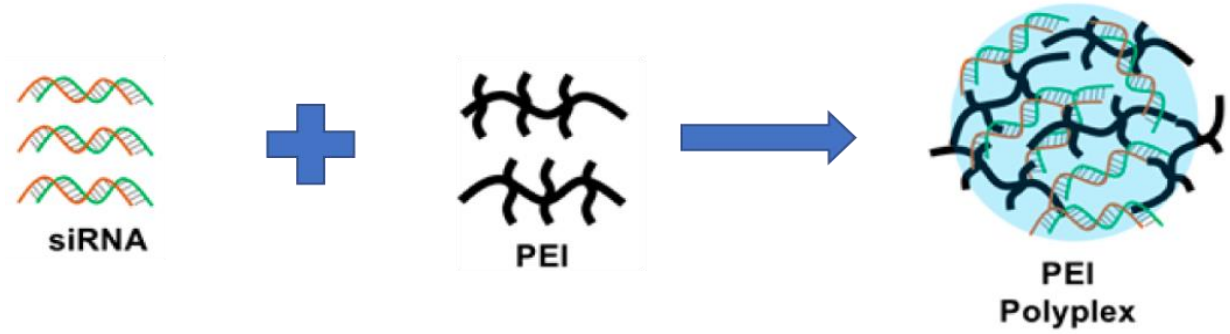

Figure 3.1 Schematic representation for polyplexes preparation of siRNA and PEI. Figure adapted and modified from: Wang et al./ Biomacromolecules (2017) 18, 77−86.

3.3.4 Cell Culture:

The B16BL6 cells were cultured and grown in Dulbecco's Modified Eagle's medium supplemented with 10% fetal bovine serum (FBS), 100 U/ml penicillin, and 100 µg/ml streptomycin at 37°C in a humidified atmosphere containing 5% CO_2.

3.3.5 MTT Assay

The MTT (3-[4, 5-dimethylthiazol-2-yl]-2, 5-diphenyl tetrazolium bromide) assay was used to assess the cytotoxicity of PEI with molecular weights 1.8, 10 and 25 KDa. Each polymer was tested for range of concentrations (10 nM-5000 nM). Cells were seeded in clear 96-well plates at 5,000 cells in 100µl of DMEM medium with 10% FBS/well. Serial concentrations of each polymer and complexes were added to the plate with 10% FBS at 37°C in 5% CO_2 for 24 hours. 10µl of MTT stock solution (5 mg/mL in PBS; pH 7.4) was placed into the wells which were incubated at 37°C for 3 hours. The crystals in each well were dissolved via adding 100 µl of dimethyl sulfoxide (DMSO) and measure the optical density (absorbance) at 544 nm on a microplate reader (Fluostar,

BMG lab-technologies, Germany). Data were expressed as mean ± SD with five replicates of each sample. Cytotoxicity was stated as a percentage relative to untreated cells (control 100%).

3.3.6 Fluorescent Microscopic Evaluation of Developed siRNA Complexes

PEI-siRNA polyplex with different molecular weights at specified N/P ratios were studied for in vitro cellular uptake utilizing a fluorescent microscope (EVOS fl Microscope, AMG, USA). B16BL6 cell line was used a model for cellular uptake evaluation. The cells were seeded at a density of $5*10^3$ per well into 96 well-plates. After 24 hours of incubation, the cells were washed three times with DPBS buffer to remove any untaken polyplexes. Then cells were fixed with 4% paraformaldehyde for around 20 minutes at room temperature. The cellular uptake was visualized for siRNA polyplex and compared to siRNA alone as a control. The visualization was through the light channel of RFP with 20X power lenses.

3.3.7 Statistical Analysis

The data were presented as mean ± S.D. Statistical significance in cytotoxicity and cellular uptake were determined using one-way ANOVA followed by a Tukey test for multiple comparison assessments. P value of <0.05 is noted as statistically significant.

3.4 Results and Discussion

Figure 3.2 describes the complexation of siRNA and PEI 1.8 KDa polymer at different N/P ratios (nitrogen is corresponding to PEI positive charge while phosphate ratio is corresponding to siRNA negative charge). The ratios were 0, 5, 10, 15, 20, 30, 50, 80 and 100. From right to left in the Figure, the existence of bands indicates the presence of un-complexed siRNA as a result of intercalation between free siRNA and ethidium bromide in the gel. Control (siRNA alone) showed a clear and bright band which indicates the presence of free siRNA. In the Figure, the band density

reduces as the N/P ratio increases. Thus, increasing PEI content ultimately enhances the binding to siRNA which leads to polyplex formation. At 50:1 ratio, the band completely disappeared which means a complete condensation with the negative charge of siRNA. The movement of the siRNA in the gel is based on charge repulsive forces.

Figure 3.3 describes the complexation of siRNA and PEI 10 KDa polymer at different N/P ratios (0, 2, 5, 10, 15, 20, 30, 50, 80 and 100). As with 1.8 KDa PEI results earlier, the existence of bands indicates the presence of un-complexed siRNA. In Figure 3.3, the band density reduces as the N/P ratio increases and the band completely disappears at 10:1 N/P ratio. Due to a higher positive charge of the higher molecular weight PEI (10 KDa), it requires less N/P ratio to induce complete complexation.

Figure 3.4 describes the complexation of siRNA and PEI 25 KDa polymer at different N/P ratios (0, 2, 5, 10, 15, 20, 30, 50, 80 and 100). Complete complexation occurs at 5:1 ratio for the 25 KDa PEI polymer. Due to an even much higher positive charge than 10 KDa PEI, the 25 KDa PEI requires much less N/P ratio to induce complete complexation and polyplex formation.

The PEI polymers with different molecular weights (1.8, 10 and 25 KDa) required varied ratios to induce polyplex formation with the siRNA. Based on gel retardation experiments, we have optimized N/P ratios for siRNA and PEI with different molecular weights. The minimum amount of polymer required to induce complete complexation (polyplex formation) was 50, 10 or 5 ratio for 1.8, 10 and 25 KDa PEI, respectively.

PEI is a cationic polymer, which has been widely used in gene delivery as a drug delivery carrier. PEI is available in branched and linear forms with varied molecular weights and with modified

functional groups (Zhang et al., 2014). In our study, we employed branched PEI polymer of three different molecular weights. Branched PEI has primary, secondary and tertiary amino groups which import a high positive charge density. The cationic charge density has an ability to condense nucleic acids and forms polyplexes in the nano-size scale. The electrostatic forces between the cationic charge of the PEI and the anionic charge of the nucleic acid are responsible for polyplex formation (Godbey et al., 1999; Jaeger et al., 2012; Kunath et al., 2003; X. Wang et al., 2015).

The main issue of using branched PEI is a relative cellular toxicity, hence these should be used at the minimal amount to induce polyplexes with nucleic acids. Therefore, we have performed MTT assay exeperiments to assess the PEI toxicity and screen the three polymers in vitro in B16BL6 melanoma cell line. Figure 3.5 shows results of the toxicity evaluation of PEI 1.8 KDa polymer at specified concentrations. The cells treated with 10 nm PEI retained about 95% viability. As the concentration of PEI increases from 50 to 5000 nM, the viability very slightly decreases from 90% to 80%. We conclude from the toxicity evaluation that PEI 1.8 KDa is practically non-toxic up to 5000 nM.

Figure 3.6 shows the toxicity evaluation of PEI 10 KDa polymer at specified concentrations. The cells treated with 10 nM PEI retained about 90% viability. The cells treated with 50 nm PEI retained about 80% viability. As the concentration of PEI increases from 100 to 5000 nM, the viability significantly decreases from 75% to 12%. These results indicate that PEI 10 KDa polymer is practically non-toxic to B16BL6 melanoma cell line up to 50 nM concentration. 100 nM to 500 nM is moderately toxic to the cells and > 500 nM, the polymer appears to be extremely toxic.

Figure 3.7 shows the toxicity evaluation of PEI 25 KDa polymer at specified concentrations. The cells treated with 10 nM PEI retained about 80% viability. The cells treated with 50 nM or 100

nM PEI concentrations retained about 70% or 65% viability, respectively. As the concentration of PEI increases from 200 to 5000 nM, the viability dramatically decreases from 50% to 5%. These results indicate that PEI 25 KDa polymer is practically non-toxic to B16BL6 melanoma cell line up to 10 nM concentration and >200 nM is very toxic. These results are based on the PEI alone with no polyplex formation. It is expected to be toxic based on the high amount of the positive charge. Attained toxicity can be explained by proton sequestration effect that leads to increase the proton pump activity within the cells. This alteration is due to osmotic swelling of endocytic compartments (leads to cell killing via mitochondria based mechanism) (Beyerle et al., 2010; Xia et al., 2009; Zhang, Li et al., 2014). Nevertheless, choosing an appropriate molecular weight and ratio is critical to balance the efficiency and cellular toxicity of PEI for siRNA delivery purposes (X. Wang, Niu et al., 2015).

Figure 3.8 shows a comparison of 1.8, 10 and 25 KDa PEI polymers in respect to their toxicity based on MTT assay. Based on these results, it is obvious that the cellular toxicity increases with increase in the molecular weight of PEI. These results are in agreement with several studies on at various cell lines (Oh et al., 2009; Thomas et al., 2002; Xia et al., 2009). Even though higher molecular weight polymers are toxic, they are required in lesser quantities to induce complete polyplex formation. In our studies, PEI 1.8 KDa polymer required a high N/P ratio (50:1) for complete complexation. However, PEI 10 KDa and 25 KDa 10:1 and 5:1, respectively, for complete complexation.

Based on gel electrophoresis results we have obtained optimum ratios (minimal amount of polymer) to form polyplexes. These polyplexes were further evaluated to determine their cytotoxicity. In Figure 3.9, 1.8 KDa PEI-siRNA (50:1) polyplex showed almost no toxicity. This

might be a consequence of cationic charge reduction due to condensation of the negative charge of siRNA. This polymer was also practically non-toxic when tested alone (Figure 3.6). On the other hand, 10 KDa PEI-siRNA polyplex showed a moderate toxicity since cell viability was around 70%. The polymer alone displayed higher toxicity as compared to its polyplex form (10:1 N/P ratio). This may be due to the presence of excess cationic charge of the polymer which is directly linked it its cytotoxicity (L. L. Wang et al., 2017). The 25 KDa PEI polyplex (5:1 N/P ratio) showed a lesser toxicity compared to the polymer alone. Even with a low polymer concentration in the polyplex (5:1 N/P ratio) the 25 KDa PEI exhibited a high toxicity 40% cell viability. Therefore, 25 KDa PEI-siRNA complex was eliminated in the cellular uptake studies.

The cellular uptake by the 1.8 KDa PEI-siRNA and 10 KDa PEI-siRNA polyplexes was evaluated (Figure 3.10). Fluorescein-tagged siRNA was incorporated in both 1.8 KDa and 10 KDa PEI polymers at 50:1 and 10:1 N/P ratios, respectively. (Figure 3.10a) No fluorescence was detected upon the application of un-complexed siRNA alone, which indicates the cellular uptake was negligent. This result is not surprising since the siRNA degrades significantly and due to its hydrophilic nature and negative charge. On the other hand, the polyplex made with 1.8 KDa PEI polymer showed bright fluorescence due to enhanced cellular uptake for siRNA (Figure 3.10b). This result is expected for the complexed siRNA which facilitates the transfer of siRNA across the cellular membrane. The fluorescence intensity was dramatically increased for 10 KDa PEI polyplex as compared to 1.8 PEI-siRNA polyplex and siRNA control. This was due to the abundant of cationic charge which facilitates the cellular uptake. We were able to achieve successful intracellular delivery of siRNA by PEI complex formation. Introducing a cationic carrier is one of

the most effective delivery methods via enhancing the electrostatic interaction between positively charged vector and negatively charged cellular membrane (Jaeger et al., 2012; Zhou et al., 2016). In our studies, 1.8 KDa PEI-siRNA at 50:1 ratio is considered least toxic and safe for the intracellular delivery in melanoma (B16BL6) cell lines. This is in contrary to certain studies, they proposed the ideal range for effective gene delivery within a range of 5 KDa to 25 KDa (Kunath et al., 2003; X. Wang et al., 2015). Their observation might be based on gene delivery with larger molecules such as DNA which required a higher cationic charge corresponding to a higher molecular weight of the carrier. siRNA is a small molecule relative to other gene cargos.

3.5 Conclusion

Delivery efficiency and low cytotoxicity are the main goals for siRNA delivery. In this study, we focused on the two aspects. Polyplexes were developed with varied N/P ratios of three different PEI polymers ranging from low, moderate and high molecular weights. The 1.8 KDa PEI-siRNA (50:1 N/P ratio) was the most suitable polyplex with respect to its safety and efficacy. 10 KDa PEI-siRNA (10:1 N/P ratio) showed reduced toxicity upon polyplex formation and a higher cellular uptake compared to 1.8 KDa PEI-siRNA polyplex. 25 KDa showed the highest efficacy in polyplex formation at a low ratio (5:1 N/P) but with an increased toxicity at a cellular level. Overall, 1.8 KDa PEI can be utilized alone as a carrier for siRNA due to its safety and efficacy while 10 KDa PEI can be used as a modifying agent or copolymer to enhance the cellular uptake.

3.6 Future Direction

Based on these results, this study is further directed to choose a model for gene targeting with specific siRNA as a therapeutic tool to knock down a mutant gene in vitro in melanoma treatment. For therapeutic efficacy, the percentage of knockdown efficiency of the gene expression and protein translation will be evaluated by q-PCR and Western Blot techniques, respectively.

3.7 References:

Acharya, R., Saha, S., Ray, S., Hazra, S., Mitra, M. K., & Chakraborty, J. (2017). siRNA-nanoparticle conjugate in gene silencing: A future cure to deadly diseases? *Mater Sci Eng C Mater Biol Appl, 76*, 1378-1400. doi:10.1016/j.msec.2017.03.009

Beyerle, A., Irmler, M., Beckers, J., Kissel, T., & Stoeger, T. (2010). Toxicity pathway focused gene expression profiling of PEI-based polymers for pulmonary applications. *Molecular pharmaceutics, 7*(3), 727-737.

Bumcrot, D., Manoharan, M., Koteliansky, V., & Sah, D. W. (2006). RNAi therapeutics: a potential new class of pharmaceutical drugs. *Nat Chem Biol, 2*(12), 711-719. doi:10.1038/nchembio839

Chiper, M., Tounsi, N., Kole, R., Kichler, A., & Zuber, G. (2017). Self-aggregating 1.8kDa polyethylenimines with dissolution switch at endosomal acidic pH are delivery carriers for plasmid DNA, mRNA, siRNA and exon-skipping oligonucleotides. *J Control Release, 246*, 60-70. doi:10.1016/j.jconrel.2016.12.005

Chiu, Y. L., Ali, A., Chu, C. Y., Cao, H., & Rana, T. M. (2004). Visualizing a correlation between siRNA localization, cellular uptake, and RNAi in living cells. *Chem Biol, 11*(8), 1165-1175. doi:10.1016/j.chembiol.2004.06.006

Geusens, B., Strobbe, T., Bracke, S., Dynoodt, P., Sanders, N., Van Gele, M., & Lambert, J. (2011). Lipid-mediated gene delivery to the skin. *Eur J Pharm Sci, 43*(4), 199-211. doi:10.1016/j.ejps.2011.04.003

Godbey, W., Wu, K. K., & Mikos, A. G. (1999). Poly (ethylenimine) and its role in gene delivery. *J Control Release, 60*(2), 149-160.

Haigh, O., Depelsenaire, A. C., Meliga, S. C., Yukiko, S. R., McMillan, N. A., Frazer, I. H., & Kendall, M. A. (2014). CXCL1 gene silencing in skin using liposome-encapsulated siRNA delivered by microprojection array. *J Control Release, 194*, 148-156. doi:10.1016/j.jconrel.2014.08.021

Huang, S. G. a. L. (2011). Nanoparticles Escaping RES and Endosome: Challenges for siRNA Delivery for Cancer Therapy. *J Nanomater, 2011*. doi:10.1155/2011/742895

Jaeger, M., Schubert, S., Ochrimenko, S., Fischer, D., & Schubert, U. S. (2012). Branched and linear poly (ethylene imine)-based conjugates: synthetic modification, characterization, and application. *Chem. Soc. Rev., 41*(13), 4755-4767.

Kunath, K., von Harpe, A., Fischer, D., Petersen, H., Bickel, U., Voigt, K., & Kissel, T. (2003). Low-molecular-weight polyethylenimine as a non-viral vector for DNA delivery: comparison of physicochemical properties, transfection efficiency and in vivo distribution with high-molecular-weight polyethylenimine. *J. Control. Release, 89*(1), 113-125.

Nam, J. P., & Nah, J. W. (2016). Target gene delivery from targeting ligand conjugated chitosan-PEI copolymer for cancer therapy. *Carbohydr Polym, 135*, 153-161. doi:10.1016/j.carbpol.2015.08.053

Oh, Y. K., & Park, T. G. (2009). siRNA delivery systems for cancer treatment. *Adv Drug Deliv Rev, 61*(10), 850-862. doi:10.1016/j.addr.2009.04.018

Reischl, D., & Zimmer, A. (2009). Drug delivery of siRNA therapeutics: potentials and limits of nanosystems. *Nanomedicine, 5*(1), 8-20. doi:10.1016/j.nano.2008.06.001

Thomas, M., & Klibanov, A. M. (2002). Enhancing polyethylenimine's delivery of plasmid DNA into mammalian cells. *Natl. Acad. Sci.*, *99*(23), 14640-14645.

Vicentini, F. T., Borgheti-Cardoso, L. N., Depieri, L. V., de Macedo Mano, D., Abelha, T. F., Petrilli, R., & Bentley, M. V. (2013). Delivery systems and local administration routes for therapeutic siRNA. *Pharm Res*, *30*(4), 915-931. doi:10.1007/s11095-013-0971-1

Wang, F., Gao, L., Meng, L. Y., Xie, J. M., Xiong, J. W., & Luo, Y. (2016). A Neutralized Noncharged Polyethylenimine-Based System for Efficient Delivery of siRNA into Heart without Toxicity. *ACS Appl Mater Interfaces*, *8*(49), 33529-33538. doi:10.1021/acsami.6b13295

Wang, L. L., Sloand, J. N., Gaffey, A. C., Venkataraman, C. M., Wang, Z., Trubelja, A., Burdick, J. A. (2017). Injectable, Guest-Host Assembled Polyethylenimine Hydrogel for siRNA Delivery. *Biomacromolecules*, *18*(1), 77-86. doi:10.1021/acs.biomac.6b01378

Wang, X., Niu, D., Hu, C., & Li, P. (2015). Polyethyleneimine-Based Nanocarriers for Gene Delivery. *Curr Pharm Des*, *21*(42), 6140-6156.

Xia, T., Kovochich, M., Liong, M., Meng, H., Kabehie, S., George, S., Nel, A. E. (2009). Polyethyleneimine coating enhances the cellular uptake of mesoporous silica nanoparticles and allows safe delivery of siRNA and DNA constructs. *ACS Nano*, *3*(10), 3273-3286. doi:10.1021/nn900918w

Xu, C.-f., & Wang, J. (2015). Delivery systems for siRNA drug development in cancer therapy. *Asian J. Pharm.*, *10*(1), 1-12. doi:10.1016/j.ajps.2014.08.011

Zhang, J., Li, X., & Huang, L. (2014). Non-viral nanocarriers for siRNA delivery in breast cancer. *J Control Release*, *190*, 440-450. doi:10.1016/j.jconrel.2014.05.037

Zhi, D., Zhao, Y., Cui, S., Chen, H., & Zhang, S. (2016). Conjugates of small targeting molecules to non-viral vectors for the mediation of siRNA. *Acta Biomater, 36*, 21-41. doi:10.1016/j.actbio.2016.03.048

Zhou, J., Wu, Y., Wang, C., Cheng, Q., Han, S., Wang, X., Dong, A. (2016). pH-Sensitive Nanomicelles for High-Efficiency siRNA Delivery in Vitro and in Vivo: An Insight into the Design of Polycations with Robust Cytosolic Release. *Nano Lett, 16*(11), 6916-6923. doi:10.1021/acs.nanolett.6b02915

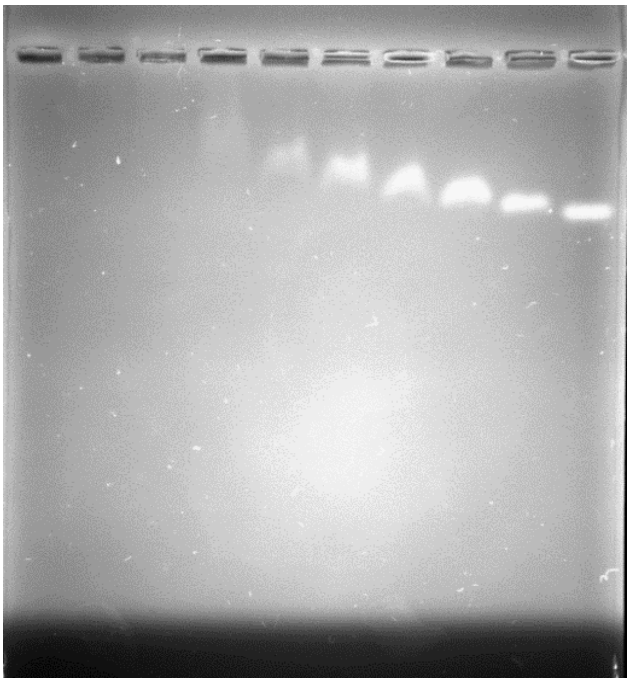

Figure 3.2 Complexation of siRNA and PEI 1.8 KDa polymer as detected by gel retardation assay: The appearance of bands represent uncomplexed siRNA while disappearance of bands indicate complete siRNA complexation. From right to left: siRNA alone as control, 5:1, 10:1, 15:1, 20:1, 30:1, 50:1, 80:1, 100:1 based on N/P ratios.

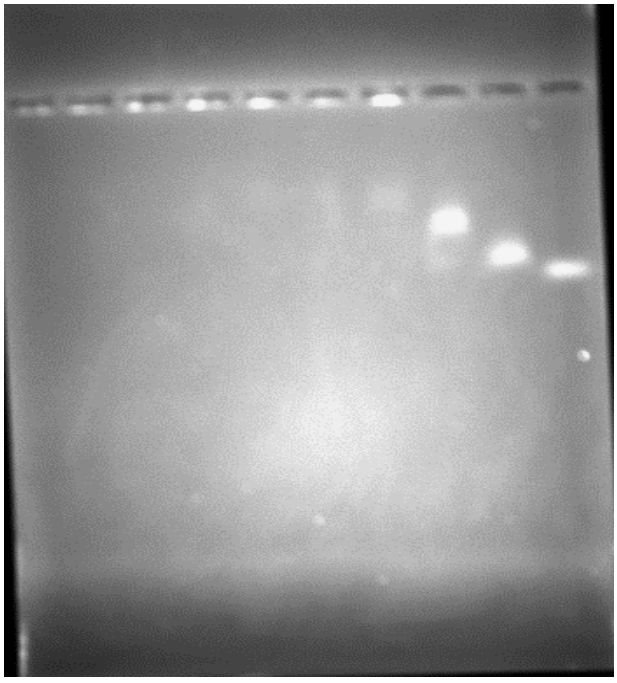

Figure 3.3 Complexation of siRNA and PEI 10 KDa polymer as detected by gel retardation assay: The appearance of bands represent uncomplexed siRNA while disappearance of bands indicate complete siRNA complexation. From right to left: siRNA alone as control, 2:1, 5:1, 10:1, 15:1, 20:1, 30:1, 50:1, 80:1 and 100:1 based on N/P ratios.

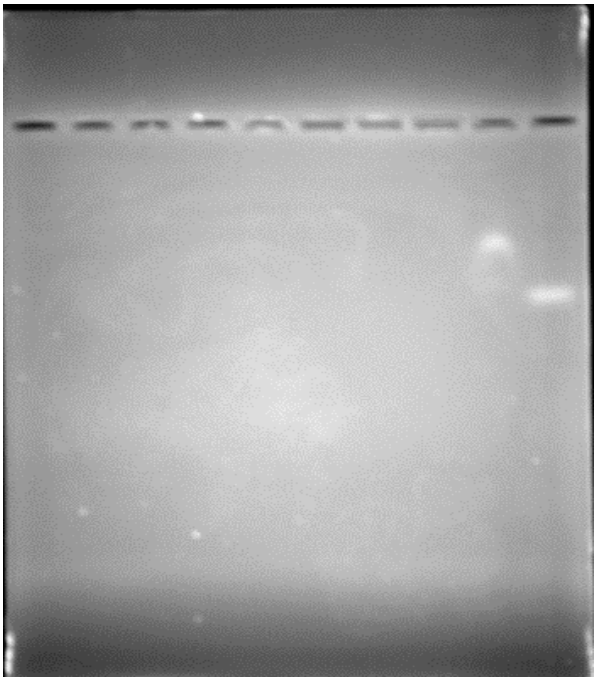

Figure 3.4 Complexation of siRNA and PEI 25 KDa polymer as detected by gel retardation assay: The appearance of bands represent uncomplexed siRNA while disappearance of bands indicate complete siRNA complexation. From right to left: siRNA alone as control, 2:1, 5:1, 10:1, 15:1, 20:1, 30:1, 50:1, 80:1 and 100:1 based on N/P ratios.

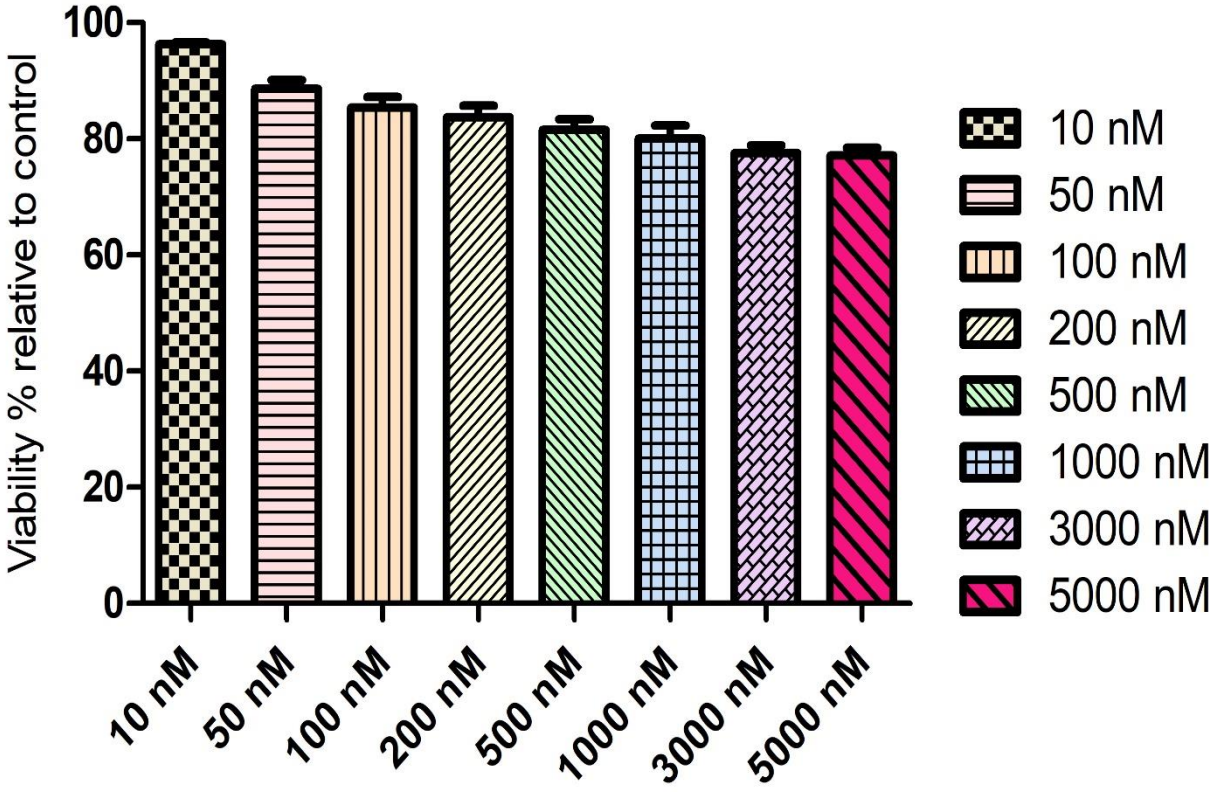

Figure 3.5 Cytotoxicity of PEI 1.8 KDa in B16BL6 melanoma cell line. (Values represent mean ± SD, N = 3).

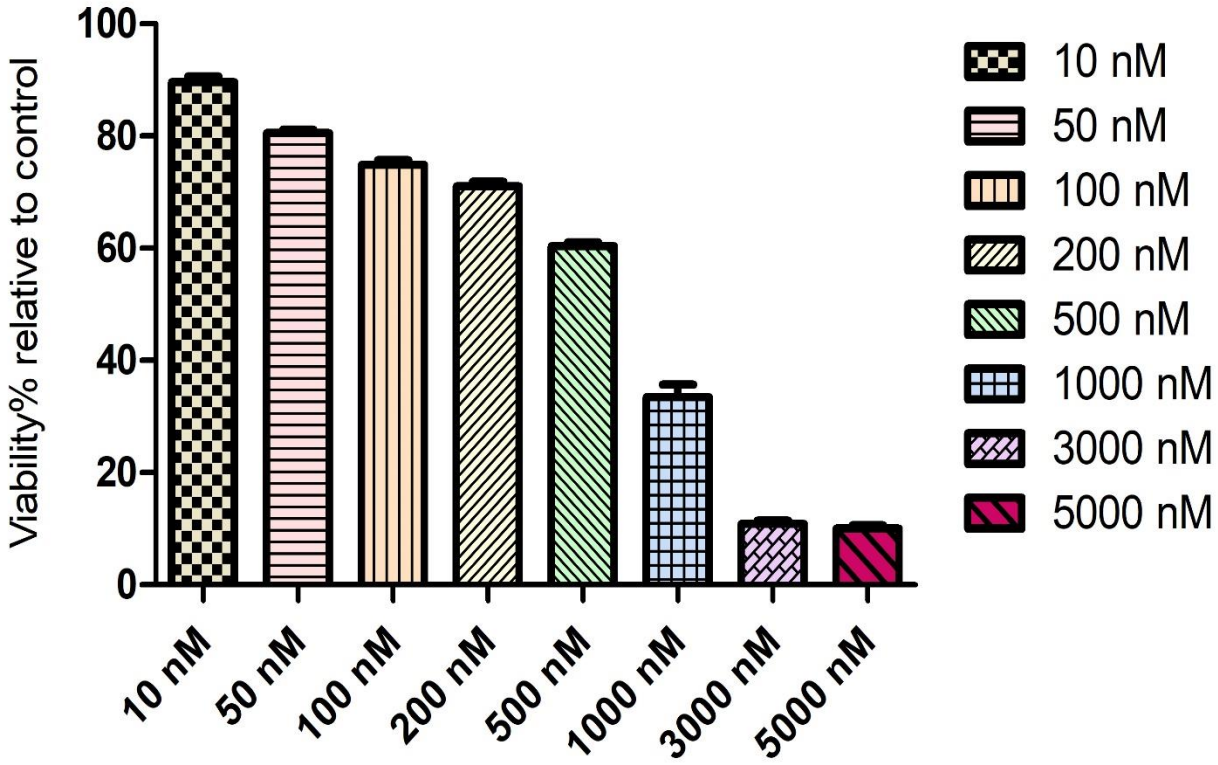

Figure 3.6 Cytotoxicity of PEI 10 KDa in B16BL6 melanoma cell line. (Values represent mean ± SD, N = 3).

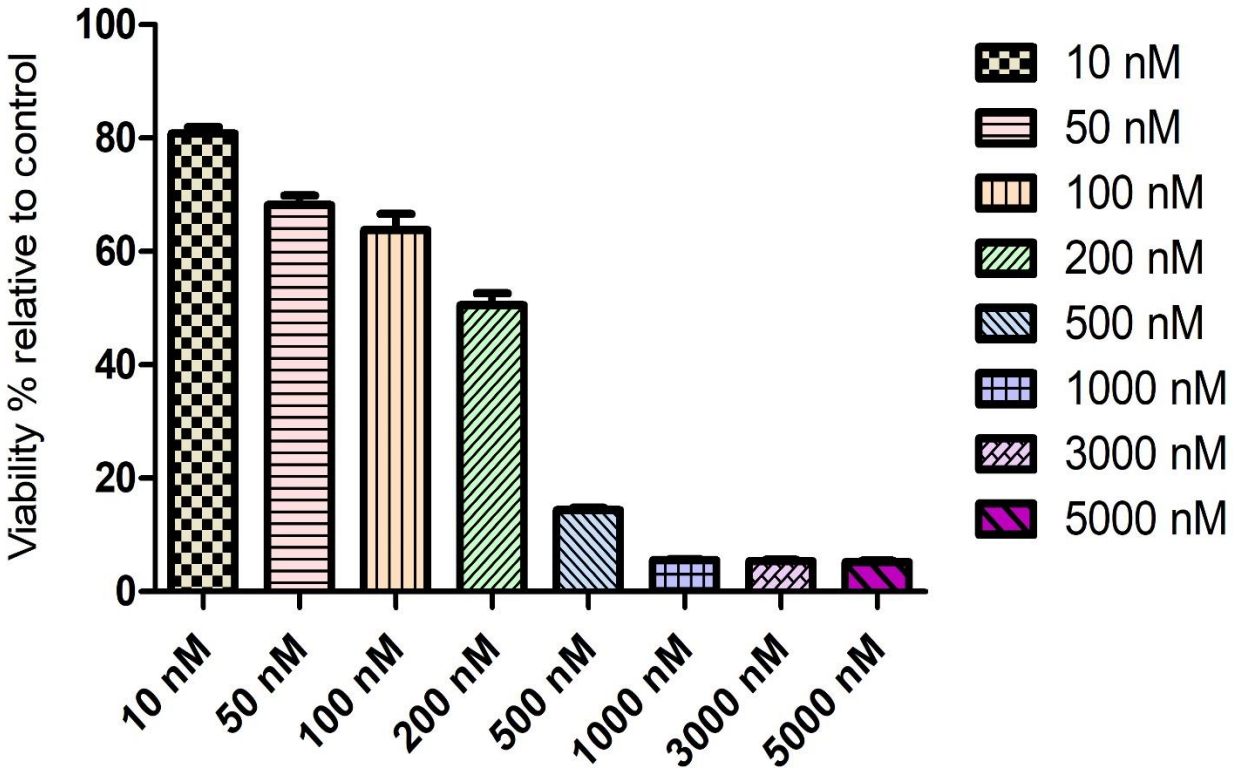

Figure 3.7 Cytotoxicity of PEI 25 KDa in B16BL6 melanoma cell line. (Values represent mean ± SD, n = 3).

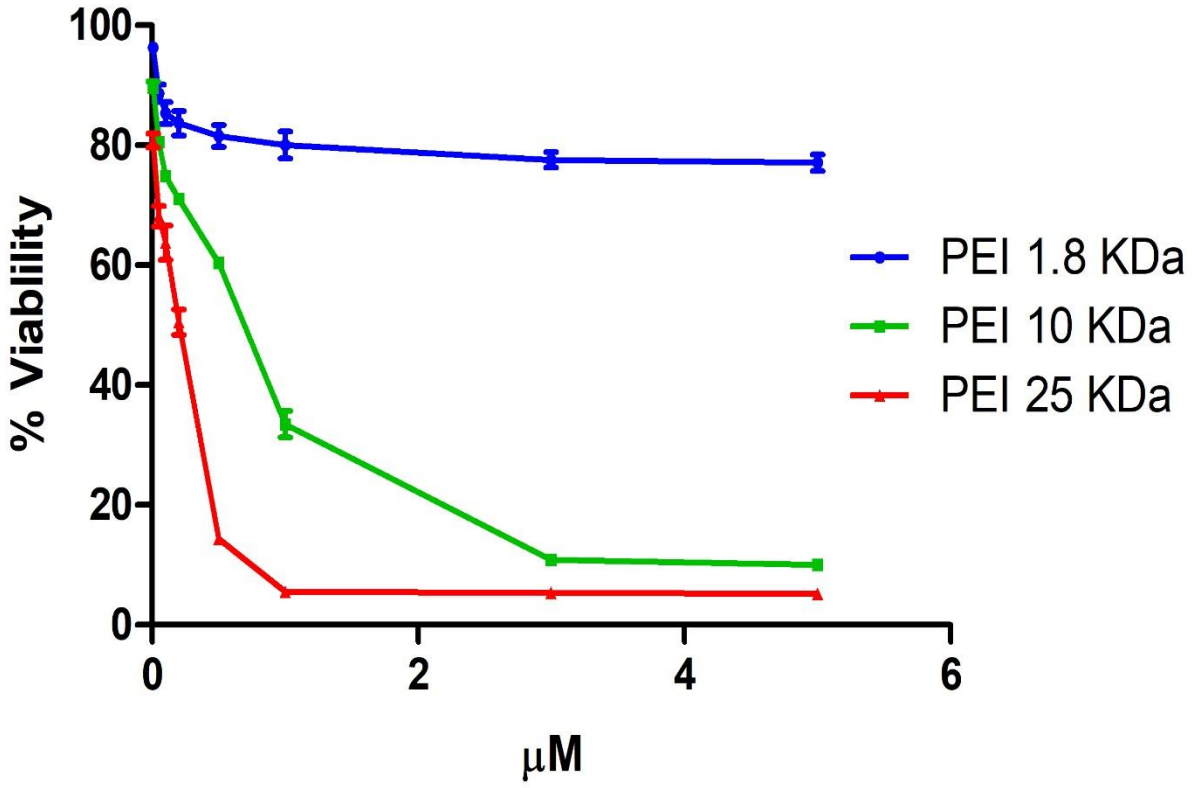

Figure 3.8 Comparion of toxcity profile of PEI in B16BL6 melanoma cell line.

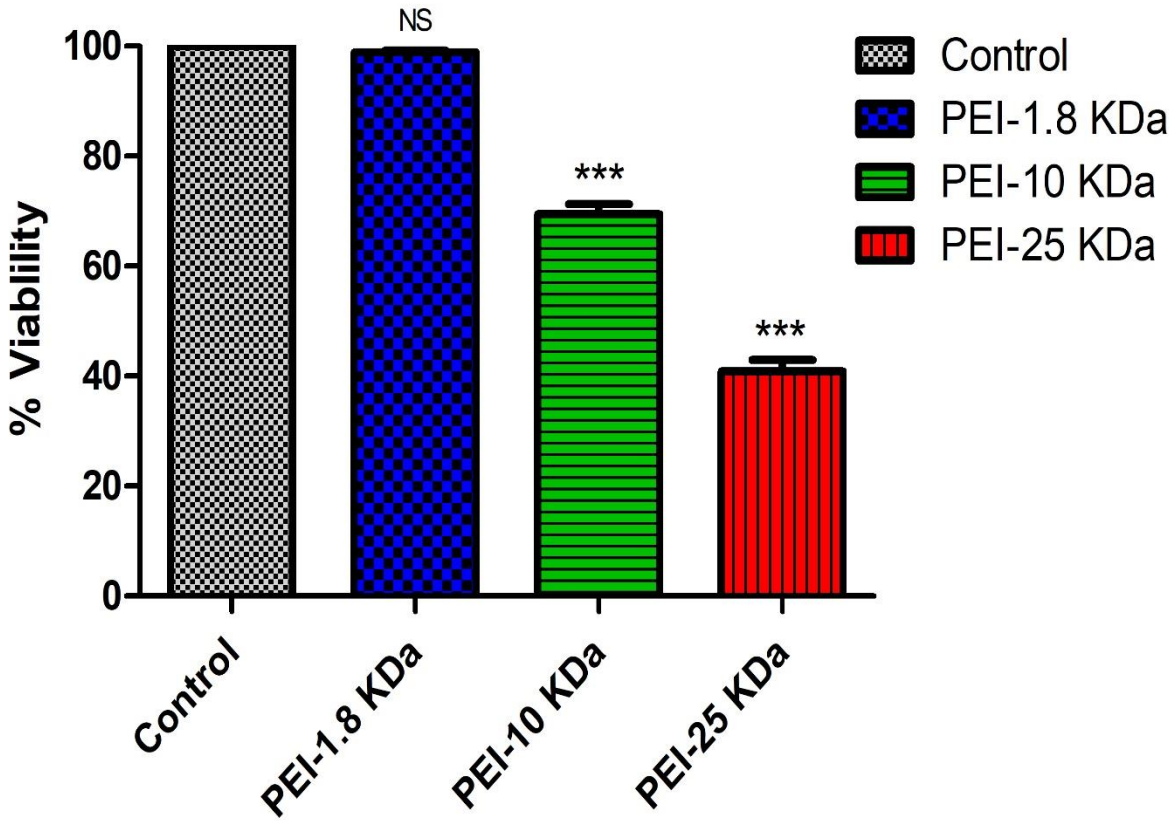

*Figure 3.9 Cytotoxicity of PEI-siRNA polyplexes at an optimal complexation based on N/P ratios in B16BL6 melanoma cell line. (Values represent mean ± SD, N = 3). Note:*** P<0.001 as compared to Control.*

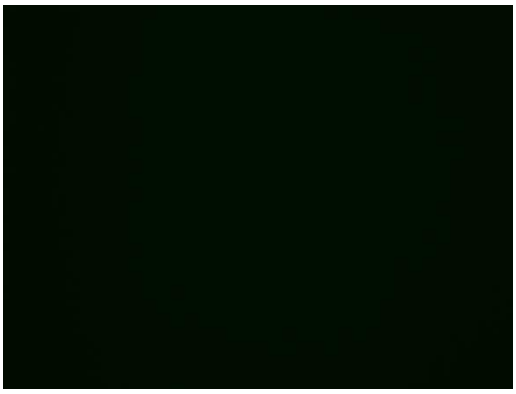

a. Cellular uptake of siRNA with no complexation

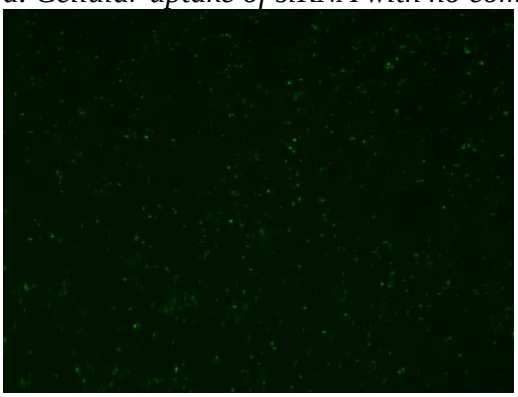

b. Cellular uptake of polyplex of siRNA with 1.8 KDa PEI

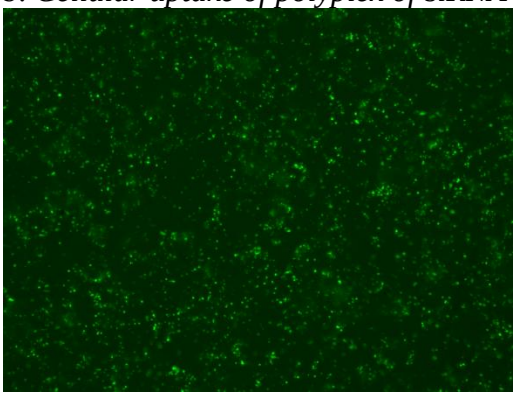

c. Cellular uptake of polyplex of siRNA with 10 KDa PEI

Figure 3.10 Cellular uptake PEI-siRNA nanoparticles into B16BL6 cells. a. siRNA alone (no PEI complexation), b. PEI 1.8 KDa at 50:1 of N/P ratio, and c. PEI 10 KDa at 10:1 of N/P ratio.

4. Acyclovir Nanogel Formulation for Enhanced Delivery across Human Cadaver Skin

4.1 Abstract

Purpose

Topical application of acyclovir is a common treatment for Herpes Labialis infection. Acyclovir demonstrates a poor skin permeability which limits the efficacy of this drug. There is a need to enhance the skin permeability of acyclovir into deep layers of skin and ultimately improve therapeutic efficacy in treating the infection. We formulated acyclovir nanoparticles based gel to enhance the drug permeation across human skin.

Methods

Acyclovir nanoparticles were prepared by ball milling method. The nano-suspension produced from ball milling was directly incorporated in carbopol® 974P NF polymer as a gelling agent. The nanogel was included with chemical penetration enhancers such as Ethanol (F3), Oleic acid (F4) or PG (F5). The particle size (P.S.) and polydispersity index (PDI) were determined by Nicomp ZLS380 Nanosizer. The nanogel viscosity was determined by Brookfield viscometer. Drug content and uniformity of acyclovir were determined by HPLC assay. In vitro release across regenerated cellulose membrane and permeation across dermatomed human cadaver skin (both normal and microneedle treated) for each formulation was studied using Franz diffusion cells and compared to the commercial product of acyclovir (Zovirax®).

Results

Ball milling produced acyclovir particle size of 270 nm with PDI of 0.321 (F1). These nanoparticles in the gel formulations (F1) showed a pH 6, viscosity 7177 cP (5 rpm), and drug content 24.9 mg/gm. All other developed formulations (with various skin permeation enhancers)

showed similar parameters with respect to particle size, polydispersity index, viscosity, drug content, and pH. The formulations F3 and F5 showed higher acyclovir release rate as compared to Zovirax®, F1 (control) or F4. In the skin permeation study, F1 formulation showed a skin permeation of 0.22 μg/cm^2/hr which is 2-fold higher than Zovirax® (0.111 μg/cm^2/hr). Incorporating 10 % ethanol (F3) in the formulation showed a synergistic permeation enhancement with 24-fold higher flux compared to Zovirax®. Inclusion of propylene glycol and oleic acid showed negligible penetration enhancement. However, microneedle treated skin showed a significant enhancement in the skin permeation as compared to passive diffusion for all formulations, F3 (10% ethanol) showed the highest enhancement skin permeation on microneedle treated skin.

Conclusion

Acyclovir nanogel formulations with ethanol as a penetration enhancer demonstrated a pronounced effect on enhancing skin permeability and drug content within deep layers upon topical application for either intact or microporated human skin. These results indicate that a nanogel formulation could be an effective treatment as a topical antiviral agent as compared to Zovirax®.

4.2 Introduction

Acyclovir is an analogue of a purine nucleoside with prospective activity as an antiviral agent, mainly via inhibiting viral DNA replication (Chaudhary et al., 2014; Ramyadevi et al., 2014). Acyclovir is very effective on treating Herps-Labialis infection caused by Herpes Virus simplex 1. Herps-Labialis infects the skin layers as well as lips and mouth area. It appears as blisters and causes severe pain which spontaneously disappears. Earlier manifestations represent a first episode of the disease progression, afterward the disease shows recurrent infection manifestation which could be triggered by environmental influences (UV-rays, cold temperature) or personal factors (psychological stress). These may last for a few days and subsequently disappear (Shukla et al., 2009). In this stage, the infection causes pain and discomfort in addition to the risk of infecting other people in direct contact with the patient (Siddoju et al., 2011). The infection is originated from ganglion nerves on the epidermis layer. Deep layers of epidermis represent the site of virus residency which raises the chances of recurrence disease manifestation under the effect of a trigger (Diez-Sales et al., 2005; Vaghani et al., 2010).

Despite the presence of new antiviral agents, acyclovir shows superiority in respect to its efficacy toward the recurrent infections. (Ramyadevi & Sandhya, 2014). In spite of its efficiency via non-topical routes, acyclovir has a limited bioavailability owing to the lower solubility, thus needing a very high oral dose (Jacobson, 1993; Talluri et al., 2008). For example, oral absorption of acyclovir is inconstant and incomplete with a low bioavailability (15-30%) and a quick clearance of around 3 hours (t1/2) (Kharia et al., 2014; Vaghani et al., 2010)**.** On the contrary**,** topical and transdermal delivery of acyclovir could provide advantages such as reduced dose and dose frequency and improved patient compliance (Patel et al., 2012; Zheng et al., 2012). However, currently available

topical acyclovir preparations show lack of efficiency on various viral infections. This due to low drug concentration in the skin layers (Parry et al., 1992; Volpato et al., 1998).

Zovirax® ointment is an FDA approved drug for the disease. Zovirax® is well known for its efficacy against Herpes Simplex Virus. Nevertheless, it displays less efficiency and low patient acceptance owing to the lower permeability of acyclovir across the skin in the affected areas (Gide et al., 2013; Masuda et al., 2012).

When an insoluble drug is formulated as nanoparticles, the drug dissolution and the thermodynamic activity are dramatically increased. The nanoparticles based formulation would enhance the permeability through various routes. The pathways are mainly through hair follicles, which increases the accumulation and the drug disposition in deeper layers of skin (Naves et al., 2017). In this study, we formulated nanoparticles in a gel for enhanced acyclovir permeation across human cadaver skin.

4.3 Materials and Methods

4.3.1 Materials

Acyclovir USP, Ethyl Alcohol 200 Proof USP, Polysorbate 80 USP-NF, and Trolamine USP-NF were obtained from Letco Medical, Decatur AL, USA. Carbopol® 974P USP-NF was obtained as a gift sample from Lubrizol, Wickliffe, OH, USA. Oleic acid and phosphate buffered saline (PBS) were purchased from Sigma-Aldrich, St. Louis, MO, USA. Propylene glycol was obtained as a gift sample from Croda Inc., NJ, USA. Ammonium acetate (HPLC Grade) was purchased from EMD Chemicals Inc., Gibbstown, NJ, USA. All other reagents were of HPLC grade.

4.3.2 Nanogel Formulation Preparations

A nanogel topical formula was prepared via suspending 5% of acyclovir in deionized water combined with 5% Tween 80 as a surfactant to enhance the dispersion of drug particles in the aqueous medium. The produced suspension was subjected to sonication for around 25 minutes. This suspension was subjected to ball milling in an in house designed equipment for four hours.

The ball milled nano-suspension was directly incorporated in Carbopol® 974P NF solution in water. The pH of the gel was adjusted to around 6.0 with Trolamine. In some cases, we have included in the nanogel formulation chemical penetration enhancers as shown in Table 2.

4.3.3 High-Pressure Liquid Chromatography for Samples Analysis

The HPLC system consisted of a Waters Alliance separation module and 2998 PDA detector. A Phenomenex C18 Luna column with 150 x 4.6 mm, 5 μm particles was used. The mobile phase consisted of (A) 0.2% formic acid in 20mM ammonium acetate in water, and (B) acetonitrile. The flow rate was 1.0 ml/min with a gradient elution as shown in Table 4.1. The detection wavelength was 254 nm and the run time was 15 minutes.

Table 4.1

Time (min)	**Solvent A** 20mM ammonium acetate with 2 ml/L formic acid	**Solvent B** Acetonitrile
0	99	1
2	99	1
5	50	50
8	50	50
10	99	1
15	99	1

4.3.4 Physiochemical Properties of Formulations

Particle size and polydispersity index (PDI) were measured by suspending each sample in deionized water with appropriate dilution. The measurement was performed with Nicomp ZLS380 Nanosizer. The PDI reflects the particle size distribution.

The nanogel viscosity was determined via a viscometer (model DV-II_, Brookfield, U.S.A.) using Spindle 51z. The reading was recorded in 30 seconds at various shearing stress values. The content and uniformity of acyclovir in the gel were determined by analyzing three samples from each nanogel formulation (top, middle and bottom of the vial). The samples (0.5 gm) were dissolved in 5 ml of 0.01 NaOH then made to volume with PBS for quantification by HPLC.

4.3.5 In Vitro Release Study

Acyclovir release from the nanogel formulations was performed using Franz diffusion cells. The diffusion cell apparatus used in this study (PermeGear, Bethlehem, PA) holds up to 6 diffusion cells in series. The apparatus has a motor to rotate magnetic beads at 600 rpm. Regenerated cellulose dialysis membrane with a molecular weight cut off 12,000 Daltons was used in the drug release studies. The membrane (pre-soaked in a buffer for 2 h) was mounted horizontally between the donor and receptor halves of the diffusion cell. The surface area of the membrane exposed to the formulation in the donor chamber was 0.64 cm^2, and the receptor cell volume was 5 ml. Approximately 100 mg of the formulation was applied on the membrane facing the donor chamber. The receptor chamber was filled with PBS pH 7.4 to mimic the physiological condition. The temperature of the jacket was maintained at 37±0.5 C^o. One millimeter of each sample was

withdrawn from receptor cell at 0, 1, 2, 4, 6, 8, 12 and 24 hours and analyzed for drug content by HPLC.

4.3.6 Skin Permeation Study

The skin permeation studies were conducted in the Franz diffusion cells as described under "drug release studies". Human skin dermatomed to ~ 0.35 mm thickness was obtained from a tissue bank (Science Care, Phoenix AZ). The skin was collected within 8 h of donor death and frozen at -70 degree C until use. The skin (1 inch x 1 inch blocks) was preserved using 50% glycerol as a cryopreservation medium. Each experiment was carried out with each formulation for at least 3 times using the skin from one donor. The frozen skin was thawed to room temperature by keeping the skin at ambient temperature for about 20 minutes. The washed skin was mounted on the cells with an epidermal surface facing the donor compartment approximately 30 minutes before the application of the formulations. The receptor chamber was filled with (5 ml) PBS. The formulation (100 mg) was applied to the surface of the epidermis gravimetrically using a syringe and occluded with Parafilm™. Periodic samples (1.0 ml) were taken from the receptor cell to measure the amount of drug transporting across the skin (0, 1, 2, 4, 6, 8, 12, and 24hours). All samples were analyzed by a validated HPLC method.

4.3.7 Drug Retention on Skin Layers

At the end of the skin permeation study, the residual drug remaining on the surface of the skin was removed by cotton swabs and by washing the surface with PBS pH 7.4. The skin surface was gently wiped with a cotton swab (Q-tips® Uniliver USA, Englewood Cliffs, NJ), 200 µl of the above buffer was added on the skin surface and the liquid was dabbed with a fresh (dry) cotton swab. This process of swabbing and dabbing was repeated 5 times. The active diffusion area was

collected with a biopsy punch (George Tiemann & Co, Hauppauge, NY) and the skin was weighed and minced with a pair of sharp point dissecting scissors into a glass vial. To these glass vials, 1 ml of above buffer was added, sonicated for 15 min. and allowed to stand overnight. The samples were sonicated again for 30 min. The samples were filtered through 0.45 µm membrane filter and the supernatants were diluted appropriately and analyzed by HPLC.

4.3.8 Permeation and Retention Studies across Microporated Skin

The skin was microporated using the metallic microneedle arrays from a Dermaroller™ (Dermaoller Deutschland s.a.r.l., Wolfenbuttel, Germany). The skin was subjected to 20 Dermaroller™ passes. The permeation and drug retention studies were conducted by the methods described in the previous sections.

4.3.9 Statistical Analysis

All results are presented as mean ± standard deviation. The statistical analysis was performed using GraphPad Prism version 5, GraphPad Software, Inc., La Jolla, CA). The data were subjected to one-way ANOVA followed by Tukey –Kramer multiple comparisons test. The mean differences were considered significant at $P < 0.05$.

4.4 Results and Discussion

Acyclovir nanoparticles were produced by a top-down approach utilizing a wet ball mill technique. Using this method, we were able to attain drug particles in the nanosize range for various batches. The mean particle diameter (d50) was in the range of 163-317 nm, and the PDI was within the acceptable limit of <0.5%. Different formula compositions are listed in Table 4.2. The F1 formulation was prepared without the addition of a penetration enhancer. Acyclovir particle size (d50) for this formulation was 270 nm with a PDI of 0.3. The pH of this formulation was around

6, and the viscosity was 7177 (cP). The acyclovir content of the gel was 99.6%, suggesting uniform drug distribution. Based on F1 composition we have slightly modified the formula composition to include selected skin penetration enhancers (F3, ethanol; F4, oleic acid and F5 propylene glycol) (Table 4.2). The formulations F3, F4 and F5 provided satisfactory results on particle size, polydispersity index, pH, viscosity and drug content. Oleic acid (F4) was chosen because of its potent effect on skin penetration as it increases the fluidity of the lipid component of SC and enhances the permeation across skin layers (Zhu et al., 2008). The physicochemical characterization of the formulation exhibited comparable properties with respect to particle size, polydispersity index, drug content and pH. However, F4 showed the lowest viscosity (6535 cP at 5 RPM) among all prepared formulations with the same percentage of the gelling agent. The lower viscosity might be a result of the oily nature of oleic acid which interacts with Carbopol and weakens its ability to form a gel. Formulations F3, F4 and F5 showed similar particle size, polydispersity index, viscosity, drug content and pH value (Table 4.3).

Drug release studies were conducted on various formulations as the gel matrix plays a role in drug retention (Diez-Sales et al., 2005). It is also essential to determine if the gel is able to release the incorporated drug for percutaneous absorption. Figure 4.1 describes the drug release from various formulations. All formulations showed a similar biphasic drug release pattern; an initial fast release up to 8 hours (F1, F4 and Zovirax®) or up to 12 hours (F3 and F5) followed by a slower release up to 24 hours. The lowest release of F4 may be due to the affinity of acyclovir to oleic acid. F3 and F5 showed higher releasing rate compared to F1. The higher release by F3 and F5 compared to F4 can be explained by the use of polar solvents (ethanol, and propylene glycol, respectively) which do not interfere with the release of drug from the formulations as with oleic acid.

Figure 4.2 illustrates permeation profiles of various acyclovir nanogel formulations across dermatomed human skin. F1 showed higher skin permeation with a flux of 0.22 μg/cm^2/hr which is 2-fold higher than Zovirax® (0.111 μg/cm^2/hr). Ethanol (F3) provided a dramatic increase in skin permeation (24-fold 2.68 μg/cm^2/hr) as compared to Zovirax®. F3 showed profound enhancement effect in comparison to F1, F4, F5 and Zovirax® ($P<0.01$). The formulations F4 and F5 did not show a significant increase in skin permeation relative to Zovirax® or F1. The enhancement effect of F3 formulation can be due to fluidization of lipid structure of the SC particularly via interaction with a polar head group of the lipids. This leads to enhance a drug transportation and accumulation across skin layers since the main barrier is the stratum corneum (Scognamiglio et al., 2013). Despite reported permeation enhancement effect of PG, in our study it did not enhance acyclovir permeation across human skin. Similar observation has been reported in another study when they used PG as co-solvent to enhance the permeability of acyclovir in vitro using hairless rat skin (Siddoju et al., 2012).

The skin retention levels of various formulations are shown in Figure 4.3. F1 (nanogel, no enhancer, control) showed a 20-fold higher skin level while F3, F4 and F5 showed 37, 22 and 2.7-fold higher skin levels than Zovirax®, respectively. The formulation F3 (ethanol as enhancer) showed 1.8-fold higher skin levels than F1 (no enhancer). Overall, the nanogel formulation greatly facilitates the accumulation of the drug in the skin as compared to Zovirax®.

In order to understand the mechanism of skin permeation enhancement by nanogel formulations, we conducted permeation studies across microneedle treated skin and the data are shown in Figure 4.4. The microporation provided a dramatic increase in the skin permeation as expected. The microneedles create pores across the stratum corneum enabling the drug to cross the barrier. It is

interesting to note that the formulation F3, which showed the highest flux by passive delivery, also showed the highest flux across microporated skin among all the formulations tested. Furthermore, F3 showed a 2-fold higher flux by microporation as compared to passive delivery. This study demonstrates the barrier nature of SC for acyclovir permeability. F5 had the lowest skin permeation by passive delivery but showed a huge increase in the permeation across microporated skin. It is interesting to note that microporated skin showed significantly lower skin levels of acyclovir as compared to passive delivery (Figure 4.5), except F4, which showed a higher skin level in the microporated skin. Zovirax® showed a higher skin level with micorporated skin; whereas F1, F3 and F4, showed lower levels versus passive delivery.

Overall, nanogel based formulations demonstrated a significantly higher skin permeation and skin levels compared to Zovirax®. This formulation should provide improved therapeutic value for acyclovir as a topical antiviral agent.

4.5 Conclusion

Acyclovir as a nanogel formulation based on a Carbopol gel matrix was effective in enhancing the drug permeability and accumulation within dermatomed human cadaver skin. Ethanol was very effective as a skin penetration enhancer for acyclovir. On the other hand, microporated skin showed variable flux results relative to passive permeation.

4.6 References:

Chaudhary, B., & Verma, S. (2014). Preparation and evaluation of novel in situ gels containing acyclovir for the treatment of oral herpes simplex virus infections. *Sci. World J., 2014,* 280928. doi:10.1155/2014/280928

Diez-Sales, O., Garrigues, T. M., Herraez, J. V., Belda, R., Martin-Villodre, A., & Herraez, M. (2005). In vitro percutaneous penetration of acyclovir from solvent systems and Carbopol 971-P hydrogels: influence of propylene glycol. *J Pharm Sci, 94*(5), 1039-1047. doi:10.1002/jps.20317

Gide, P. S., Gidwani, S. K., & Kothule, K. U. (2013). Enhancement of transdermal penetration and bioavailability of poorly soluble acyclovir using solid lipid nanoparticles incorporated in gel cream. *Indian J Pharm Sci, 75*(2), 138-142.

Jacobson, M. A. (1993). Valaciclovir (BW256U87): the L-valyl ester of acyclovir. *J Med Virol, Suppl 1*, 150-153.

Kharia, A. A., & Singhai, A. K. (2014). Effective parameters for formulation of gastro adhesive nanoparticles: screening by design-of-experiments approach. *J Microencapsul, 31*(4), 399-405. doi:10.3109/02652048.2013.863398

Masuda, T., Yoshihashi, Y., Yonemochi, E., Fujii, K., Uekusa, H., & Terada, K. (2012). Cocrystallization and amorphization induced by drug-excipient interaction improves the physical properties of acyclovir. *Int J Pharm, 422*(1-2), 160-169. doi:10.1016/j.ijpharm.2011.10.046

Naves, L., Dhand, C., Almeida, L., Rajamani, L., Ramakrishna, S., & Soares, G. (2017). Poly(lactic-co-glycolic) acid drug delivery systems through transdermal pathway: an overview. *Prog Biomater*. doi:10.1007/s40204-017-0063-0

Parry, G. E., Dunn, P., Shah, V. P., & Pershing, L. K. (1992). Acyclovir bioavailability in human skin. *J Invest Dermatol, 98*(6), 856-863.

Patel, K. K., Kumar, P., & Thakkar, H. P. (2012). Formulation of niosomal gel for enhanced transdermal lopinavir delivery and its comparative evaluation with ethosomal gel. *AAPS PharmSciTech, 13*(4), 1502-1510. doi:10.1208/s12249-012-9871-7

Ramyadevi, D., & Sandhya, P. (2014). Dual sustained release delivery system for multiple route therapy of an antiviral drug. *Drug Deliv, 21*(4), 276-292. doi:10.3109/10717544.2013.839368

Scognamiglio, I., De Stefano, D., Campani, V., Mayol, L., Carnuccio, R., Fabbrocini, G., De Rosa, G. (2013). Nanocarriers for topical administration of resveratrol: a comparative study. *Int J Pharm, 440*(2), 179-187. doi:10.1016/j.ijpharm.2012.08.009

Shukla, C., Friden, P., Juluru, R., & Stagni, G. (2009). In vivo quantification of acyclovir exposure in the dermis following iontophoresis of semisolid formulations. *J Pharm Sci, 98*(3), 917-925. doi:10.1002/jps.21474

Siddoju, S., Sachdeva, V., Friden, P. M., & Banga, A. K. (2011). Iontophoretic delivery of acyclovir: intradermal drug monitoring using microdialysis and quantification by skin extraction. *PDA J Pharm Sci Technol, 65*(5), 432-444. doi:10.5731/pdajpst.2011.00756

Siddoju, S., Sachdeva, V., Friden, P. M., & Banga, A. K. (2012). Evaluation of acyclovir cream and gel formulations for transdermal iontophoretic delivery. *Ther Deliv, 3*(3), 327-338.

Talluri, R. S., Samanta, S. K., Gaudana, R., & Mitra, A. K. (2008). Synthesis, metabolism and cellular permeability of enzymatically stable dipeptide prodrugs of acyclovir. *Int J Pharm, 361*(1-2), 118-124. doi:10.1016/j.ijpharm.2008.05.024

Vaghani, S. S., Gurjar, M., Singh, S., Sureja, S., Koradia, S., Jivani, N. P., & Patel, M. M. (2010). Effect of iontophoresis and permeation enhancers on the permeation of an acyclovir gel. *Curr Drug Deliv, 7*(4), 329-333.

Volpato, N. M., Nicoli, S., Laureri, C., Colombo, P., & Santi, P. (1998). In vitro acyclovir distribution in human skin layers after transdermal iontophoresis. *J Control Release, 50*(1-3), 291-296.

Zheng, D., Giljohann, D. A., Chen, D. L., Massich, M. D., Wang, X. Q., Iordanov, H., Paller, A. S. (2012). Topical delivery of siRNA-based spherical nucleic acid nanoparticle conjugates for gene regulation. *Proc Natl Acad Sci U S A, 109*(30), 11975-11980. doi:10.1073/pnas.1118425109

Zhu, W., Yu, A., Wang, W., Dong, R., Wu, J., & Zhai, G. (2008). Formulation design of microemulsion for dermal delivery of penciclovir. *Int J Pharm, 360*(1-2), 184-190. doi:10.1016/j.ijpharm.2008.04.008

Table 4.2 Composition of nanogel formulations

Ingredient %	**F1**	**F3**	**F4**	**F5**
Acyclovir	5.00	5.00	5.00	5.00
Carbopol 974p	0.50	0.50	0.50	0.50
Polysorbate 80	5.00	5.00	5.00	5.00
Trolamine	0.35	0.35	0.35	0.35
Ethanol	-	10.00	10.00	-
Oleic acid	-	-	5.00	-
PG	-	-	-	10.00
Water	**89.15**	**79.15**	**74.15**	**79.15**

Table 4.3 Physical properties of nanogel formulations

Formula	**F1**	**F3**	**F4**	**F5**
Particle size (nm)	270	317	314	163
Particle Size distribution (PI)	0.321	0.284	0.235	0.140
pH	6.03	6.50	6.40	6.09
Viscosity (cP)	7177	7477	6535	9362
Drug Content %	99.6	100.5	101.0	100.8

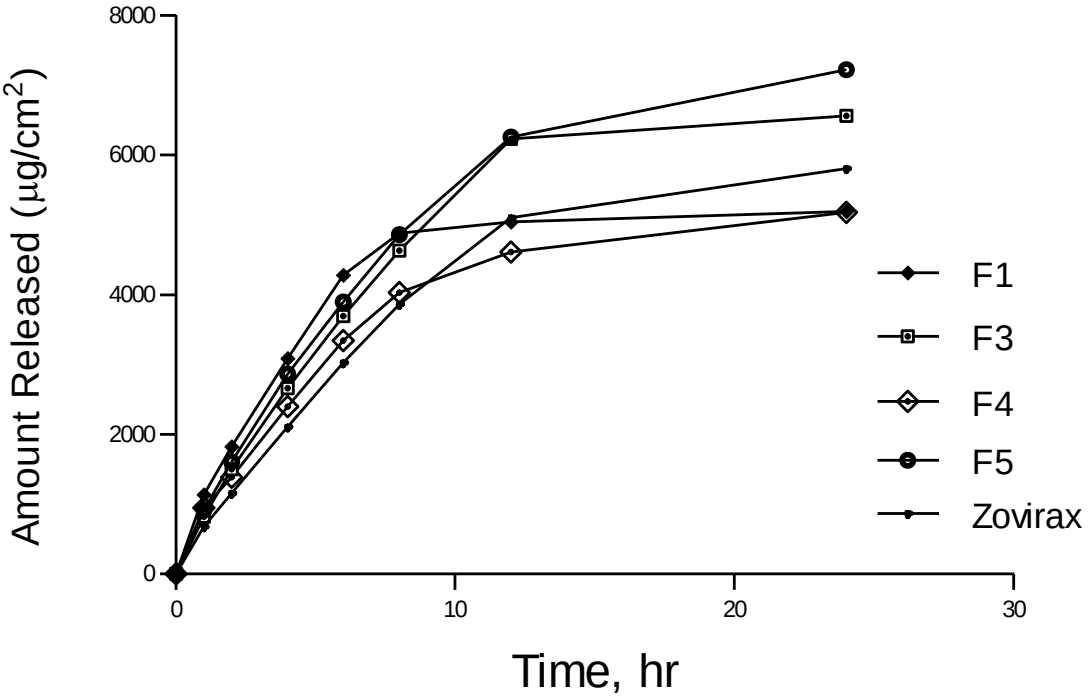

Figure 4.1 In vitro release across dialysis membrane. Each study was performed in triplicate (N=3).

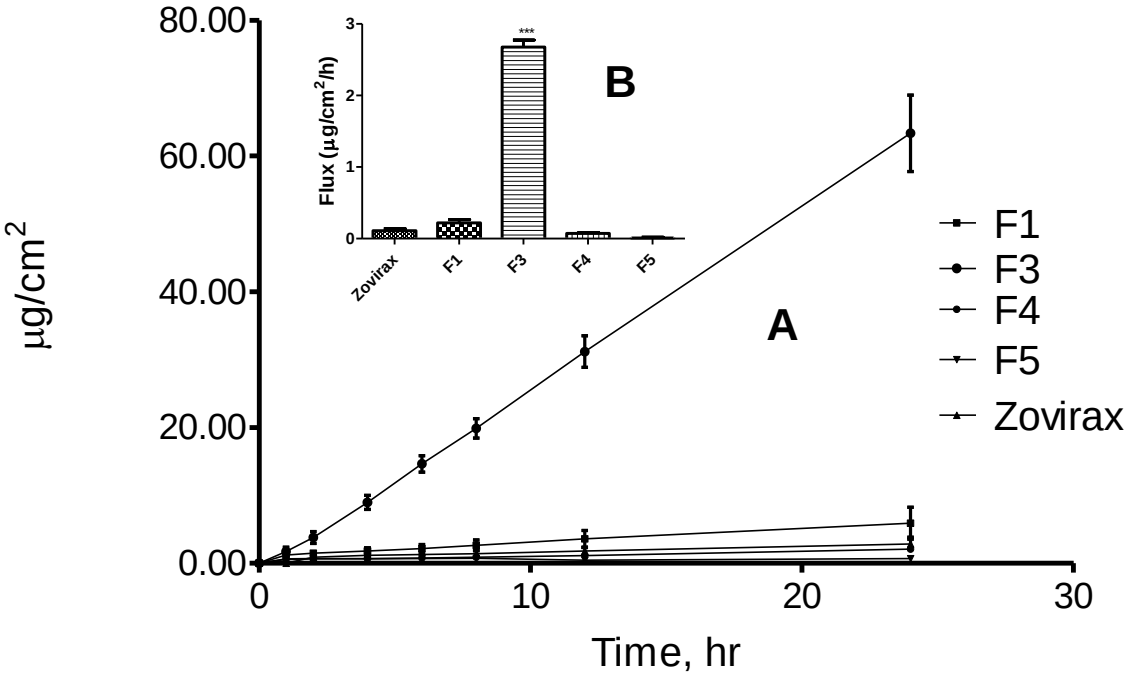

*Figure 4.2 Passive skin permeation: A. Passive skin permeation: A. Skin permeation for F1, F3, F4, F5 and Zovirax®. B. Flux of F1, F3, F4, F5 and Zovirax®. Each formula was evaluated in triplicate (N=3). Note: *** P<0.001 as compared to Zovirax®.*

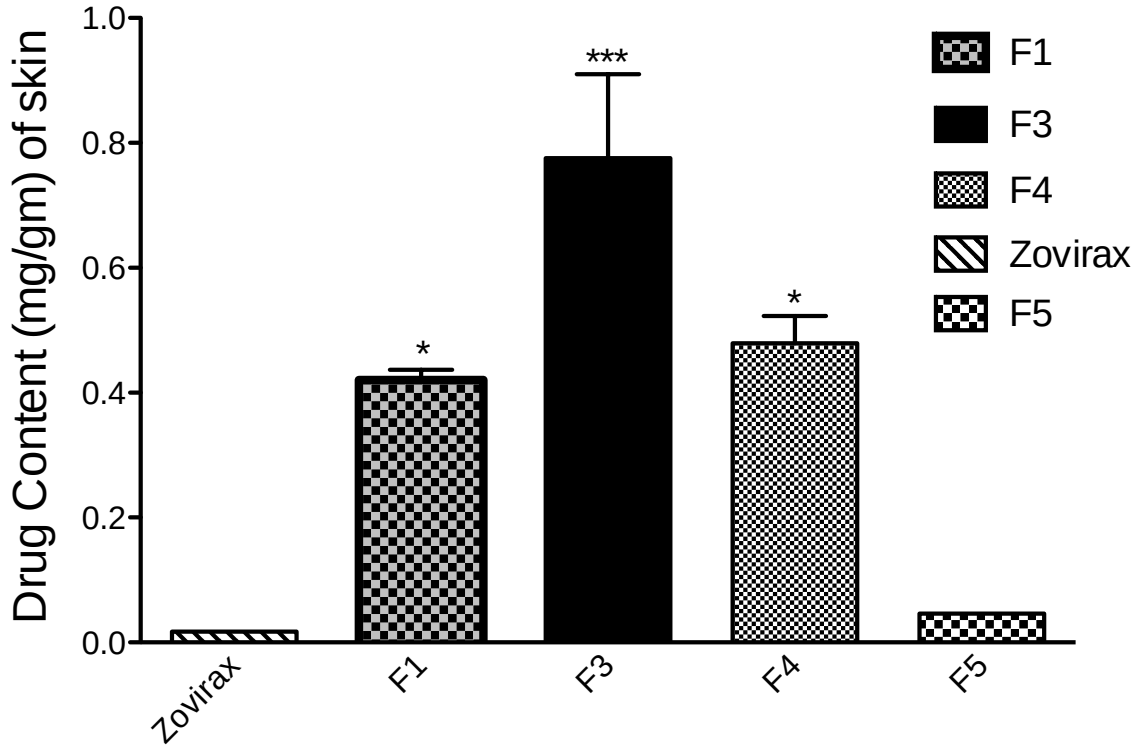

*Figure 4.3 Acyclovir retention within skin for passive permeations. Each formula was evaluated in triplicate (N=3). Notes: *p < 0.05 as compared with Zovirax®.; *** P<0.001 as compared to Zovirax®.*

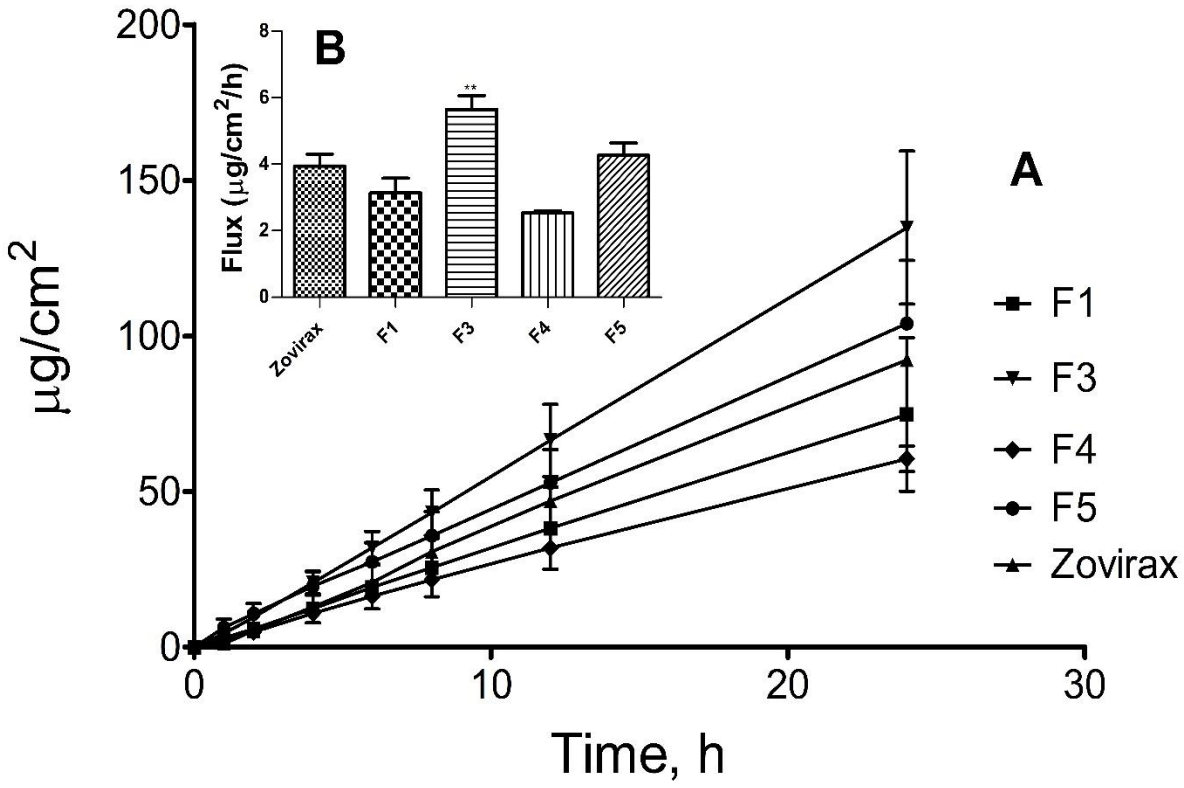

*Figure 4.4 Microneedle treatment for percutaneous permeation: A) Skin permeation. B) Flux. Each formula was evaluated in triplicate (N=3). Note: **p < 0.01 as compared with Zovirax®.*

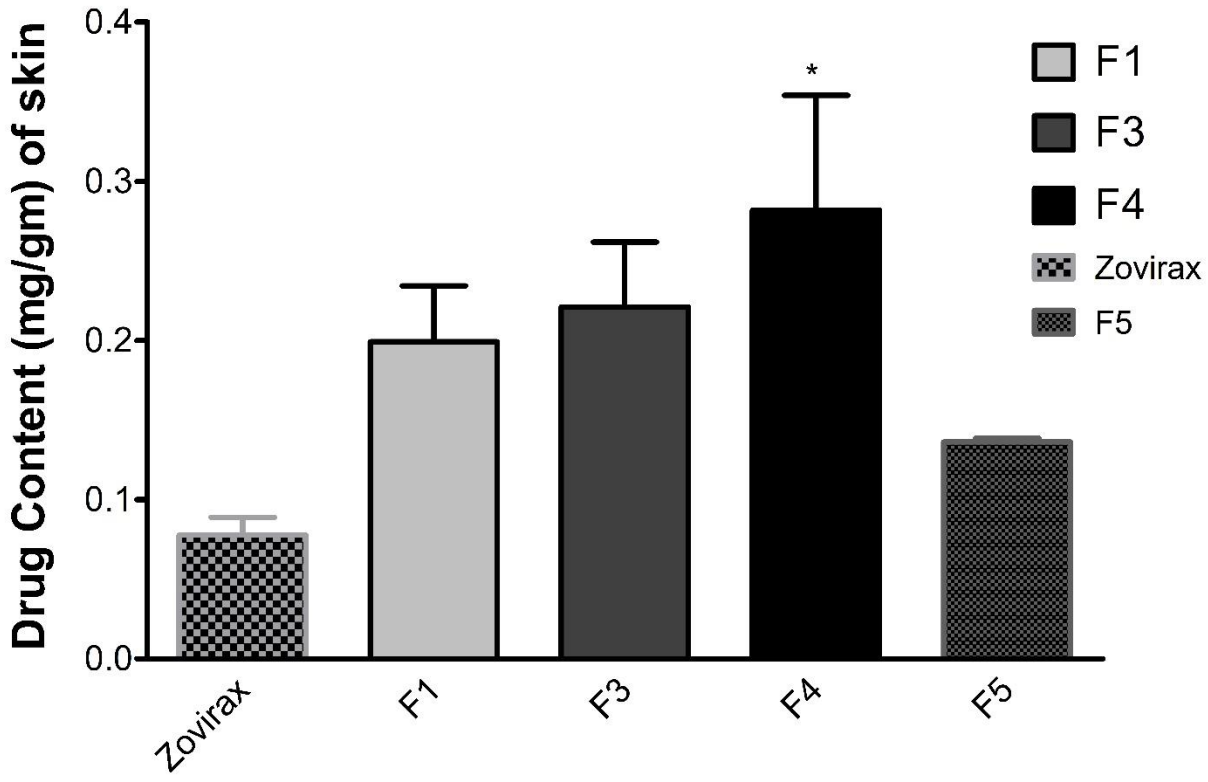

*Figure 4.5 Acyclovir content within skin for microporated permeation. Each formula was evaluated in triplicate (N=3).: *p < 0.05 as compared with Zovirax®.*

5. Pharmacokinetic Evaluation of a Novel Buccal Midazolam Gel in Healthy Dogs

5.1 Abstract

Objective: To determine the physical properties of the gels on the pharmacokinetics of novel midazolam buccal gel formulations in comparison to intravenous (IV) midazolam solution in healthy dogs. The effect of two different gel dosages on plasma midazolam levels following buccal administration was studied.

Animals: Five healthy adult hound dogs (three females, two males)

Procedure: Midazolam buccal gels were formulated with Pluronic F127 (T18) or hydroxyl propyl methylcellulose (HPMC) K100M (T19) as the base polymers. Based on the promising release and pharmacokinetic data, the T19 gel was reformulated with increased midazolam concentrations and higher gel viscosity (T29). The formulations (T18, T19, T29 and a commercially available 5 mg/mL midazolam hydrochloride IV solution) were administered once to each hound at a dose of 0.3 mg/kg with at least three days between the administration of different formulations. Similarly, T29 was administered at a higher dose of 0.6 mg/kg. Blood samples were collected at various time points and drug levels were quantified via liquid chromatography–tandem mass spectrometry.

Results: The formulations T19 and T29 with significantly higher release rates than T18 were also effectively absorbed through buccal administration in dogs. Following buccal administration at a dose of 0.3mg/kg, T19 and T29 produced a C_{max} of 98.3±26.5 and 106.3±35.2 ng/ml respectively, which are approximately two-fold higher as compared to T18 (47.7±38.5 ng/ml). Furthermore, T29 at higher dose (0.6mg/kg) produced a C_{max} of 187.0±104.3ng/mL.

Conclusions and Clinical Relevance: Results of this study show promise for buccal administration of midazolam gel, but further evaluation of the efficacy of this medication in a clinical setting are needed prior to recommendations for routine use.

5.2 Introduction

Seizures are the most common manifestation of neurologic disease in small animals (Munana, 2013). While most seizures are isolated self-limiting episodes, status epilepticus and cluster seizures are two conditions that require more urgent medical intervention (Lowenstein et al., 1999; Monteiro et al., 2012; Saito et al., 2001). Status epilepticus is a life-threatening condition characterized by generalized seizures lasting longer than five minutes or two seizures occurring in tandem without an interictal recovery of consciousness. Cluster seizures are defined as two or more seizures occurring in a 24-hour period with return to normal mentation between each event (Mariani, 2013).

In the hospital setting, intravenous benzodiazepine administration is considered the first line of therapy for status epilepticus (Dewey, 2006). In non-hospital settings, where intravenous access is nearly impossible, alternative routes of drug administration are necessary. The use of rectal diazepam is well established in both human and veterinary medicine (Baysun et al., 2005; Bhattacharyya et al., 2006; Nakken et al., 2011; Podell, 1995). Unfortunately, variable absorption and a prolonged onset of action have been reported for rectal administration for both diazepam (Probst et al., 2013) and midazolam (Schwartz et al., 2013). Intranasal dosing of benzodiazepines in veterinary patients has also been reported (Eagleson et al., 2012; Musulin et al., 2011; Platt et al., 2000). This method is generally more pleasant for owners with the added advantage that hepatic first-pass effects, encountered with drug administration in the cranial portion of the colon, are avoided (Musulin et al., 2011; Schwartz et al., 2013). Limitations for intranasal administration lie in the volume of medication that can be administered without pharyngeal runoff and the potential for patients to sneeze following administration (Eagleson, Platt et al., 2012; Musulin,

Mariani et al., 2011; Platt, Randell et al., 2000). Additionally, in veterinary medicine, nasal administration of drugs can be difficult due to the small size of the nares in many dogs and cats.

In human patients, buccal administration of midazolam is another route of administration that circumvents the high first-past effect of rectal or oral dosing (Scott et al., 1999). Buccal midazolam in epileptic adults and children is reported to be both efficacious and well tolerated (Baysun, Aydin et al., 2005; Camfield, 1999; Kutlu et al., 2003; McIntyre et al., 2005; Scott, Besag et al., 1999; Talukdar et al., 2009; Wiznitzer, 2005). There is one previous veterinary report of oral mucosal absorption of midazolam, but the administration was completed on anesthetized animals using an unknown dosage (Zhang et al., 2002). A pH-dependent absorption of this medication was determined, with greater levels of absorption reported for formulations with a pH between 3 and 4 (Zhang et al., 2002).

There is a need in veterinary medicine to be able to provide veterinarians and owners with a safe, reliable and easy treatment solution for their pet when experiencing acute repetitive seizures in the clinic or at-home environment. Based on this, the purpose of the current study was to demonstrate the safety and pharmacokinetics of novel gel-formulations of midazolam after buccal administration in healthy dogs and compared to intravenous administration of a commercially available midazolam solution. A secondary objective was to determine the effect of different dosages on plasma midazolam levels following buccal administration. We hypothesized that a suitably formulated midazolam gel would provide rapid detectable plasma levels following buccal administration.

5.3 Materials and Methods:

5.3.1 Materials

All solvents and chemicals used in the preparation of formulations were procured from Letco Medical, Decatur, AL and PCCA, Houston, TX. Methocel™ K100M HPMC provided as a gift sample by Colorcon Inc, Montgomeryville PA. Prepared in-house using a Milli-Q water purifier system, Millipore Elix, Germany. Trapasol® HP-beta- was obtained from CD, CTD Inc, Alachua, FL. CVO 100 Bohlin Rheometer, Malvern Instruments, Southborough, MA. PermeGear Bethlehem, PA. Alliance 2695 Separation module and 2998 PDA detector. Phenomenex, Luna® C18, Phenomenex Inc., Torrance, CA. All chromatographic solvents and reagents were procured from VWR International, Suwannee, GA. Agilent 1290 UHPLC system, Agilent Technologies, Santa Clara, CA. Agilent 6460 triple quadrapole mass spectrometer, Agilent Technologies, Santa Clara, CA. Zorbax SB-C8 column, Agilent Technologies, Santa Clara, CA. GraphPad Prism software version 3, GraphPad Software, Inc., La Jolla, CA

5.3.2 Study Design

In the first phase, buccal gel formulations T18 and T19 containing 1% midazolam were developed and administered to dogs. Based on the pharmacokinetic data, the formulation T19 was further optimized by increasing the midazolam loading to 2% in a more viscous formulation T29, and a second pharmacokinetic study was performed. The time gap between the first and second pharmacokinetic study was 2 months on the same group of dogs.

5.3.3 Preparation of Formulations

The formulation compositions are given in Table 5.1. The Pluronic gel (T18) was prepared using Pluronic F127 (Poloxamer 407) as the base polymer. Midazolam (1%) was dissolved in ethanol.

Phosphoric acid (diluted 50:50 with deionized water, 43.3%) was added to maintain the solubility of midazolam in the formulation. Pluronic 30% aqueous gel (F127) as a cold solution (4ºC) was added to the alcoholic solution of midazolam and mixed for 15 min.

The HPMC gel (T19 or T29) was prepared using HPMC K100M as a base polymer which forms a strong gel at low concentrations. Midazolam (1% and 2% in T19 and T29, respectively) was dissolved in ethanol. Phosphoric acid (diluted 50:50 with deionized water, 43.3%) was added to maintain the solubility of midazolam in the formulation. HPβCD was dissolved in water (50% w/w) under stirring and added to the midazolam solution. HPMC K100M was dissolved in water (3%) and added to the drug solution under stirring for 15 min.

5.3.4 Rheology Evaluation of Gel Formulations

The rheological properties were studied using CVO 100 Bohlin rheometer. cone-plate geometry arrangement with an angle 2° and 40 mm of diameter. One milliliter of each sample was withdrawn by a syringe and placed in the cone for evaluation. The gap between the cone and plate was 1 mm. Samples were allowed to stabilize for 5 min before conducting rheological measurements such as equilibration time after loading the sample on the sensor system. The measurements were performed with an increasing ramp of shear rates between 0.1 s−1 and 100 s−1 for 100 s, remaining at 150 s−1 for 120 s, and finally descending from 100 s−1 to 0.1 s−1 for 100 s. All assays were performed in triplicate at different temperatures (25, 30, 35, 40, 50oC). The output shear rate was converted to revolutions per minute (Shear rate = C2 x angular velocity, where C2 = 14.324).

5.3.5 In Vitro Release of Midazolam across Dialysis Membrane

The diffusion cell apparatus used in this study holds up to 6 diffusion cells in series. The apparatus has motor to rotate magnetic beads at 600 rpm. The regenerated cellulose membrane (molecular weight cut-off 12,000) was soaked in 0.01 M PBS (pH 7.4) solution for an hour prior to use. The membrane was mounted horizontally between the donor and receptor halves of the diffusion cell. The surface area of the dialysis membrane exposed to the formulation in the donor chamber was 0.64 cm^2, and the receptor cell was filled with 5 ml of PBS pH 7.4. A water circulation jacket (37 ^oC) surrounds the receptor cell in order to control the temperature at physiologic level. The donor chamber was covered with a Parafilm M®. The experiment was carried out with each formulation for at least 3 times. The formulation (~50 mg) was placed on the dialysis membrane gravimetrically using a syringe. At predetermined time points (0, 1, 2, 4, 6, 8, 12, and 24 hours) the whole receptor medium was collected and replaced with the fresh PBS pH 7.4. This ensures sink condition for midazolam in the experiment. The midazolam content of the samples was assayed by HPLC as described later.

5.3.6 In Vivo Buccal Administration in Dogs

Five purpose-bred research hounds (three females and two males) weighing between 16.9 and 22.4 kg were used for the study. Serum biochemistry profiles and complete blood cell counts were completed and found to be unremarkable in all dogs prior to the study. All in vivo procedures were conducted in accordance with protocols approved by the University of Georgia's Institutional Animal Care and Use Committee.

All four midazolam formulations (T18, T19 and T29 buccal gel formulations and a commercially available 5 mg/mL midazolam hydrochloride intravenous solution) were administered once to each

hound at a dose of 0.3 mg/kg with at least three days between the administration of different formulations. The gel was pre-loaded into syringes and required 1.0 to 1.3 ml volume based on the weight of dogs. One of the formulations, T29 required half the volume because this formulation has double midazolam concentration (2%). The half-life of midazolam following intravenous administration of a dosage of 0.2mg/kg in the dog has been reported as up to 161minutes with this washout period of three days far exceeding seven to ten half-lives (Eagleson et al., 2012). The T29 buccal gel formulation was also administered an additional time to each dog at a higher dosage (0.6 mg/kg) at least three days following administration of any of the previous formulations or dosages. The hounds were fasted for 12 hours with free access to water prior to midazolam dosing and throughout the 480 minutes of blood collection following drug administration. Vital parameters including heart rate, respiratory rate, and indirect blood pressure were recorded just prior to drug administration. Heart rate was monitored through auscultation or peripheral pulse palpation every 5 minutes for the first 30 minutes following each midazolam dosage. Respiratory rates and indirect blood pressures were recorded at 15 and 30 minutes following midazolam dosing.

Buccal midazolam gel formulations were administered with needleless 1 cc plastic syringes along the inner cheek pouch between the teeth and buccal mucosa. The cheeks and lips were gently massaged on the side of administration for five to ten seconds immediately after dosing and the dogs' heads were kept elevated at least 30 degrees for 60 seconds following buccal dosages. Intravenous midazolam solutions were administered over five to ten seconds through sterile intravenous cephalic catheters or through direct needle intravenous injections into the cephalic

vein. Heparinized saline solution (0.5 cc) was used to flush the midazolam solution through the needles or catheters following injection.

Peripheral blood samples (2 cc of venous blood in standard lithium heparin tubes) were collected through sterile intravenous cephalic vein catheters or via jugular venipuncture. Blood samples were collected just prior to and at 3, 6, 9, 12, 15, 20, 30, 60, 120, 240 and 480 minutes following administration of midazolam. Samples were stored on ice for a maximum of two hours prior to centrifugation. Harvested plasma samples were stored in polypropylene vials at -70 ^{o}C until midazolam concentration assays could be performed. All the samples were assayed within 14 days of plasma collection.

5.3.7 HPLC Analysis of Midazolam from in Vitro Release Samples

Midazolam samples from the in vitro release studies were analyzed using Water HPLC System equipped with a PDA-UV detector and a 5 µm, 150 x 4.6 mm column. The separation was performed with an isocratic mode. The mobile phase was a mixture of 10mM sodium acetate trihydrate and acetonitrile (55:45, v/v). The run time was 10 minutes with a flow rate of 1 mL/min at room temperature. The injection volume was 10 µl and the U.V. absorbance of the eluent was collected at 220 nm.

5.3.8 LC-MS/MS Quantification of Midazolam Concentration in Plasma:

The liquid chromatography was carried out through an ultra HPLC system coupled to a triple quadrapole mass spectrometer. Chromatographic quantification was achieved with a 2.1×50 mm, 1.8 µm column using a mobile phase composed of A: 10 mM ammonium formate, B: Acetonitrile with gradient elution as following composition: 0 min (40% A, 60% B), 1.0 min (20% A, 80% B).

The flow rate was 0.5 ml/min, the column temperature was set at 40 ^{o}C and the injection volume was 1 µl and samples introduced into the mass spectrometer using electrospray ionization. The analysis time was set at 1 min and mass detection was achieved using MRM. The MRM ion-pair parameters are precursor ion (326.1, 326.1 m/z), product ion (291.1, 249.1 m/z), fragmentor (160 V) and collision energy (26, 40 V) as quantifying pattern and qualifying for midazolam, respectively. The MRM parameters are precursor ion (285.1, 285.1 m/z), product ion (193.1, 154 m/z), fragmentor (140 V) and collision energy (32, 26 V) as quantifying pattern and qualifying for diazepam (internal standard), respectively.

A) Method Validation

10 mg of midazolam was weighed and dissolved in 100 mL of methanol to obtain a stock solution of 100 µg/mL. This solution was diluted further to get a concentration of 6 µg/mL. The plasma from each study dog was collected and pooled. The plasma samples were spiked with midazolam at 1000, 500, 250, 125, 62.5, 31.3, 15.6, 7.81, 3.91, 1.95, 0.977, 0.488, 0.244 ng/mL concentrations and used to construct a calibration curve. The calibration curve was prepared, each time plasma samples were assayed. A stock solution of diazepam (internal standard) at 150 ng/mL was prepared. The lower limit of quantification was considered as the lowest concentration of the drug in plasma that could be quantified with acceptable precision and accuracy under the experimental conditions (variation in precision was within 85% - 110%). The analyte response at the lower limit of quantitation was found to be 5 times the response of the blank response. The limit of detection was determined by injecting the serial diluted standard solutions to obtain a signal-to noise ratio of 3. The volume of internal standard added to the samples was 50 µL. Depending on the calibration curve, four concentrations were selected (0.244, 3.906, 62.5 and 500 ng/ml) as quality

control samples representing the higher, medium and lower limit of quantification. 10 milligrams of midazolam was weighed and dissolved in 100 ml of methanol and dilutions were prepared to obtain a stock solution with concentration of 1 µg/mL. The concentrations of midazolam in dog plasma were chosen depending on the lower limit of quantification from calibration curve to represent a low, medium and high-quality control samples in triplicate with accuracy range from 88-115%.

B) Quantification of Midazolam from Dog Plasma

Fifty µL of diazepam (internal standard; 150 ng/mL) was added to 100 µL of dog plasma, and vortex mixed for 1 min. To the above sample, 50 µL of 0.1 M sodium hydroxide was added and vortex mixed for 30 sec. To the above sample, 0.8 mL of diethyl ether was added and vortex mixed for 10 min. The samples were centrifuged at 3000 g for 5 min at room temperature. After centrifugation, the vials were transferred into freezer set at -80 ^{o}C for 20 min. The organic layer was separated and transferred into 5 mL radioimmunoassay vials and evaporated under the gentle stream of nitrogen gas at 40 ^{o}C. The residue was reconstituted in 100 µL acetonitrile and the drug content was quantified via LC-MS/MS. Recovery of the extraction procedure was calculated at the QC levels of 0.244, 3.906, 62.5 and 500 ng/ml with at least 4 replicates of each concentration level. The recovery % for all QC samples were within 80 - 120% of the expected concentration.

5.3.9 Pharmacokinetic and Statistical Analysis

Various pharmacokinetic values were determined for the plasma midazolam concentration-time profiles. The area under the concentration/time curve (AUC) was calculated using the linear trapezoidal rule method. The intravenous midazolam hydrochloride solution was used as the reference formulation for the calculation of relative bioavailability using the mean AUC. The

maximum plasma midazolam concentration (Cmax) was that observed from the data, with the time to maximum concentration (tmax) defined as the time of the first occurrence of Cmax. Half-life and other pharmacokinetic values were calculated by use of standard equations.

Mean and standard error of means between various treatments were calculated using commercially available software. One-way analysis of variance (ANOVA) was used to determine the level of significance between various treatments. Mean values were considered to differ significantly at a $P < 0.05$.

5.4 Results

The optimized formulation compositions and their physical properties are presented in Table 5.1. The T18 formulation was made with Pluronic F127 gel whereas the T19 and T29 were prepared from HPMC K100M as gelling agents (Table 5.1). In the first set of pharmacokinetic experiments we used T18 and 19 gels, but based on the plasma concentrations and the AUC values obtained, our goal was to further improve the plasma concentration as well as the AUC of midazolam in dogs. Hence, we modified T19 formulation to further increase its viscosity as well the midazolam drug concentration. All formulations were clear gels, the pH of the formulations was between 3.2 and 3.8, assay values were closer to the input drug loading (100%) in the gels. The viscosity of T18 formulation was about 30 and 10 fold higher as compared to the T19 and T29 formulations, respectively. Further, its viscosity was not altered appreciably at different temperatures (25 to 50 ^{o}C) (Figure 5.1). The HPMC formulations T19 and T29 showed a 3- and 4-fold decrease in the viscosity with temperature. At the room temperature, all formulations had optimum rheological properties and adequate syringability for buccal administration in dogs.

To ensure that the drug from the formulations is readily diffused and available for absorption at the buccal mucosal surface, midazolam release studies across a dialysis membrane were conducted. The drug readily diffused from T19 and T29 gels, whereas the T18 gel (Pluronic gel, higher viscosity) showed significantly lower diffusion than T19 or T29 (Figure 5.2). At 4 h T18 showed 54.2±8.8% drug release, whereas T19 and T29 showed 80.5±1.2% and 91.1±0.0% drug release, respectively ($P < 0.001$). This study suggests the T19 or T29 gels have optimal release properties for in vivo administration and buccal absorption.

Following IV administration, midazolam showed a C_{max} of 717 ng/ml and a $t_{1/2}$ of 68.7 min (Figure 5.3, Table 5.2). Formulations T18 and T19 had similar $t_{1/2}$ (around 60 min), but the C_{max} values were 47.74 and 98.26, respectively. The bioavailability of T18 and T19 gels was 25.2% and 28.4%, respectively. In order to achieve higher C_{max} levels in dogs, a formulation with higher viscosity and drug loading (T29) was used. The formulation was administered at the same dose (T29) and two times the dose (T29 2x) in terms of midazolam. In the second set of pharmacokinetic studies (Figure 5.4, Table 5.3), IV administration showed a C_{max} (609 ng/ml) but showed a slightly prolonged $t_{1/2}$ (90.7 min). The formulation T29 resulted in a significantly higher C_{max} (106 ng/ml) and bioavailability (40.8%) as compared to T19 or T18. Further, the T29 gel two-folds midazolam dose resulted in significantly higher C_{max} (187 ng/ml) as compared to T29 at its normal dose.

All formulations were well tolerated in the dogs with the exception of some self-limited drooling in two of the dogs following administration of the 0.6mg/kg dosage of the T29 gel. One of the dogs that drooled following administration of the buccal gel similarly drooled following administration of midazolam intravenously at a 0.3mg/kg dosage.

5.5 Discussion

The results of this study demonstrate that the midazolam gel formulations tested were absorbed effectively following buccal administration with peak plasma concentrations achieved within 15 minutes and with varied bioavailability values ranging from (25 to 41%) as compared to IV administration. Minimum plasma midazolam concentrations required to effectively treat seizures have not been established, though accepted doses range from 0.06-0.5 mg/kg administered intravenously or 0.2 mg/kg intranasally to achieve plasma drug concentrations in the range of 860±360ng/mL and 450± 90ng/mL respectively (Eagleson et al., 2012; Horikawa et al., 1990; Patterson, 2014; Schwartz et al., 2013). While plasma concentrations and bioavailability following intravenous administration of midazolam were clearly superior to buccal administration, the plasma concentrations achieved with the higher dosage in this study (0.6 mg/kg) are comparable to those reported with intranasal midazolam gel administration and superior to those of rectal administration of a midazolam solution within a similar time frame (Court et al., 1992; Eagleson et al., 2012). In addition, the AUC, a reflection of bioavailability and clearance of a drug, was similar if not superior following buccal administration to previously reported AUCs for intramuscular administration of midazolam (Schwartz et al., 2013).

The ability to achieve peak concentrations within 15 minutes opens the possibility for the use of buccal midazolam gel in status epilepticus or cluster seizure therapy when intravenous access is not possible. In humans, changes were noted on electroencephalography within five minutes of buccal midazolam administration, even prior to detectable venous blood levels (Scott et al., 1998). The theory behind this finding was that buccally absorbed midazolam might be distributed rapidly to the brain and fat from the arterial blood, resulting in lower venous drug concentrations of the

initial samples obtained during the first few minutes of sampling. Venous blood levels obtained in the human subjects (C_{max} 86.7 ng/mL) however, were far lower than plasma concentrations obtained in the dogs in this study (C_{max} 187 ng/mL). Electroencephalography studies and arterial sampling following buccal midazolam administration would be needed in dogs to demonstrate this effect in dogs; however, the possibility of effects on the central nervous system prior to peak plasma levels is an intriguing possibility. The peak plasma levels and time to peak concentrations are higher and faster in this study than those previously reported for rectal routes of midazolam administration presumably with absorption not impeded by technical skill or the presence of fecal matter. This is similar to reports on epileptic children in which time for administration and onset of effect were considerably lower for buccal midazolam versus rectal diazepam (Ashrafi et al., 2010; McIntyre et al., 2005). The buccal administration also circumvents the limited volume of drug permissible with intranasal administration of midazolam, a concern in heavier patients requiring a large volume (Eagleson et al., 2012), as the oral cavity is considerably larger and more easily accessible during seizures. Intramuscular administration of midazolam is a good alternative when intravenous access is not possible, but may be beyond the technical ability and comfort of some owners (Schwartz et al., 2013).

The optimized formulations T18 (made with Pluronic F127), T19 and T29 (made with HPMC K100M) had similar pH but different viscosity values to achieve bioadhesion and better absorption. The formulation with the greatest viscosity (T18) showed lowest C_{max} and bioavailability. Apparently, this formulation showed decreased release (as shown in the dialysis study), in vitro and the drug was not readily available for absorption by the buccal mucosa. However, the T19 formulation with the least viscosity and better drug release characteristics

showed increased C_{max} and bioavailability as compared to that of T18. The formulations T19 and T29 had a drug solubilizer and buccal permeation enhancer, HPβCD at larger concentrations (17.6 and 22%, respectively), which provided better buccal absorption for midazolam. HPβCD has been reported as a mucosal permeation enhancer for drugs such as ropinirole and bupivacaine (Jug et al., 2010; Kontogiannidou et al., 2016).

In human studies on buccal midazolam, formulations of the drug varied from standard injectable solutions to commercially available oral syrups (Ashrafi et al., 2010; Baysun et al., 2005; McIntyre et al., 2005; Scott et al., 1998; Scott et al., 1999). Previous studies in dogs on intranasal midazolam administration demonstrated superior drug absorption from a 0.4% HPMC gel formulation rather than standard injectable formulations (Eagleson et al., 2012). The gel formulation was theorized to improve retention and mucosal contact-time in the nasal cavity. A similar HPMC gel was used in this study to improve retention of solution in the oral cavity. The absorption of midazolam from the oral mucosa in the dog has previously been shown to be pH dependent with ideal absorption between pH 3 and 4 (Zhang et al., 2002). Midazolam requires an acidic solution to maintain solubility; however, at pH values below 3, encountered in certain intravenous or commercially available oral solutions of midazolam, oral mucosal absorption may be impeded (Zhang et al., 2002). The gel used in this study was carefully formulated to maintain a pH between 3 and 4.

Concerns with buccal or sublingual administration of any medication during status epilepticus include swallowing of the medication, aspiration, or inadvertent bite wounds to the administrator (Scott et al., 1999). Swallowing of the medication is a valid concern as gastric absorption of midazolam may reduce peak concentrations due to hepatic first-pass effects (Schwartz et al., 2013; Zhang et al., 2002). One of the dogs in this study exhibited excessive salivation following both

intravenous and buccal administration of midazolam. Drooling could contribute to increased swallowing or loss of drug from the oral cavity and adversely affect absorption. Aspiration following oral dosing of medication during seizures is another concern, although administered doses of the buccal 2% (w/v or v/v) midazolam gel formulation used in this study are expected to be under two milliliters, even in patients weighing 50 kg or more. Bite wounds during buccal medication administration are a valid concern for caregivers of humans and veterinary species. Fortunately, oral mucosa is readily accessible, arguably more so than nasal mucosa, and does not require insertion of objects between the teeth. Administration of buccal midazolam in children and adults is reported to be well tolerated, even if clenched teeth are encountered during administration as the tip of the syringe is simply inserted in the space between teeth and lips (Kutlu et al., 2003; Scott et al., 1999). In addition to being well tolerated by the animals, buccal dosing was quick and did not pose a technical challenge for drug administrators in this study.

With the social stigma associated and poor compliance with rectal drug administration for human patients, there has been a trend towards intranasal and buccal administration of benzodiazepines in human epileptics (Baysun et al., 2005; Chakupurakal et al., 2010; Kutlu et al., 2003; McIntyre et al., 2005; Scott et al., 1999; Talukdar et al., 2009; Wiznitzer, 2005). Similar, if not superior, drug absorption and onset of efficacy have been demonstrated with buccal midazolam over rectal diazepam in human adults and children (Ashrafi et al., 2010; Baysun et al., 2005; McIntyre et al., 2005; Nakken et al., 2011; Scott et al., 1999). The relative ease of administration and social acceptability of administering solutions into the mouth, rather than rectally, make this a preferable option for owners and veterinary staff when intravenous access in a seizure patient is not possible. This is the first study to examine the dose-dependent pharmacokinetics of buccal administration

of midazolam formulation in dogs. Future investigations into formulation concentration or dosage are required to determine if higher plasma concentrations or more rapid absorption can be achieved. Long-term stability and shelf life of the gel formulation should also be determined prior to recommendation for use in a clinical setting. Pharmacokinetic studies in patients receiving long term anti-convulsant therapy are also needed as chronic administration of phenobarbital can affect plasma concentrations of benzodiazepines (Wagner et al., 1998). Results of this study show promise for buccal administration of midazolam gel, but further evaluations of the efficacy of this medication in a clinical setting are needed prior to recommendations for routine use.

5.6 Abbreviations:

AUC- Area under the curve

Cmax- Peak concentration

Tmax- Time to observed peak concentration

$t_{1/2}$- Plasma half-life

HPMC- Hydroxypropyl methylcellulose

HPβCD- Hydroxypropyl β-cyclodextrin

HPLC- High-performance liquid chromatography

PBS- Phosphate buffered saline

LC-MS/MS- Liquid chromatography–tandem mass spectrometry

MRM- Multiple reaction monitoring

5.7 References:

Ashrafi, M. R., Khosroshahi, N., Karimi, P., Malamiri, R. A., Bavarian, B., Zarch, A. V., Kompani, F. (2010). Efficacy and usability of buccal midazolam in controlling acute prolonged convulsive seizures in children. *Eur J Paediatr Neurol, 14*(5), 434-438. doi:10.1016/j.ejpn.2010.05.009

Baysun, S., Aydin, O. F., Atmaca, E., & Gurer, Y. K. (2005). A comparison of buccal midazolam and rectal diazepam for the acute treatment of seizures. *Clin Pediatr (Phila), 44*(9), 771-776. doi:10.1177/000992280504400904

Bhattacharyya, M., Kalra, V., & Gulati, S. (2006). Intranasal midazolam vs rectal diazepam in acute childhood seizures. *Pediatr Neurol, 34*(5), 355-359. doi:10.1016/j.pediatrneurol.2005.09.006

Camfield, P. R. (1999). Buccal midazolam and rectal diazepam for treatment of prolonged seizures in childhood and adolescence: a randomised trial. *J Pediatr, 135*(3), 398-399.

Chakupurakal, R., Sobithadevi, D. N., Choules, A. P., & Ahmed, M. (2010). Buccal midazolam: are we ready yet? *Seizure, 19*(5), 310. doi:10.1016/j.seizure.2010.04.004

Court, M. H., & Greenblatt, D. J. (1992). Pharmacokinetics and preliminary observations of behavioral changes following administration of midazolam to dogs. *J Vet Pharmacol Ther, 15*(4), 343-350.

Dewey, C. W. (2006). Anticonvulsant therapy in dogs and cats. *Vet Clin North Am Small Anim Pract, 36*(5), 1107-1127, vii. doi:10.1016/j.cvsm.2006.05.005

Eagleson, J. S., Platt, S. R., Strong, D. L., Kent, M., Freeman, A. C., Nghiem, P. P., White, C. A. (2012). Bioavailability of a novel midazolam gel after intranasal administration in dogs. *Am J Vet Res, 73*(4), 539-545. doi:10.2460/ajvr.73.4.539

Horikawa, H., Tada, T., Sakai, M., Karube, T., & Ichiyanagi, K. (1990). Effects of midazolam on the threshold of lidocaine-induced seizures in the dog--comparison with diazepam. *J Anesth, 4*(3), 265-269. doi:10.1007/s0054000040265

Jug, M., Maestrelli, F., Bragagni, M., & Mura, P. (2010). Preparation and solid-state characterization of bupivacaine hydrochloride cyclodextrin complexes aimed for buccal delivery. *J Pharm Biomed Anal, 52*(1), 9-18. doi:10.1016/j.jpba.2009.11.013

Kontogiannidou, E., Andreadis, D. A., Zografos, A. L., Nazar, H., Klepetsanis, P., van der Merwe, S. M., & Fatouros, D. G. (2016). Ex vivo buccal drug delivery of ropinirole hydrochloride in the presence of permeation enhancers: the effect of charge. *Pharm Dev Technol*, 1-5. doi:10.3109/10837450.2015.1135343

Kutlu, N. O., Dogrul, M., Yakinci, C., & Soylu, H. (2003). Buccal midazolam for treatment of prolonged seizures in children. *Brain Dev, 25*(4), 275-278.

Lowenstein, D. H., Bleck, T., & Macdonald, R. L. (1999). It's time to revise the definition of status epilepticus. *Epilepsia, 40*(1), 120-122.

Mariani, C. L. (2013). Terminology and classification of seizures and epilepsy in veterinary patients. *Top Companion Anim Med, 28*(2), 34-41. doi:10.1053/j.tcam.2013.06.008

McIntyre, J., Robertson, S., Norris, E., Appleton, R., Whitehouse, W. P., Phillips, B., Choonara, I. (2005). Safety and efficacy of buccal midazolam versus rectal diazepam for emergency

treatment of seizures in children: a randomised controlled trial. *Lancet, 366*(9481), 205-210. doi:10.1016/S0140-6736(05)66909-7

Monteiro, R., Adams, V., Keys, D., & Platt, S. R. (2012). Canine idiopathic epilepsy: prevalence, risk factors and outcome associated with cluster seizures and status epilepticus. *J Small Anim Pract, 53*(9), 526-530. doi:10.1111/j.1748-5827.2012.01251.x

Munana, K. R. (2013). Update: seizure management in small animal practice. *Vet Clin North Am Small Anim Pract, 43*(5), 1127-1147. doi:10.1016/j.cvsm.2013.04.008

Musulin, S. E., Mariani, C. L., & Papich, M. G. (2011). Diazepam pharmacokinetics after nasal drop and atomized nasal administration in dogs. *J Vet Pharmacol Ther, 34*(1), 17-24. doi:10.1111/j.1365-2885.2010.01186.x

Nakken, K. O., & Lossius, M. I. (2011). Buccal midazolam or rectal diazepam for treatment of residential adult patients with serial seizures or status epilepticus. *Acta Neurol Scand, 124*(2), 99-103. doi:10.1111/j.1600-0404.2010.01474.x

Patterson, E. N. (2014). Status epilepticus and cluster seizures. *Vet Clin North Am Small Anim Pract, 44*(6), 1103-1112. doi:10.1016/j.cvsm.2014.07.007

Platt, S. R., Randell, S. C., Scott, K. C., Chrisman, C. L., Hill, R. C., & Gronwall, R. R. (2000). Comparison of plasma benzodiazepine concentrations following intranasal and intravenous administration of diazepam to dogs. *Am J Vet Res, 61*(6), 651-654.

Podell, M. (1995). The use of diazepam per rectum at home for the acute management of cluster seizures in dogs. *J Vet Intern Med, 9*(2), 68-74.

Probst, C. W., Thomas, W. B., Moyers, T. D., Martin, T., & Cox, S. (2013). Evaluation of plasma diazepam and nordiazepam concentrations following administration of diazepam

intravenously or via suppository per rectum in dogs. *Am J Vet Res, 74*(4), 611-615. doi:10.2460/ajvr.74.4.611

Saito, M., Munana, K. R., Sharp, N. J., & Olby, N. J. (2001). Risk factors for development of status epilepticus in dogs with idiopathic epilepsy and effects of status epilepticus on outcome and survival time: 32 cases (1990-1996). *J Am Vet Med Assoc, 219*(5), 618-623.

Schwartz, M., Munana, K. R., Nettifee-Osborne, J. A., Messenger, K. M., & Papich, M. G. (2013). The pharmacokinetics of midazolam after intravenous, intramuscular, and rectal administration in healthy dogs. *J Vet Pharmacol Ther, 36*(5), 471-477. doi:10.1111/jvp.12032

Scott, R. C., Besag, F. M., Boyd, S. G., Berry, D., & Neville, B. G. (1998). Buccal absorption of midazolam: pharmacokinetics and EEG pharmacodynamics. *Epilepsia, 39*(3), 290-294.

Scott, R. C., Besag, F. M., & Neville, B. G. (1999). Buccal midazolam and rectal diazepam for treatment of prolonged seizures in childhood and adolescence: a randomised trial. *Lancet, 353*(9153), 623-626. doi:10.1016/S0140-6736(98)06425-3

Talukdar, B., & Chakrabarty, B. (2009). Efficacy of buccal midazolam compared to intravenous diazepam in controlling convulsions in children: a randomized controlled trial. *Brain Dev, 31*(10), 744-749. doi:10.1016/j.braindev.2008.11.006

Wagner, S. O., Sams, R. A., & Podell, M. (1998). Chronic phenobarbital therapy reduces plasma benzodiazepine concentrations after intravenous and rectal administration of diazepam in the dog. *J Vet Pharmacol Ther, 21*(5), 335-341.

Wiznitzer, M. (2005). Buccal midazolam for seizures. *Lancet, 366*(9481), 182-183. doi:10.1016/S0140-6736(05)66884-5

Zhang, J., Niu, S., Zhang, H., & Streisand, J. B. (2002). Oral mucosal absorption of midazolam in dogs is strongly pH dependent. *J Pharm Sci, 91*(4), 980-982.

Table 5.1 *Composition and physical properties of the three midazolam buccal gel formulations: T18 (midazolam 1%, pluronic gel formulation), T19 (midazolam 1%, HPMC with HPβCD formulation), T29 (midazolam 2%, HPMC with HPβCD formulation).*

Ingredients	**Quantity, g/100g**		
	T18	**T19**	**T29**
Midazolam USP	1	1	2
Ethanol USP	10	10	20
Pluronic Gel 30% (F127)	88	0	0
Phosphoric Acid (86.6% assay)	0.5	0.5	0.5
Hydroxypropyl betacyclodextrin (Trapasol®)	0	17.6	22
Hydroxypropyl methylcellulose (Methocel K100 M)	0	0.88	0.99
Water q.s.	100	100	100
Appearance	Clear	Clear	Clear
pH	3.5	3.2	3.8
Assay %	101.2	101.3	100.8
Viscosity. Pas, 22 rpm	124	3.92	12.5

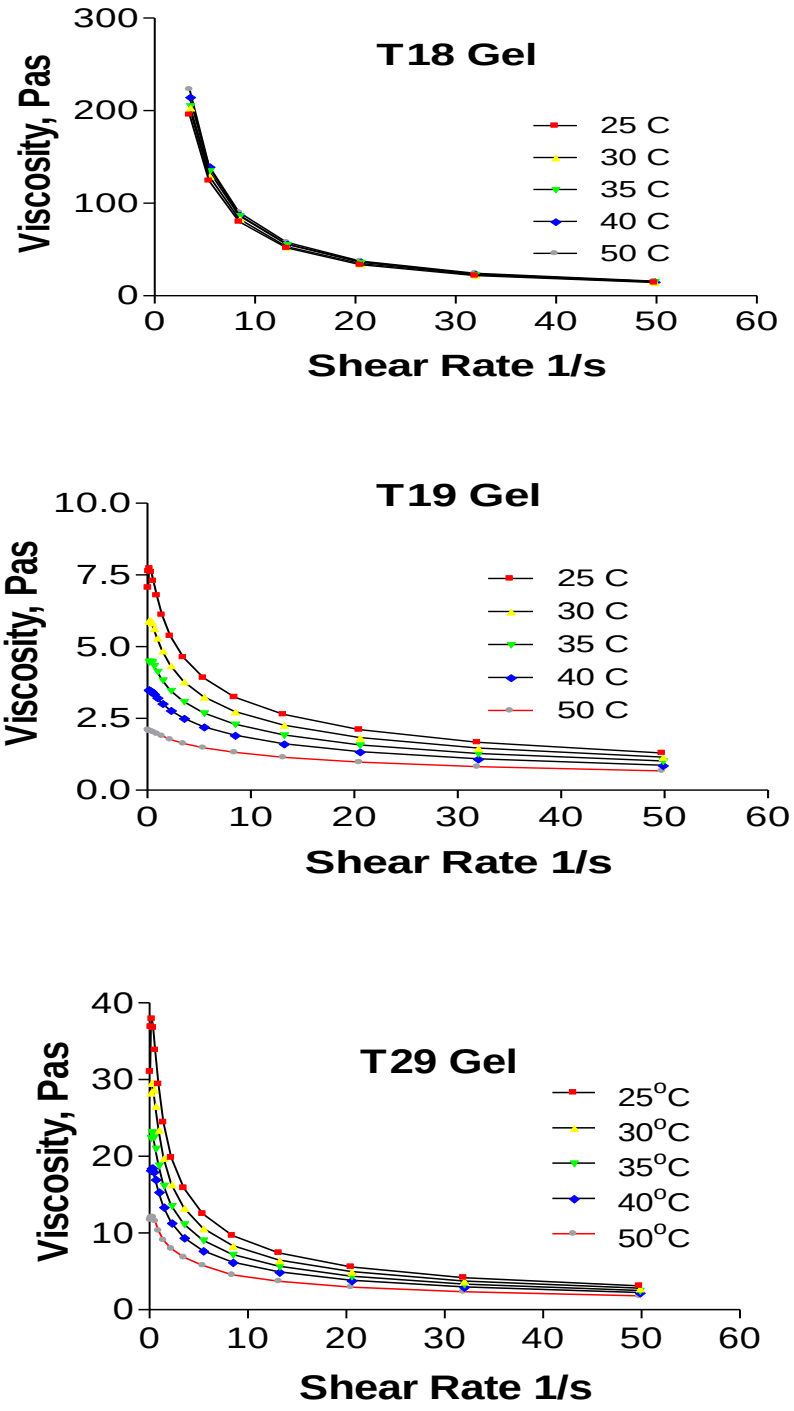

Figure 5.1 Rheological properties, as assessed by viscosity vs shear rate at temperatures ranging from 25 to 50°C, of three different midazolam gel formulations: A. T18 (midazolam 1%, pluronic gel formulation), B. T19 (midazolam 1%, HPMC with HPβCD formulation), C. T29 (midazolam 2%, HPMC with HPβCD formulation).

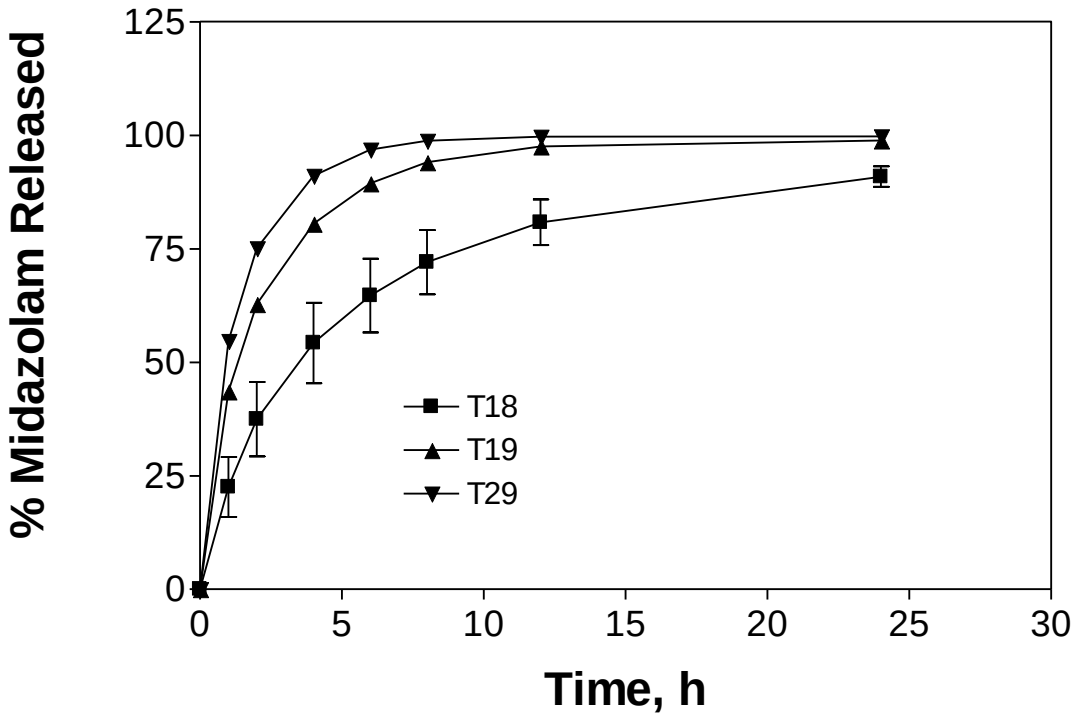

Figure 5.2 Drug diffusion and release of various midazolam gel formulations across a dialysis membrane. T18 (midazolam 1%, pluronic gel formulation), T19 (midazolam 1%, HPMC with HPβCD formulation), T29 (midazolam 2%, HPMC with HPβCD formulation).

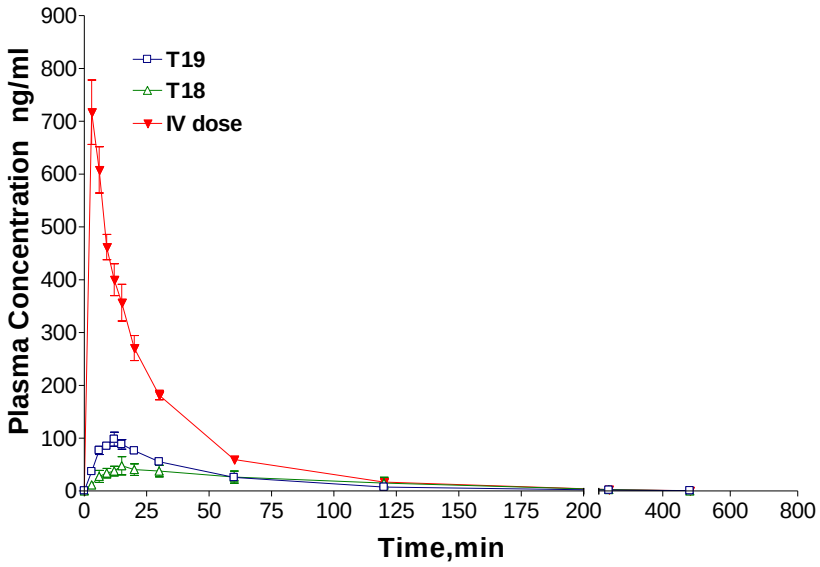

Figure 5.3 Plasma concentrations (ng/mL) of midazolam after buccal administration of two gel formulations and intravenous administration of an injectable solution at a dosage of 0.3mg/kg. T18 (midazolam 1%, pluronic gel formulation), T19 (midazolam 1%, HPMC with HPβCD formulation).

Table 5.2 *Pharmacokinetic variables after buccal administration of two different midazolam gel formulations (T18 and T19) and intravenous administration of an injectable midazolam solution. All solutions administered at a dosage of 0.3mg/kg to five healthy adult hound dogs. T18 (midazolam 1%, pluronic gel formulation). T19 (midazolam 1%, HPMC with HPβCD formulation).*

Parameter	**Unit**	**T19**	**T18**	**IV**
t1/2	min	63.8±44.9	58.7±16.6	68.7±36.7
Tmax	min	12.0	15.0	3.0
Cmax	ng/ml	98.3±26.5	47.7±38.5	717±138
AUC 0-t	ng/ml*min	5,170.1±330	4,620±4530	18,400±2,400
AUC 0-inf	ng/ml*min	5,230±300	4,630±4,550	18,400±2,40
AUMC 0-inf	ng/ml*min^2	365947.7±54907.6	402037±535400	719912±230301
Vz/F	(mg)/(ng/ml)	0.176±0.138	0.183±0.164	0.0538±0.0295
Bioavailability	%	28.4	25.2	NA

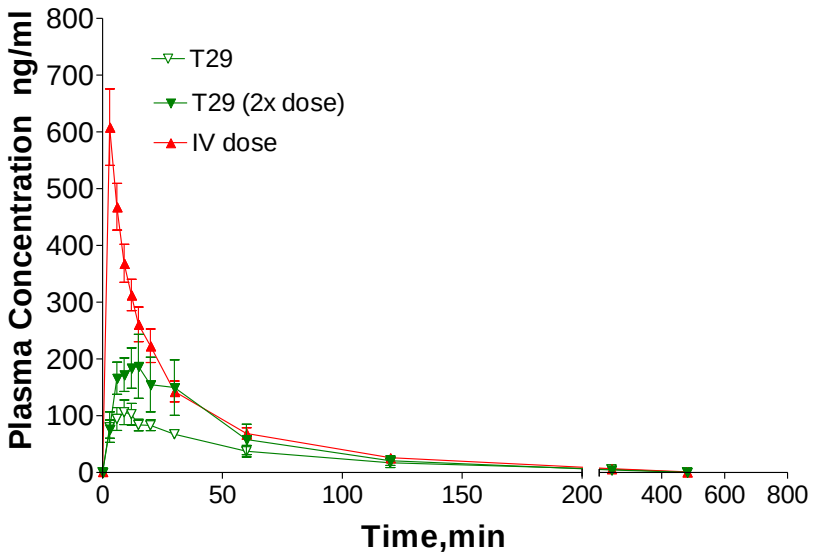

Figure 5.4 Plasma concentrations (ng/mL) of midazolam after buccal administration of the T29 formulation (midazolam 2%, HPMC with HPβCD formulation) at a dosage of 0.3mg/kg and 0.6mg/kg and intravenous injection of an injectable.

Table 5.3 *Pharmacokinetic after buccal administration of a 2% midazolam gel formulation (T29) at a dosage of 0.3mg/kg and 0.6mg/kg in comparison to intravenous administration of an injectable midazolam solution at a dosage of 0.3 mg/kg.*

Parameter	**Unit**	**T29**	**T29 2x dose**	**IV**
t1/2	min	75.3±18.7	71.3±13.8	90.7±15.4
Tmax	min	9.0	15.0	3.0
Cmax	ng/ml	106.3±35.2	187.0±104.3	608.5±150.9
AUC 0-t	ng/ml*min	7805.8±3598.8	12101.9±8902.8	19001.4±4578.2
AUC 0-inf	ng/ml*min	7873.9±3626.9	12162.4±8954.1	19312.3±4641.1
AUMC 0-inf	ng/ml*min^2	677800±663759	788994±704905	1261242±408388
Vz/F	(mg)/(ng/ml)	0.1380±0.0705	0.0845±0.0532	0.0678±0.0155
Bioavailability	%	40.77	31.48	NA

`

6. Resveratrol Nanogel Formulation for Enhanced Transdermal Delivery Across Human Skin

6.1 Abstract

Purpose: Resveratrol, a natural polyphenol found in grapes and berries, has strong anti-oxidant properties and is believed to be beneficial in treating many disease conditions including skin cancer. This compound is insoluble in many topical vehicles/solvents, leading to problems in developing a topical product. In this study, we prepared a nanoparticle based gel (nanogel) formulation and obtained skin permeation data on resveratrol.

Methods: The saturation solubility of resveratrol in topical vehicles such as ethanol, polyethylene glycol 400, Labrfil® 2125, Labrfil® 1944, Lauroglycol FCC, Transcutol®P, Labrasol®, Capryol™ PGMC and Capryol™90 was determined. Labrasol® showed a higher solubility for resveratrol and was used in the nanogel formulation. Resveratrol was solubilized in Labrasol® and added to 1% Pluronic®F68 solution under stirring. This resultant suspension was subjected to ultrasonication and high-pressure homogenization to achieve a nanosuspension. The suspension was then gelled using Methocel®K4M (F3). The drug release and skin permeation of the nanogel formulation were determined using dialysis membrane and dermatomed human cadaver skin, respectively. The size and size distribution of nanoparticles was determined by Nicomp ZLS 380, and drug concentration was determined by a HPLC method.

Results: The solubility of resveratrol was high in Labrasol®, Transcutol®P, Arlasolve® and polyethylene glycol 400 (>100 mg/ml). However, Labrasol was chosen as a solubilizer for the nanogel formulation because this solvent provided proper viscosity and compatibility with the gel components. All other solvents failed to retain the viscosity for the nanogel. The mean diameter

of particles in the nanogel formulation F3 was 120 nm. The F3 formulation showed an amount of drug release (1647.2 µg/cm^2) which was 1.6 and 1.1 fold higher compared to F1 and F2 (control formulations), respectively. In the skin permeation study, F3 showed a flux (1.31±0.08 µg/cm^2/h) which was 12 and 3-fold higher compared to F1 and F2, respectively. The skin retention of F3 (234± 45.9 µg/g of skin) was approximately 12 and 5 fold higher compared to F1 and F2, respectively.

Conclusion: An enhancement of resveratrol delivery was observed when a nanogel formulation was compared to microparticles incorporated in a gel formulation of the same drug percentage. This enhancement was shown in skin permeation as well as drug retention within skin layers. A high skin permeation for therapeutic quantities of resveratrol is possible when the nanogel is applied on a larger surface area of the body.

6.2 Introduction

Resveratrol (RV) is 3,5,4'-trihydroxystilbene and is widely present in certain types of wine (polyphenols red wines) (Baur et al., 2006a). Resveratrol was discovered and extracted originally from Polygonum cuspidatum's root; which was employed in traditional Japanese and Chinese medicine. Additionally, resveratrol is naturally available from grapes, peanuts and berries plants. These plants produce resveratrol in response to exterior stress, for instance, UV irradiation and microbial infection (Amri et al., 2012; Ansari et al., 2011; Park et al., 2013). Chemically, it is a member of the stilbene class of polyphenolic compounds. It exists in two isomeric forms (Figure 6.1): cis-resveratrol and trans-resveratrol, the latter preferred due to better biological activity and chemical stability (Baxter, 2008).

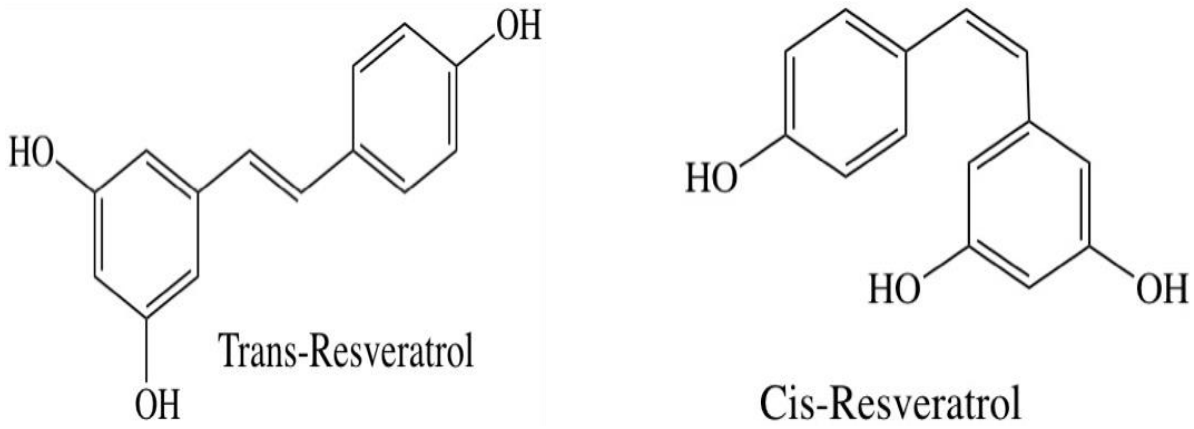

Figure 6.1 Two isoforms for resveratrol.

Oxidative stress and prolonged inflammation are two conditions associated with several diseases such as cancer, diabetes, atherosclerosis, pulmonary infections, and Alzheimer's disease. This highlights the importance of counteracting the inflammation and oxidative stress via antioxidant

and anti-inflammatory agents (Aldawsari et al., 2016; Reuter et al., 2010). Resveratrol possesses a strong anti-oxidant effect in addition to its anti-inflammatory, cardioprotective, neuroprotective, chemopreventive, and anti-aging properties (Athar et al., 2007; Francioso et al., 2014; Pando et al., 2013). However, it exhibits poor water solubility (rate limiting step for dissolution), low oral bioavailability and short half-life (8-14 minutes) as a result of extensive first-pass metabolism. This necessitates higher oral doses to compensate for the loss, which consequently raises the cost (Baur et al., 2006b; Hung et al., 2008).

Several studies have shown that resveratrol exerts chemopreventive action specifically on the skin at various stages of cancer progression (Afaq et al., 2003; Nassiri-Asl et al., 2016). Resveratrol in a topical formulation has beneficial effects such as preventing keratinocyte proliferation specifically in epidermal cells, acting as antimicrobial and antiviral agent for skin infections, protecting the skin from damage due to UV exposure, accelerating wound healing process, inhibiting the production of melanin and reducing skin irritations (Afaq et al., 2003; Hung et al., 2008; Park et al., 2008; Scognamiglio et al., 2013). Hence, resveratrol both as topical and transdermal formulations would be a beneficial alternative to oral administration (Zhang et al., 2007; Zhou et al., 2015) . Studies explored topical application of resveratrol as an emulsion, solution, and gel for improved drug delivery (S Kobierski et al., 2009). A common issue was that resveratrol is insoluble in many topical vehicles/solvents, leading to problems in developing a product. Nanotechnology for drug delivery has shown several benefits such as improved solubility, absorption, and bioavailability from topical/transdermal formulations (Dianzani et al., 2014; Liu et al., 2012; Scognamiglio et al., 2013; P. P. Shah et al., 2012; Tsai et al., 2016). In this study, we

obtained solubility data of resveratrol and selected appropriate solvents in the formulation of a nanoparticle based gel (nanogel) for enhanced topical delivery of resveratrol.

6.3 Materials and Methods:

6.3.1 Materials

Resveratrol was purchased from AvaChem Scientific, San Antonio,TX, USA. Pluronic®F68 (Poloxamer 188, NF) was purchased from Spectrum Chemical Corp., Gardena, CA, USA. Hydroxypropyl Methylcellulose (Methocel® K4M) was obtained as a gift from Colorcon, Grinnell, Iowa, USA. Phosphate buffered saline 0.01 M (NaCl 0.138 M; KCl - 0.0027 M, pH 7.4) for reconstitution was purchased from Sigma-Aldrich, St. Louis, MO, USA. Transcutol P®, Labrafil M 2125 CS®, Labrafil M 1944 CS®, Lauroglycol FCC®, Labrasol®, Arlasolve®, Capryol 90® and Capryol PGMC® were obtained from Gattefosse Sas, Saint-Priest Cedex, France. Polyethylene glycol (PEG) 400 NF was purchased from Fisher Scientific. All other chemicals and reagents were HPLC or analytical grade.

6.3.2 Resveratrol Solubility Determination

An excess amount of resveratrol was added to 2 ml of the following solubilizers: Labrafil 2125®, Labrafil 1944®, Capryol PGMC®, Capryol 90®, Lauroglycol FCC®, Transcutol P®, Labrasol®, Arlasolve®, PEG 400), in glass vials. The vials were capped and sealed with Parafilm® and subjected to continuous shaking at for 72 hours at ambient room temperature. Before drug solubility analysis, the solutions were allowed to stand for 24 h for settling of the excess drug. The supernatant was then filtered through 0.45 um Nylon membrane filter. The filtered solutions were diluted 100 times with Methanol: Water (1:1) and assayed by HPLC.

6.3.3 Resveratrol Nanogel Preparation

Based on resveratrol solubility and compatibility with HPMC, Labrasol® was chosen as a solvent for resveratrol. Resveratrol was solubilized in Labrasol® and added to 1% Pluronic®F68 aqueous solution under constant stirring to obtain a resveratrol suspension. The suspension was subjected to ultrasonication and homogenization by a high-pressure homogenizer. The homogenization process was performed at 22000 PSI for five cycles to achieve resveratrol nanoparticles. Methocel® K4M as a powder was added to the nanosuspension in a uniform manner. Upon the addition, mixture was under the effect of a magnetic stirrer for 1 h (F3). The first control formulation was prepared with no labrasol, and no high-pressure homogenization (F1). Also, the second control formulation was prepared with same (F3) preparation procedure but without high-pressure homogenization use (F2). The formulation compositions are listed in Table 6.2**.**

6.3.4 HPLC-UV Analysis of Resveratrol

The HPLC instrumentation and method consists of Waters Agilent HPLC System with PDA detector interfaced to Empower 3 software. A reversed phase, C18 Luna 150 x 4.6 mm, 5-µm particles loaded HPLC column (Phenomenex, Torrance CA) was used. A mobile phase containing methanol and water (51:49) at a flow rate of 0.9 ml/min was used. The injection volume was 20 µl and the detection wavelength was 306 nm. The run time was 10 min.

6.3.5 Particle Size and Size Distribution Measurements

Particle size (P.S.) and polydispersity index (PI) were measured at room temperature after diluting each sample in deionized water (1:100). Nicomp ZLS380 was utilized to obtain z-average value in nm along with the PI that reflects the distribution of the particle sizes in the medium.

6.3.6 In Vitro Release Evaluation of Resveratrol Nanogel Formulations

The release behavior of resveratrol nanogel was evaluated by Franz diffusion cell apparatus using a cellulose membrane. The receptor medium was (50:50) ethanol: PBS with pH 7.4 to maintain the sink condition for resveratrol. The cellulose membrane was positioned in between the receptor and the donor compartments. 0.5 gm of each formulation was placed in the donor compartment and spread evenly on the membrane in occlusive condition (the donor cell was sealed with Parafilm®). At 1, 2, 4, 6, 8, 12, 24 and 26 hours samples were withdrawn and replenished with fresh receptor medium. The samples were assayed by HPLC. All studies were performed under protection from light owing to the sensitivity of resveratrol to photo degradation.

6.3.7 Skin Permeation Study of Resveratrol Nanogel Formulations

The percutaneous permeation study was performed in the same pattern as the in vitro release procedure using Franz diffusion cell. Instead of the cellulose membrane, dermatomed human skin (Sciencecare, Phoenix AZ) was used. The skin was mounted with stratum corneum facing the donor and receptor cell was filled with (50:50) ethanol: PBS to maintain the sink condition. An infinite dose (0.5 gm) was applied on donor side under occlusive condition (the donor cell was sealed with Parafilm®).

At the end of the skin permeation study, the residual drug remaining on the surface of the skin was removed by cotton swabs and by washing the surface with PBS. The skin surface was gently wiped with a cotton swab (Q-tips® Uniliver USA, Englewood Cliffs, NJ), 200 µl of the above buffer was added on the skin surface and the liquid was dabbed with a fresh (dry) cotton swab. This process of swabbing and dabbing was repeated 5 times. The active diffusion area was collected with a biopsy punch (George Tiemann & Co, Hauppauge, NY) and the skin was weighed and minced

into pieces with a pair of sharp point dissecting scissors into a glass vial. To these glass vials, 1 ml of above buffer was added, sonicated for 15 min. and allowed to stand overnight. The samples were sonicated again for 30 min, the next day and filtered through 0.45 µm membrane filter and the supernatant was diluted appropriately and analyzed by HPLC.

6.3.8 Statistical Analysis

All results were presented as means ± standard deviations. The statistical analysis was performed using GraphPad Prism version 5, GraphPad Software, Inc., La Jolla, CA. The data were subjected to one-way ANOVA followed by Tukey –Kramer multiple comparisons test. The mean differences were considered significant at $P < 0.05$.

6.4 Results and Discussion

The solubility of resveratrol in several solvents are shown in Table 6.1. From the table, the highest solubility was observed with four solvents, Labrasol, Transcutol p, Arlsolve and PEG 400. All displayed a solubility greater than 100 mg/ml of resveratrol. However, only Labrasol was chosen as a solubilizer at 0.5 % w/w resveratrol based on proper gel formation and compatibility. Nanogel could not be achieved beyond 0.5% w/w resveratrol because of the interference of excess Labrasol® (beyond 10%) in gel formulation. Three formulations were prepared and denoted as F1 (no Labrasol®), F2, and F3. The physicochemical properties of formulations are listed in Table 6.2. The PS for F3 was 120.3 nm with a PI of 0.31 indicating particle size uniformity in the formulation.

Viscosity for F1, F2 and F3 were 890 cP, 125 cP, and 96 cP, respectively. Since the proposed formulation is intended for topical application, it needs to have an appropriate viscosity (adhesive

and retention) for prolonged contact time to achieve a better drug accumulation and enhanced absorption through a biological membrane (Punit P Shah et al., 2012). From viscosity measurements, all formulations are expected to have a sufficient retention on skin which facilitates drug release and enhances drug retention. F1 showed the highest viscosity which might be explained by the absence of Labrasol®. While the presence of Labrasol® in F2 and F3 formulations was responsible for the significantly lower viscosity of the gel, along with other formulation properties such as solubility. pH values for all formulations were closely akin with no significant variations (Table 6.2).

Incorporating nano-particulate drug within gel matrix provided a uniform dispersion of the drug and better contact (based on increased surface area of drug nanoparticles, increases contact with skin) of drug for enhanced skin permeation (Batheja et al., 2011; P. P. Shah et al., 2012). Furthermore, the nanoparticles in the formulation maintain a high thermodynamic activity of the drug in the formulation (Baroli, 2010). Prior to incorporating in a gel matrix, the nanoparticles were stabilized by 1% of Pluronic® F68 as a surfactant to prevent drug particles from aggregation (S Kobierski et al., 2009).

All three formulations had good drug release. However, F3 (1647.2 µg/cm^2) showed the highest release, followed by F2 (1448.5 µg/cm^2) and F1 (1047.4 µg/cm^2). The release behavior of the gels might be reduced with increasing viscosity which is correlated with drug diffusion (Baumgartner et al., 2002).

Skin permeation of resveratrol nanogel formulations are shown in Figure 6.3. The cumulative amount of drug permeated for F3 is around 32 µg/cm^2, whereas F2 and F1 showed significantly

less drug permeation (11.8 and 2.6 µg/cm^2, respectively). The steady state flux of F3 was highest (1.31±0.083 µg/cm^2/h), followed by F2 (0.47 ±0.014 µg/cm^2/h) and F1 (0.11± 0.01 µg/cm^2/h). Thus, F3 and F2 exhibited a significant enhancement in transdermal flux, approximately 12 and 4-fold higher, respectively, as compared to F1 (control).

The skin retention (deposition) for resveratrol is presented in Figure 6.4. F3 showed the highest drug accumulation (234.0±45.9 µg/gm of skin) followed by F2 (43.0±12.0 µg/gm) and F1 (20±2.0 µg/gm). Thus, the skin retention of F3 was 12 and 5 fold higher than F1 and F2, respectively.

The therapeutic value of resveratrol is hampered by its poor permeability and aqueous solubility. To enhance skin permeability and deliver adequate amounts of the drug into the systemic circulation, formulation studies were conducted. From Table 6.1, both F3 and F2 have the same formula composition, but with a different particle size (F2, microparticles; F3, nanoparticles). The nanosize particles in F3 demonstrated significantly higher permeation and skin deposition as compared to F2. However, both F2 and F3 showed enhanced skin permeation of resveratrol over F1 (control, no Labrasol®). The increased surface area of drug particles (increased drug contact with skin) and a higher thermodynamic activity of drug in F3 might be responsible for higher skin permeation (S. Kobierski et al., 2011; Vitorino et al., 2015). These results agree with studies on nanoparticles for enhancing percutaneous permeation of topically applied drugs (Pando et al., 2015; Piao et al., 2008; P. P. Shah et al., 2012; Shen et al., 2016; Valenzuela et al., 2012).

6.5 Conclusion

An enhancement of resveratrol delivery was observed when nanogel formulation was compared to microparticles incorporated in a gel formulation. This enhancement was shown in skin permeation as well as drug retention within skin layers. Skin permeation in the therapeutic quantities of resveratrol can be possible when applied on a larger surface area of the body.

6.6 References:

Afaq, Adhami, & Ahmad. (2003). Prevention of short-term ultraviolet B radiation-mediated damages by resveratrol in SKH-1 hairless mice. *Toxicol Appl Pharmacol, 186*(1), 28-37.

Aldawsari, Aguiar, Wiirzler, Aguayo-Ortiz, Aljuhani, Cuman, Velazquez-Martinez. (2016). Anti-inflammatory and antioxidant properties of a novel resveratrol-salicylate hybrid analog. *Bioorg Med Chem Lett, 26*(5), 1411-1415. doi:10.1016/j.bmcl.2016.01.069

Amri, Chaumeil, Sfar, & Charrueau. (2012). Administration of resveratrol: What formulation solutions to bioavailability limitations? *J Control Release, 158*(2), 182-193. doi:10.1016/j.jconrel.2011.09.083

Ansari, Vavia, Trotta, & Cavalli. (2011). Cyclodextrin-based nanosponges for delivery of resveratrol: in vitro characterisation, stability, cytotoxicity and permeation study. *AAPS PharmSciTech, 12*(1), 279-286. doi:10.1208/s12249-011-9584-3

Athar, Back, Tang, Kim, Kopelovich, Bickers, & Kim. (2007). Resveratrol: a review of preclinical studies for human cancer prevention. *Toxicol Appl Pharmacol, 224*(3), 274-283. doi:10.1016/j.taap.2006.12.025

Baroli. (2010). Penetration of nanoparticles and nanomaterials in the skin: fiction or reality? *J Pharm Sci, 99*(1), 21-50. doi:10.1002/jps.21817

Batheja, Sheihet, Kohn, Singer, & Michniak-Kohn. (2011). Topical drug delivery by a polymeric nanosphere gel: Formulation optimization and in vitro and in vivo skin distribution studies. *J Control Release, 149*(2), 159-167. doi:10.1016/j.jconrel.2010.10.005

Baumgartner, Kristl, & Peppas. (2002). Network structure of cellulose ethers used in pharmaceutical applications during swelling and at equilibrium. *Pharm. Res., 19*(8), 1084-1090.

Baur, Pearson, Price, Jamieson, Lerin, Kalra, Sinclair. (2006a). Resveratrol improves health and survival of mice on a high-calorie diet. *Nature, 444*(7117), 337-342. doi:10.1038/nature05354

Baxter. (2008). Anti-aging properties of resveratrol: review and report of a potent new antioxidant skin care formulation. *J Cosmet Dermatol, 7*(1), 2-7. doi:10.1111/j.1473-2165.2008.00354.x

Dianzani, Zara, Maina, Pettazzoni, Pizzimenti, Rossi, Barrera. (2014). Drug delivery nanoparticles in skin cancers. *Biomed Res Int, 2014,* 895986. doi:10.1155/2014/895986

Francioso, Mastromarino, Masci, d'Erme, & Mosca. (2014). Chemistry, stability and bioavailability of resveratrol. *Med Chem, 10*(3), 237-245.

Hung, Lin, Huang, & Fang. (2008). Delivery of resveratrol, a red wine polyphenol, from solutions and hydrogels via the skin. *Biol Pharm Bull, 31*(5), 955-962.

Kobierski, Ofori-Kwakye, Muller, & Keck. (2011). Resveratrol nanosuspensions: interaction of preservatives with nanocrystal production. *Pharmazie, 66*(12), 942-947.

Kobierski, Ofori-Kwakye, Müller, & Keck. (2009). Resveratrol nanosuspensions for dermal application–production, characterization, and physical stability. *Pharmazie, 64*(11), 741-747.

Liu, Xie, Zhang, & Zhang. (2012). A mini review of nanosuspensions development. *J Drug Target, 20*(3), 209-223. doi:10.3109/1061186X.2011.645161

Nassiri-Asl, & Hosseinzadeh. (2016). Review of the Pharmacological Effects of Vitis vinifera (Grape) and its Bioactive Constituents: An Update. *Phytother Res, 30*(9), 1392-1403. doi:10.1002/ptr.5644

Pando, Caddeo, Manconi, Fadda, & Pazos. (2013). Nanodesign of olein vesicles for the topical delivery of the antioxidant resveratrol. *J Pharm Pharmacol, 65*(8), 1158-1167. doi:10.1111/jphp.12093

Pando, Matos, Gutierrez, & Pazos. (2015). Formulation of resveratrol entrapped niosomes for topical use. *Colloids Surf B Biointerfaces, 128*, 398-404. doi:10.1016/j.colsurfb.2015.02.037

Park, Elias, Hupe, Borkowski, Gallo, Shin, Uchida. (2013). Resveratrol stimulates sphingosine-1-phosphate signaling of cathelicidin production. *J Invest Dermatol, 133*(8), 1942-1949. doi:10.1038/jid.2013.133

Park, & Lee. (2008). Protective effects of resveratrol on UVB-irradiated HaCaT cells through attenuation of the caspase pathway. *Oncol Rep, 19*(2), 413-417.

Piao, Kamiya, Hirata, Fujii, & Goto. (2008). A novel solid-in-oil nanosuspension for transdermal delivery of diclofenac sodium. *Pharm Res, 25*(4), 896-901. doi:10.1007/s11095-007-9445-7

Reuter, Gupta, Chaturvedi, & Aggarwal. (2010). Oxidative stress, inflammation, and cancer: how are they linked? *Free Radic Biol Med, 49*(11), 1603-1616. doi:10.1016/j.freeradbiomed.2010.09.006

Scognamiglio, De Stefano, Campani, Mayol, Carnuccio, Fabbrocini, De Rosa. (2013). Nanocarriers for topical administration of resveratrol: a comparative study. *Int J Pharm, 440*(2), 179-187. doi:10.1016/j.ijpharm.2012.08.009

Shah, Desai, Patel, & Singh. (2012). Skin permeating nanogel for the cutaneous co-delivery of two anti-inflammatory drugs. *Biomaterials, 33*(5), 1607-1617. doi:10.1016/j.biomaterials.2011.11.011

Shen, Xu, Shen, Min, Li, Han, & Yuan. (2016). Nanogel for dermal application of the triterpenoids isolated from Ganoderma lucidum (GLT) for frostbite treatment. *Drug Deliv, 23*(2), 610-618. doi:10.3109/10717544.2014.929756

Tsai, Lu, Fu, Fang, Huang, & Wu. (2016). Nanocarriers enhance the transdermal bioavailability of resveratrol: In-vitro and in-vivo study. *Colloids Surf B Biointerfaces, 148*, 650-656. doi:10.1016/j.colsurfb.2016.09.045

Valenzuela, & Simon. (2012). Nanoparticle delivery for transdermal HRT. *Nanomedicine, 8 Suppl 1*, S83-89. doi:10.1016/j.nano.2012.05.008

Vitorino, Sousa, & Pais. (2015). Overcoming the skin permeation barrier: challenges and opportunities. *Curr Pharm Des, 21*(20), 2698-2712.

Zhang, Flach, & Mendelsohn. (2007). Tracking the dephosphorylation of resveratrol triphosphate in skin by confocal Raman microscopy. *J Control Release, 123*(2), 141-147. doi:10.1016/j.jconrel.2007.08.001

Zhou, He, Yang, Jian, Chen, & Ding. (2015). Formulation, characterization and clinical evaluation of propranolol hydrochloride gel for transdermal treatment of superficial infantile

hemangioma. *Drug Dev Ind Pharm, 41*(7), 1109-1119. doi:10.3109/03639045.2014.931968

Table 6.1 *Resveratrol solubility determination in mg per ml*

Vehicles	**Solubility (mg/ml)**
Capryol PGMC®	10.78
Capryol 90®	14.21
Labrafil 2125®	4.43
Lauroglycol FCC®	2.95
Labrafil 1944®	2.93
Labrasol®	>100
Transcutol P®	>100
Arlasolve®	>100
PEG 400	>100

Table 6.2 *Formulations composition*

Batch No.	F1	F2	F3
Resveratrol	*0.50%*	*0.50%*	*0.50%*
Labrasol®	-	*5.00%*	*5.00%*
Pluronic acid F68	-	*1.00%*	*1.00%*
HPMC	*2.00%*	*2.00%*	*2.00%*
Water	*97.5%*	*91.50%*	*91.50%*
Particle size	*>1µm*	*>1µm*	*120.3 nm*
Polydispersity Index	-	-	*0.308*
Viscosity at 5 RPM	*890 cP*	*125 cP*	*96 cP*
PH	*5.20*	*4.83*	*4.9*

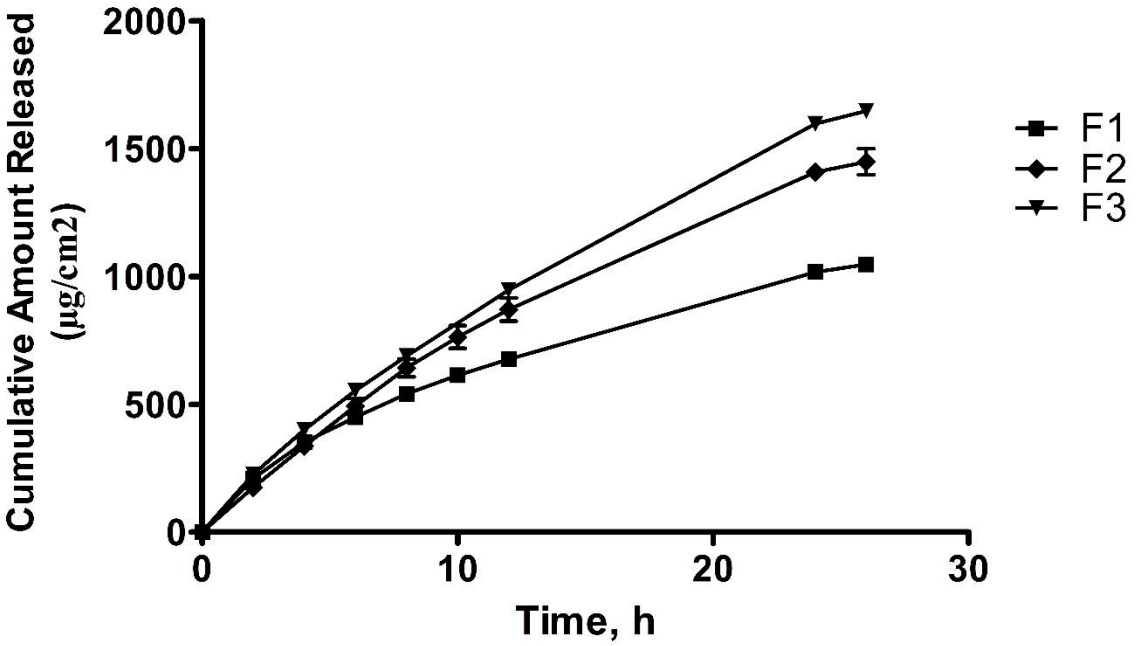

Figure 6.2 Cumulative release of resveratrol from nanogel formulations. Each experiment was performed in triplicate (N=3).

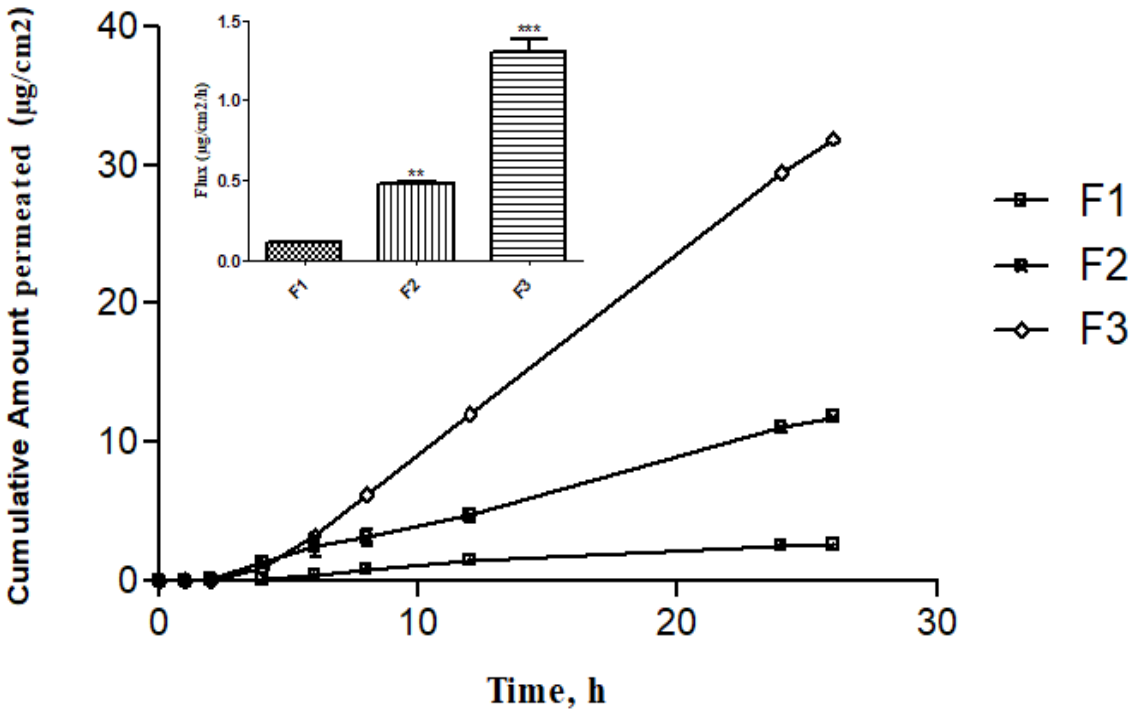

Figure 6.3 A. Cumulative amount of resveratrol permeated. B. Flux quantity of resveratrol. Each experiment was performed in triplicate (N=3). Notes: ***p < 0.01 compared with F1; ***p < 0.001 compared with F1.*

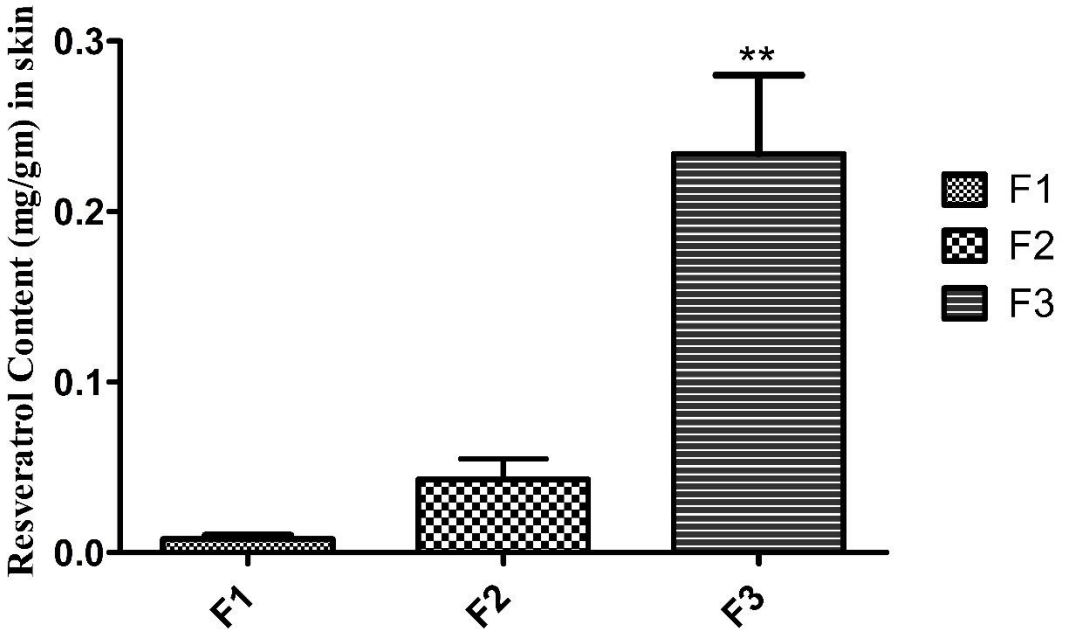

*Figure 6.4 Drug deposition of resveratrol within skin layers. Each experiment was performed in triplicate (N=3). Note: **p < 0.01 compared with F1.*

7. Summary

Topical and trans-mucosal drug delivery are potential routes for a variety of drugs with limited oral bioavailability. Hydrogel and nanogel formulations are efficient in enhancing the delivery of such drugs. Incorporating drug in the form of nanoparticles within a gel matrix has potential in enhancing the poorly permeable drug for topical and transdermal drug delivery. On the other hand, a hydrogel showed promising results on delivering drugs via buccal mucosa. The hydrogel showed a superiority based on its retention and adhesive properties for better absorption. In the dissertation, a nanogel and hydrogel were developed and evaluated as a platform for topical and trans-mucosal drug delivery, respectively. In addition, siRNA-PEI polyplexes were developed and optimized as a suitable platform for effective delivery of siRNA for melanoma treatment.

We have prepared siRNA-PEI polyplexes at different N/P ratios with three different molecular weights of PEI (1.8 KDa, 10 KDa, and 25 KDa). The complexation efficiency, cellular toxicity, as well as cellular uptake, were evaluated. The 1.8 KDa PEI-siRNA (50:1 N/P ratio) was most suitable with respect to safety and efficacy. 10 KDa PEI-siRNA (1:10 N/P ratio) showed reduced toxicity upon polyplex formation and a higher cellular uptake compared to 1.8 KDa PEI-siRNA polyplex. On the other hand, 25 KDa showed the highest efficacy in polyplex formation at a low ratio (5:1 N/P) but with an increased toxicity at a cellular level. Overall, 1.8 KDa PEI can be utilized as a carrier for siRNA due to its safety and efficacy. Based on these results, this study is further directed to choose a model for gene targeting with specific siRNA as a therapeutic tool to knock down a mutant gene in vitro for melanoma treatment. Furthermore, gene expression, as well as protein quantification, should be evaluated with respect to efficacy by q-PCR and Western

Blot techniques, respectively. Based on obtained results, further research is directed towards evaluating the optimal polyplexes efficiency for in vivo study.

Topical delivery of acyclovir is hampered by its low percutaneous permeability. We developed a nanogel formulation of acyclovir for enhanced topical drug delivery. Acyclovir nanogel (F1) formulation showed an enhanced skin permeation (2-fold higher flux) compared to Zovirax®, a commercial product. Incorporating 10 % ethanol (F3) in the formulation showed a synergistic permeation enhancement with 24-fold higher flux compared to Zovirax®. Microporated skin permeation studies were performed to illustrate the permeation behavior with interrupted stratum corneum. The results showed a significant enhancement in skin permeation compared to the passive diffusion; F3 (10% ethanol) still showed the highest enhancement. Acyclovir nanogel formulation with ethanol as a penetration enhancer demonstrated a pronounced effect on enhancing acyclovir skin permeability and content upon topical application.

Gel formulations of midazolam were developed and evaluated for buccal administration. All formulations were evaluated for physical properties, rheology behavior and in vitro release. Furthermore, a pharmacokinetic study in healthy dogs was performed. The formulations T19 and T29 (both HPMC based) with significantly higher release rates than T18 (Pluronic F127 based) were also effectively absorbed through buccal administration in dogs. At a dose of 0.3mg/kg, T19 and T29 produced a Cmax of 98.3±26.5 and 106.3±35.2 ng/ml, respectively, which are approximately two-fold higher compared to T18 (47.7±38.5 ng/ml). Furthermore, T29 at higher dose (0.6mg/kg) produced a Cmax of (187.0±104.3ng/ml). Results of this study show promise for the treatment of seizures in dogs. Future investigations into formulation concentration or dosage are required to determine if higher plasma concentrations or more rapid absorption can be

achieved. Long-term stability and shelf life of the gel formulation should also be determined prior to recommendation for use in a clinical setting.

Finally, resveratrol in nanoparticle based gel formulation was developed for enhancing transdermal flux on human skin. The solubility of resveratrol was determined in several common topical solvents. Based on solubility and compatibility results, Labrasol® was chosen for resveratrol nanogel formulation development. Resveratrol nanoparticles produced by high pressure homogenization were gelled using Methocel®K4M (F3). The F3 formulation showed a much higher amount of drug release, 1.6 and 1.1-fold higher compared to F1 and F2 (control formulations), respectively. In the skin permeation study, F3 showed 12 and 3-fold higher flux compared to F1 and F2, respectively. The skin retention of F3 was approximately 12 and 5-fold higher compared to F1 and F2, respectively. Nanogel formulation showed an enhancement of resveratrol delivery compared to same drug percentage in microparticles incorporated in gel formulations. The enhanced contact of nanoparticles on the skin as well as their faster dissolution of particles to replace the depleted (permeated) drug might be the reasons for better skin permeation. This enhancement was observed for the drug retention within skin layers as well.